This is to certify that the

thesis entitled

The Role of Surface Oxidation in Enhancing the Hydrogasification Rate of Coal Char.

presented by

Martin Edward Toomajian

has been accepted towards fulfillment
of the requirements for

M.S. degree in Chem. Engr.

Dennis J Miller
Major professor

Date 5/10/91

The Role of Surface Oxidation in Enhancing the Hydrogasification Rate of Coal Char

By

Martin Edward Toomajian

A THESIS

Submitted to
Michigan State University
in partial fulfillment of the requirements
for the degree of

MASTER OF SCIENCE

Department of Chemical Engineering

1991

ABSTRACT

The Role of Surface Oxidation in Enhancing the Hydrogasification Rate of Coal Char

By

Martin Edward Toomajian

This study uses a bituminous coal char and Saran char to study the effects of demineralization, preoxidation, intermittent oxidation, and outgassing on hydrogasification rate. Also, the usefulness of total surface area, surface pH, active surface area (ASA), and surface oxygen concentration (O/C ratio) as predictors of reactivity are investigated. Preoxidation of the fresh chars has no effect on the hydrogasification rate, but preoxidation of outgassed chars and intermittent oxidation (oxidation of partially gasified chars) enhances the rate two-fold. Outgassing chars prior to gasification decreases the gasification rate up to ten-fold. The ASA, as measure by oxygen chemisorption at 295°C, and surface oxygen concentration (O/C ratio), as measured by x-ray photoelectron spectroscopy, are the best predictors of reactivity. The ASA normalized rate for the fresh chars was ~1.0ccCH_4/ min*m^2 and the rate normalized with the O/C ratio was ~65cc CH_4/min*g carbon*unit O/C.

To my wife, Jennifer, whose love and encouragement kept me focused on the important things in life, and to my family whose continued support has helped me pursue and complete this degree.

ACKNOWLEDGEMENTS

I would like to thank Dr. Dennis Miller, my graduate advisor, for his continued guidance and encouragement throughout the completion of this research and Thesis.

The assistance of Dr. Kevin Hook, formerly of the Composite Materials and Structures Center at Michigan State University, is greatly appreciated in learning how to analyze samples using the XPS.

Finally, I would like to thank the United States Army for giving me the opportunity to attend Graduate School.

TABLE OF CONTENTS

LIST OF TABLES

LIST OF FIGURES

Chapter 1
Background

1.1 INTRODUCTION

The conversion of coal into synthetic fuels is not a new process, yet it is still not commercially widespread today. The first evidence of coal gasification can be traced back to 1670; yet, the commercial use of this process did not start until the early 1800s in Britain and the United States [1]. This early use was limited to supplementing the fledgling commercial natural gas industry. The process was not widely used because its low yields and the high cost of production made it uneconomical. The first major use of coal gasification came in the latter stage of World War II, when military necessity overrode poor economics. During the war, the Germans imported most of their oil from occupied Romanian oil fields; however, since these fields were vulnerable to attack (and were eventually destroyed), they maintained a fledgling synthetic fuel industry. Their primary production process was the Fischer-Tropsch Process, which produced approximately 200 million gallons of fuel per year [2] by the end of 1943. Germany's use of synthetic fuels ceased in May 1944 when Allied bombing destroyed the production facilities. After World War II, the abundance of oil, both in the United States and abroad, eliminated the desire to pursue coal conversion as a reliable energy source.

In the past two decades, both export and import embargoes interrupted the world supply of oil. The first major interruption occurred in the early 1970's when the 1973 Arab-Israeli War threatened secured oil exports from the Middle East. The second interruption occurred in 1974, when OPEC sought to reduce the World's supply to drive the price higher. This latter incident sparked a need in the United States to develop alternative fuel sources.

Several of the alternative fuels looked at were nuclear, solar, natural gas, and coal. Coal is the most abundant fossil fuel in the United States; however, it was not the most attractive option. Increased concern over the environmental impact of burning coal greatly reduced its desirability. Solar power, although the most environmentally safe power source, was still developing. This left natural gas as the next major source of fuel in the United States. The sudden increase in demand for natural gas threatened to decrease the nation's inventory to a 10 year supply by 1975 [3].

As energy experts looked for alternative fuels, they pursued several methods of increasing the natural gas supply. These methods included:

- Reforming of oil
- Importing LNG
- Importing more Canadian gas
- Pipelining Alaskan gas
- Producing pipeline quality gas from coal

The last method, coal gasification, seemed the best alternative to reducing America's dependence of foreign fuels.

1.2 COAL GASIFICATION PROCESSES

In the early 1970s, there were few commercially available processes. The processes that focused on methane production included the Lurgi, BI-GAS, Synthane, CO_2 Acceptor, and the HYGAS processes [3]. The Lurgi process consists of 13 fixed beds in which gasification occurs when steam and oxygen pass through the bottom of the bed. The Lurgi process is the only one that produces a synthetic pipeline gas; however, the initial product gas has a low heating value and requires catalytic methanation to upgrade it. Because of their caking properties, most U.S. bituminous coals cannot be used in the Lurgi process; however, if they undergo a prior carbonization step, they can be used. The Lurgi process produces approximately 5% methane in product gas, the smallest amount produced from any of the above gasification processes.

Unlike the Lurgi process, which uses a fixed bed, other processes use continuous fluid beds, falling beds, or entrained beds to produce synthetic natural gas. Furthermore, they produce at least one-third of their methane via direct hydrogasification of the coal.

In the HYGAS process, pulverized coal reacts with a hydrogen-rich gas containing some steam in a fluidized bed. The reaction occurs at temperatures between 1200 and 1750°F and a nominal pressure of 1000psig; this process produces up to 20% methane. Since bituminous coals tend to agglomerate during hydrogasification, they also require pretreatment for use in the HYGAS process.

The CO_2 Acceptor process is similar to the HYGAS process but uses calcined dolomite or limestone to catalyze the reaction. This process, originally designed for lignite, should work well with the subbituminous

coals found in the western United States [3]. This process produces approximately 17% methane.

The BI-GAS process reacts oxygen and steam with spent char to produce hydrogen, carbon oxides, and steam. This gas rises in the column and entrains freshly ground coal. Hydrogasification occurs as the gas and coal make contact. A cyclone separates the product gas from the spent coal char. The product gas proceeds to a methanation and purification step, while the spent coal char recycles to the bottom of the column. This process produces approximately 50% less methane than the CO_2 Acceptor process [3].

The Synthane process is the only process designed for bituminous coals and generally produces 15% methane. In this process, coal enters the reactor at the top, while steam and oxygen enter at both the top and bottom of the reactor. As the coal, steam, and oxygen enter the reactor, the steam and oxygen effectively pretreat the coal. As the pretreated coal enters the gasification zone, it reacts with the bottom feed of oxygen and steam. This reaction produces methane and carbon oxides [3].

By the late 1970s, only the Lurgi process was operating commercially, although the other processes had pilot plants operating. Of the above alternative fuel processes, the Synthane process was the most expensive and the Hygas (steam-oxygen) process was the least expensive, yet all of the processes were still commercially uneconomical. The cost of producing natural gas by the Hygas process was comparable to Alaskan natural gas but almost twice as expensive as regulated natural gas. The Synthane process produced natural gas that was almost three times higher than regulated natural gas [4].

The Exxon Catalytic Coal Gasification Process [1] is a newer generation gasification process for producing methane. In the Exxon process, coal and

steam react at high temperature to form methane. The intermediate products in the process are carbon monoxide and hydrogen, which are recycled back over the coal bed.

One additional process, the Hydrocarb Process [5], is not currently used commercially but it is important to this study since it is primarily a hydrogasification process. In the Hydrocarb Process, bituminous coal reacts with hydrogen to form methane and water and liberate additional hydrogen from the coal. The methane is then thermally decomposed to form carbon black and hydrogen. The carbon black is the desired product and can be used as a high quality fuel. The addition of limestone to the process removes unwanted sulfur, and sulfur can also be removed by forming hydrogen sulfide and using a gas scrubber.

1.3 GASIFICATION CHEMISTRY

Currently, there are several different processes for coal gasification under development in the United States. Steam gasification is the most common process, but hydrogen gasification is also an important process.

The route to methane formation in steam gasification is relatively simple. Coal is mixed with steam at high temperatures and pressures to produce hydrogen and carbon monoxide. An intermediate reaction, called the water shift reaction, produces carbon dioxide and additional hydrogen, which combines with carbon monoxide or directly with feed coal to produce methane. The following reaction sequence describes the process chemistry of steam gasification.

{1} $C(s) + H_2O(g) \longrightarrow H_2(g) + CO(g)$

{2} $CO(g) + H_2O(g) \longrightarrow H_2(g) + CO_2$ Water Shift Rxn

{3} $3H_2(g) + CO(g) \longrightarrow CH_4(g) + H_2O$

The overall reaction is

{4} $2C(s) + 2H_2O(g) \longrightarrow CH_4(g) + CO_2(g)$

Hydrogen gasification is much simpler and more direct than steam gasification. In hydrogasification, the coal char reacts directly with molecular hydrogen to form methane.

{5} $Coal + 2H_2(g) \longrightarrow CH_4(g)$

As previously discussed, the Hydrocarb Process is not a true gasification process since the final product is solid carbon black. The reaction sequence, however, is important to this study because methane is formed directly from hydrogen and coal in an intermediate reaction step. The reaction steps for the Hydrocarb Process are as follows:

{6} $Coal + 2H_2 + 0.016CaCO_3 \longrightarrow CH_4 + 0.08H_2O + 0.32H_2 + 0.008N_2 + 0.016CaS$

{7} $CH_4 \longrightarrow C + 2H_2$

where: Coal = $CH_{.8}O_{.08}S_{.016}N_{.016}$

The overall reaction is

{8} $Coal + 0.016CaCO_3 \text{----> } C + 0.08H_2O + 0.32H_2 + 0.008N_2 + 0.016CaS$

1.4 SCOPE OF THIS STUDY

This study investigates the role of oxygen in the production of methane via direct hydrogasification. Hydrogasification is used instead of other gasification methods because it is a direct route to methane production. Unlike gasification in steam and CO_2, gasification in pure hydrogen eliminates all external sources of oxygen. Thus, any influence that oxygen has on gasification must be caused by oxygen initially present on the sample surface or in the bulk sample. Hydrogasification also eliminates the need for the water shift reaction because excess hydrogen is added to the system in the reactor feed stream. This makes it easier to isolate the effect of oxygen on the reaction.

This study uses an Illinois #6 bituminous coal (PSOC 1493) and a DOW Saran resin powder (DOW MA 127) to investigate the role of oxygen in hydrogasification. Both samples are pyrolyzed to form chars to prevent them from caking in the hydrogasification reactor. The effects of oxidation, both preoxidation and intermittent oxidation, and outgassing are investigated for these samples. Gasification kinetics are compared to char properties as determined by XPS, pH measurements, and surface area measurements to gain insight into the role of oxygen.

Chapter 2
Literature Review

2.1 GASIFICATION

Compared to other processes for coal gasification, hydrogasification is not well studied. Although some significant research has been done in this field, reviewing other forms of coal gasification and carbon based char gasification is important. These other gasification methods can answer questions concerning the reactivity of coal in different gasification environments.

Hydrogasification can be related to steam gasification because the extra hydrogen produced in the water shift reaction may react with fresh coal, in addition to carbon monoxide, to form methane. Also, the effects of char preparation and pretreatment will be similar in both gasification processes. These coal char pretreatments include oxidation, catalysis, and outgassing, and they all have an effect on the reactivity of a coal char.

2.1.1 EFFECT OF PREPARATION METHOD ON CHAR PROPERTIES

The first step in coal conversion is pyrolysis to form chars. Charring is important because it removes volatiles found in coal and ultimately determines the char properties. The severity of pyrolysis (ie. the maximum temperature and time) is an important factor in determining char reactivity. For example, increasing the severity of the heat treatment has been reported to decrease the active surface area of the char [6].

Miura et al. [7] showed that the reactivity of coal chars gasified in air at 550°C decreases with an increase in the severity of the pyrolysis conditions. They also determined that demineralization greatly reduces the reactivity of the char. This reduction in rate results from the removal of minerals in the coal which catalyze gasification.

2.1.2 HYDROGEN GASIFICATION

Hydrogen gasification of coal char has not been studied as extensively as steam, oxygen, or carbon dioxide gasification, but there have been a few in-depth reviews [8,9,10,11]. Walker et al. [12] compared gasification rates in hydrogen with rates in other media. They determined that the gasification rate relative to carbon dioxide is 1×10^5 for oxygen, 3 for steam and 3×10^{-3} for hydrogen. For calcium-catalyzed gasification, Linares-Solano et al. [13] found the rate relative to CO_2 to be 5×10^4 for oxygen, 16 for steam, and 5.4×10^{-4} for hydrogen.

Blackwood [8] conducted one of the early in-depth studies of hydrogasification on coconut and wood chars. He found that the rate of methane formation is linearly proportional to the partial pressure of hydrogen in the reactor. The total pressure in the reactor does not affect the methane formation rate. Blackwood also studied steam and carbon dioxide gasification but he found no relationship between the CO_2 or CO partial pressure and the rate of methane formation. In hydrogasification of wood chars, Blackwood found that the methane rate formation is linearly proportional to the oxygen content of the char. He also found that a sharp decrease in the reaction rate corresponds to a sharp decrease in the oxygen content of the wood char.

Blackwood investigated the effect of intermittent oxidation and outgassing on the reactivity of the char and found that these treatments had no effect. This observation was later disputed by Anthony and Howard [9]. They studied the hydrogasification of coals and found that outgassing the coal at 680°C in an inert gas reduces the reactivity in hydrogasification. They also found that in hydrogasification at 927°C and 100atm the reaction proceeds rapidly up to ~40% carbon conversion. They assumed that the initial rapid reaction was due to the hydrogenation of volatile components evolving from the coal. They did not take into account different reactivities of the surface carbon atoms.

Previous work in this laboratory by Zoheidi and Miller [14] and Treptau and Miller [15] studied the effects of different pretreatments on the hydrogasification rate of carbon black and coconut char. They determined that outgassing at high temperature (1270°K) decreases the reactivity of a carbon black [14]. Zoheidi also found that even after pretreatment, only basic oxygen groups remain on the carbon surface during hydrogasification.

Surface annealing and the loss of carbonyl groups causes the rapid decrease in hydrogasification rate when unreactive chromene groups replace the carbonyl groups.

Treptau [15] found that outgassing carbon blacks at 1270°K reduces the surface oxygen content to almost zero. More importantly, he found that outgassing reduces the gasification rate by six-fold. Heating coconut char to gasification temperatures (1023°K) had no effect on reactivity; however, outgassing at 1273°K anneals active sites and reduces the reaction rate by a factor of two. This mild reduction in reaction rate, as compared to the six-fold decrease in rate for carbon black, is attributed to the higher bulk oxygen content of the char. The activity that remains after outgassing remains constant with carbon conversion. This is probably due to basic oxygen groups desorbing from the bulk char at a constant rate.

A suggested mechanism for non-catalyzed hydrogasification [16,17,18] starts with hydrogen successively and dissociatively chemisorbing onto the prismatic edge faces of graphite. The breakage of the C-C bond occurs when the third hydrogen atom adsorbs [18]; this is the rate controlling step. Since hydrogen attacks the edge atoms and not the basal plane atoms, increasing the number of edge sites should increase the gasification rate. The following diagram shows the suggested mechanism.

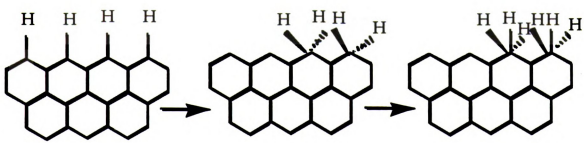

Shaw [19] suggested a different mechanism for hydrogasification, where the hydrogen associatively adsorbs onto the sample surface. He based his model on the data found by Blackwood [8] who explained his results using the dissociative model described above. Shaw reinterpreted Blackwood's data and developed a four step mechanism where each step is reversible. The mechanism can be simplified into two main steps where in the first step hydrogen adsorbs at an active site on the surface. This forms a CH_2 group that is attached to the carbon lattice. In the second step, another hydrogen molecule adsorbs on the first CH_2 group, breaking the carbon-carbon bond and evolving a methane molecule. The two step mechanism is described below.

$$\{9\} \qquad C_f + H_2 \underset{k_{-1}}{\overset{k_1}{<=\!=>}} CH_2..... \qquad\qquad \{10\} \qquad CH_2.... + H_2 \underset{k_{-2}}{\overset{k_2}{<=\!=>}} CH_4 + C_f.....$$

C_f represents an active site on the carbon surface and k_1,k_{-1}, k_2, and k_{-2} are specific rate constants for the reaction steps. The following series of diagrams depict how active sites are formed by desorbing surface oxygen groups and how associative hydrogen chemisorption occurs at these active sites.

ACTIVE SITE FORMATION

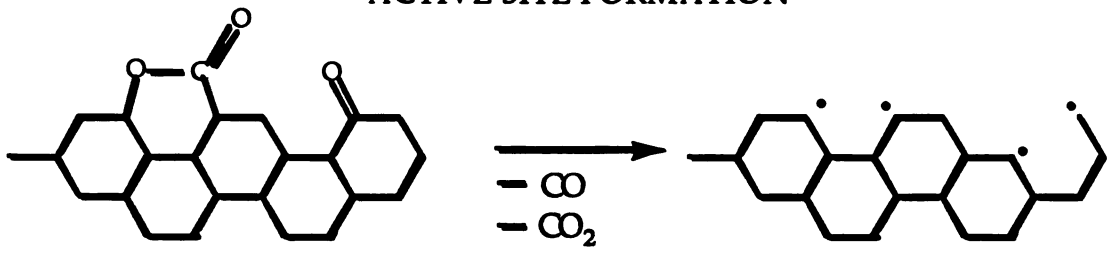

ASSOCIATIVE HYDROGEN CHEMISORPTION

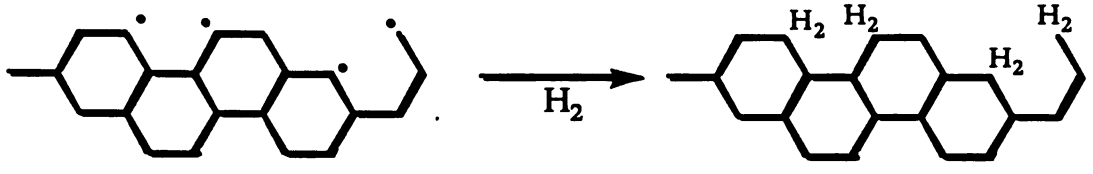

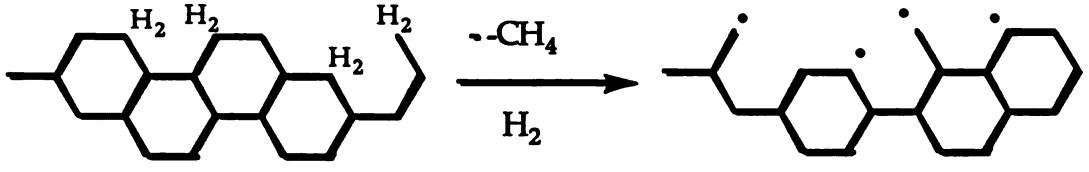

2.1.3 CATALYSIS OF HYDROGASIFICATION

Hydrogasification is generally strongly catalyzed by metals such as iron and platinum. Also, alkali salts such as calcium and potassium make good catalysts. Matsumoto and Walker [10] investigated the synergism between iron and potassium catalysts and good methanation catalysts. The methanation catalysts used were nickel and cobalt-molybdenum supported on aluminum oxide. The Saran char they used was loaded with 2.58% iron or

11.0% potassium. The methanation catalysts were loaded to 67wt% nickel on gamma aluminum oxide and 3wt% Co and 10wt% Mo as MoO_3 on gamma aluminum oxide. In the absence of a methanation catalyst, the maximum iron-loaded char reactivity was 31%/hour. Adding the nickel catalyst increased the reactivity to 100%/hour and adding the Co-Mo catalyst increased the reactivity to 77%/hour. Without iron, the methanation catalysts have little effect on the char reactivity. The maximum reaction rate with nickel is only 6.6%/hour and the Co-Mo shows little activity. The reaction rate with potassium was 36%/hour but the majority of Matsumoto's study of potassium concerned the effects of sulfur poisoning and will be discussed later.

In hydrogasification, the most commonly used alkali salt is potassium. The advantage of using potassium instead of other salts, like calcium, is that the potassium is highly mobile on the char surface. Potassium will distribute itself on the surface of the coal char, whereas calcium must be atomically dispersed throughout the coal char to obtain good activity [20].

The effectiveness of potassium as a catalyst in hydrogasification was studied by Zoheidi [21]. He used 5-10wt% K_2CO_3 on carbon black. For fresh carbon black, the reaction rate per unit area stays approximately constant with at least a 5wt% catalyst loading. This is significant because the rate per unit area decreases with conversion for uncatalyzed samples. Zoheidi also showed that catalyzing previously gasified samples will increase the hydrogasification rate. He added 10wt% K_2CO_3 to previously outgassed carbon blacks and the rate per unit area increased by twenty-fold.

Saber et al. [22] suggested a mechanism for explaining how potassium catalyzes the carbon dioxide gasification of carbon black. They found that the carbonate complex is not part of the catalytic cycle. The active catalyst

alternates between the potassium metal and a potassium-oxygen-carbon complex. They suggest that between 500°K and 1000°K, potassium carbonate forms complexes with surface carbon atoms, or surface carbon oxides. These complexes exchange carbon and oxygen with the gas phase; however, carbon from the substrate does not exchange.

Zoheidi [21] applied Saber's mechanism to potassium catalyzed hydrogasification. He suggested that the basic oxygen (carbonyl) surface groups interact with alkali-carbonates and produce stable complexes (C-O-K) that enhance reactivity. Treptau [15] showed that preoxidation of the catalyzed char increases the gasification rate by two-fold for partial combustion in air and three-fold for nitric acid oxidation. This is supported by work done by Keleman et al. [23] and Saber et al. [24], who showed that surface oxygen groups have a stabilizing effect on alkali salt catalysts and that oxygen groups also aid the activation of the catalysts. Zoheidi also suggests that the surface oxygen groups formed by burning in air at 400°C depend on the structure of the surface and can form either stable or unstable (active) potassium complexes. These unstable complexes increase the reactivity by readily desorbing from the surface and leaving new active sites.

Sulfur inhibition is a major problem in catalyzed hydrogasification. Matsumoto and Walker [10] studied the effects of sulfur poisoning in the hydrogasification of Saran char. They found that iron is especially susceptible to sulfur poisoning. The addition of only 1 ppm H_2S in the hydrogen feed stream will poison 60% of the surface iron sites and reduce the reactivity of the char to a negligible rate. Potassium is also strongly retarded by sulfur in a wet hydrogen environment. Matsumoto and Walker added their Co-Mo catalyst to a Saran char loaded with 2.8 mmole potassium/g char and found that the sulfur contained in the catalyst support was enough to stop the

hydrogasification reaction. The aluminum oxide catalyst support had only 0.23wt% sulfur. Sulfur will inhibit both potassium and iron because they strongly bind sulfur to their surface. Once the sulfur is bound, it is extremely difficult to remove.

2.1.4 OXIDIZED COAL GASIFICATION

Oxidation of coal chars prior to gasification is potentially a simple method for increasing the hydrogasification rate of coal chars. Oxidation is effective because methane formation is directly related to the desorption of oxygen complexes [25]. The most common methods of preoxidation are burning the sample in air or contacting it with aqueous nitric acid. Burning a sample in air at temperatures below 450°C primarily fixes acidic oxygen groups on the carbon surface and burning in air at temperatures above 600°C primarily fixes basic oxygen groups on the char surface. The following diagram shows several different types of basic and acidic oxygen complexes bonded to a carbon surface.

BASIC OXYGEN GROUPS

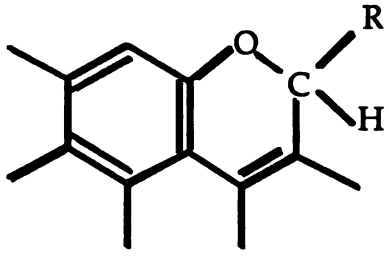

CHROMENE

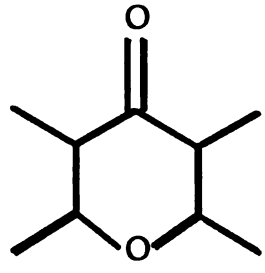

PYRONE

ACIDIC OXYGEN GROUPS

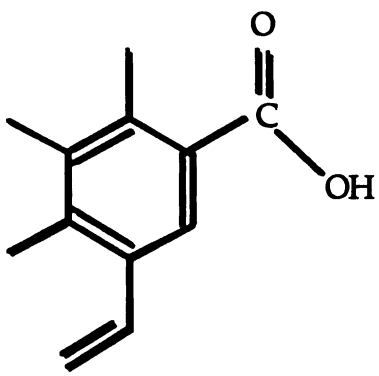

CARBOXYLIC

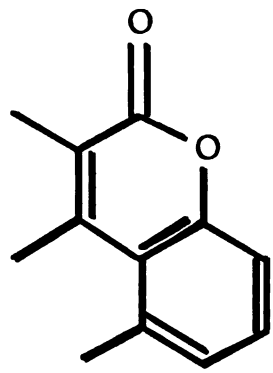

LACTONE

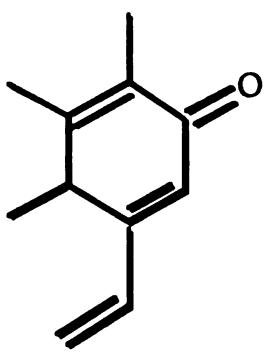

QUINONE

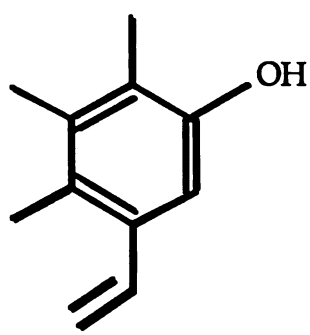

PHENOLIC

Also, Sellitti et al. [26] found that nitric acid oxidation produces a carbon structure with carboxyl, phenol, amine, carbonyl, and ester groups bound to the surface. An example of this structure is shown below.

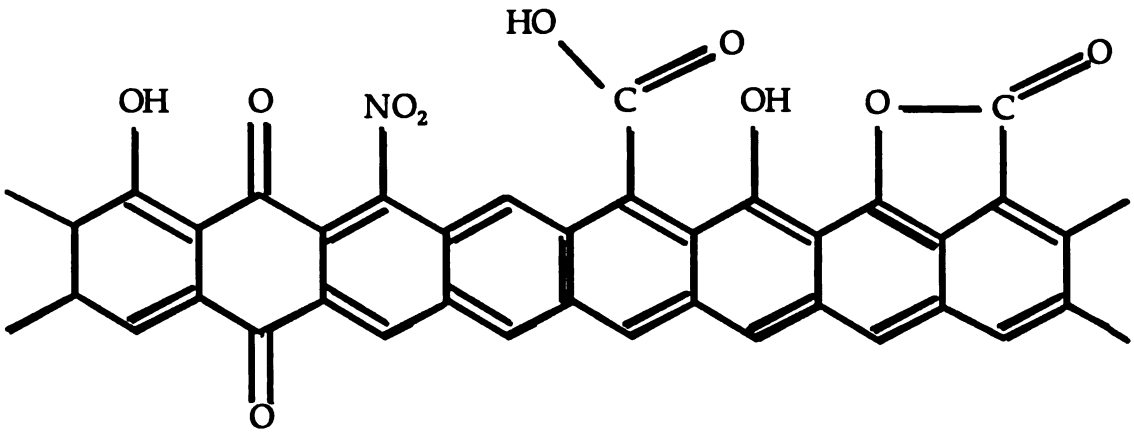

The mechanism by which oxygen desorbs from the char surface is the key to understanding how it enhances the methane formation. Once oxygen chemisorbs on a carbon surface, it will not desorb in its atomic or molecular form. It only desorbs as carbon monoxide or carbon dioxide. This desorption cleaves a carbon atom from the surface leaving an active, or nascent, site [27]. Molecular hydrogen then attacks these new active sites, forming a methane molecule.

Pretreatment by contacting with nitric acid is especially useful in studying the effect of oxidation because the surface chemical properties of the sample can be altered without affecting the surface area or structure [28]. Oxidizing a sample by contacting it with aqueous nitric acid increases the rate six-fold in catalyzed steam gasification [29]. This was supported by Mims and Krajewski [30] who determined that in catalytic gasification, the catalyst activity is related to the presence of surface oxygen groups.

Treptau [15] studied the effect of subsequent oxidation on fresh and outgassed carbon black and coconut char. He found that preoxidation fixes additional oxygen groups on the surface of the samples and enhances the hydrogasification rate of carbon black and coconut char. Preoxidizing fresh carbon black with aqueous HNO_3 only increases the hydrogasification rate by

30% to 50%, while preoxidation via partial combustion gave as much as a two-fold rate increase. Preoxidizing the coconut char with aqueous nitric acid significantly increases the rate in both fresh and outgassed samples. He found that oxidizing outgassed carbon blacks by burning in air at 400°C, increases the hydrogasification rate two-fold, but contacting with nitric acid only increases the rate by 5-10%. Treptau also found that the coconut char behaved somewhat similarly to the carbon black. The main difference between the two samples was the higher bulk oxygen content in the coconut char. The coconut char contained 2.8% oxygen versus 0.2% for carbon black. For the outgassed coconut char, the rate increases almost to that of the fresh char, but the effect decays with carbon conversion.

Zoheidi [31] compared the surface pH of carbon black samples after oxidation via burning in air and oxidation via contacting with aqueous nitric acid. The pH tests confirmed that both contacting with nitric acid and burning in air at 400°C fix acidic oxygen groups on the surface, whereas burning in air at 800°C fixes basic groups on the surface. Nitric acid oxidation takes up to 15 hours to saturate the surface with oxygen, while partial combustion will saturate the surface in only 15 minutes.

Another method using oxygen to enhance hydrogasification is to add a small amount of oxygen directly to the hydrogen feed stream. It is extremely important to keep the oxygen concentration below the explosive level. Cao and Back [11] used this method and showed that adding just 0.1% oxygen to hydrogen in the feed stream increases the rate of methane formation by an order of magnitude in the hydrogasification of carbons [11].

2.2 REVIEW OF SURFACE CHARACTERIZATION TECHNIQUES

The ability to characterize the char surface is extremely important in studying coal gasification in order to understand the surface structure and nature of surface groups present. Surface characterization involves determination of total surface area, pore structure, active surface area, ΔpH, and concentration of elements on the char surface. Each parameter will be discussed in detail in the following sections.

2.2.1 TOTAL SURFACE AREA AND POROSITY

Generally, the first step in characterizing a carbon sample is to determine the total surface area (TSA) and porosity. Historically, however, the porosity was not a useful parameter for characterizing the reactivity of a carbon. Although the porosity of a coal increases with oxidation, the oxidation rate only slightly increases [32]. There is no large increase in the activity because the new surface has pores in the micro- and mesopore range. Slow diffusion in these pores restricts molecular oxygen so the oxidation rate does not significantly increase. Comparing the pore structure and active surface area evolution with hydrogenation rates shows that the macropore surface area increases after 55% conversion. This is primarily due to the meso- and micropores broadening into the macropore size [33].

The TSA of a sample is also not a good parameter for characterizing the reactivity of a coal char. Radovic et al. [6] showed that TSA, from CO_2

adsorption and calculated by assuming micropore volume equal to the monolayer capacity, is not a relevant parameter for normalizing reactivity. Also, DeKoranyi [34] found that the reactivity of coal chars in CO_2 gasification will increase by no more than two-fold while the TSA increases by as much as twenty-five-fold. The oxygen chemisorption capacity of a char is a better index of the gasification reactivity because it is related to the active surface area of the sample.

2.2.2 ACTIVE SURFACE AREA

With coal char and model carbons, most of the sample surface area is unreactive. Generally, edge carbon atoms are more reactive than basal plane carbon atoms because of either a geometric factor or an impurity factor [35]. The edge carbon atoms are more reactive because they have unpaired sigma electrons that are available to form bonds, whereas the basal plane carbon atoms have sigma electrons in chemical bonds with adjacent carbon atoms. Impurities may be a factor because they diffuse to and concentrate at the edges during heat treatment at high temperatures. These impurities may help catalyze the gasification reaction or desorb to leave vacancies in the basal plane structure.

This leads to the idea of active surface area (ASA). The ASA is the actual area on the sample where gasification reactions occur. The ASA of a sample consists of the active, or edge, sites located along the edges of the carbon basal planes and at vacancies left when impurities desorb from the surface [35].

Walker [36] pioneered the use of oxygen chemisorption to measure the ASA of graphite in the absence of carbon gasification. He suggests a two step mechanism for carbon gasification. In the first step, molecular oxygen dissociatively chemisorbs onto the carbon surface, forming a C-O complex.

{11} $$2C_f + O2_{(g)} \text{-----> } 2\,C(O)$$

The C-O complexes dissociate to form two surface carbonyl groups.

{12} $$2C(O) \text{ -----> } 2CO$$

In the second step, the surface carbonyl groups desorb as carbon monoxide.

{13} $$CO \text{ -----> } 2\,CO_{(g)}$$

This dissociative oxygen chemisorption only occurs at the edges of basal planes (edge sites) and defect sites. The first step is not reversible; once chemisorbed, oxygen only desorbs as CO or CO_2. There is negligible chemisorption of molecular oxygen on the basal planes of graphite.

Walker [36] suggested that oxygen chemisorption may not find the exact ASA of a carbon. He found that the ASA of oxidized carbon blacks as determined by oxygen chemisorption at 300°C did not agree with the ASA found by accounting for oxygen desorbed as CO and CO_2 during sample heating. There are two possible theories for this difference. First, some active sites may require higher activation energies not reached by oxygen chemisorption at 300°C; and second, at higher gasification temperatures the mobility of some oxygen atoms is high enough for them to migrate onto the

basal plane surfaces. Using oxygen chemisorption at temperatures higher than 300°C may fix more ASA, but it also may lead to CO_2 gasification of the carbon surface. Since oxygen desorbs as CO and CO_2, the activation energy required for desorption is greater than that for adsorption.

Walker also investigated the mobility of surface oxygen complexes. He selectively adsorbed O^{18} and O^{16} at different temperatures to place them in surface groups with varying activation energies. He then desorbed the surface oxygen groups at different temperatures and measured the ratio of O^{18} to O^{16}. He found that this ratio remained relatively constant at each desorption temperature. Since both O^{18} and O^{16} desorbed at all temperatures, the oxygen atoms must be able to migrate between different surface groups; ie. a carboxyl oxygen can exchange with a carbonyl oxygen.

2.2.3 SURFACE SPECTROSCOPIC STUDIES

X-ray photoelectron spectroscopy (XPS) is an excellent analysis technique for determining the concentration of elements on a sample surface. In XPS , electrons from a radioactive source bombard the sample surface and dislodge 1s, 2s, 2p, etc. electrons from the inner shells of surface elements. The dislodged electrons are collected and analyzed to determine a spectra of the primary photoelectrons [37]. Auger electrons are also collected and analyzed so XPS is often the preferred surface chemical analysis technique.

In coal research, the primary use of XPS is to determine the concentrations of surface elements and to provide information about the chemical state of the surface elements. A shift in the elemental peak for carbon will occur when some elements, like oxygen, nitrogen, and sulfur, are

bonded to the carbon. The degree of shift in the peak location indicates what type of atoms are attached and their bonding states.

XPS studies [38, 39, 40] of oxidized carbons have showed that an approximate 1.5 eV shift in the position of the carbon C1s peak occurs with each C-O bond. These researchers determined the following locations of oxygen-carbon complexes:

Structure and Chemical Representation		Peak Position
graphite structure	-C--C-	284.4 eV
phenol groups	-C--OH	286.0 eV
quinone groups	-C=O	288.0 eV
ester groups	-C=OOC-	288.0 eV
carboxyl groups	-C=OOH	289.2 eV

Other researchers [41, 42, 43] identified the chemical shifts of the carbon C1s peak when carbon atoms are bonded to different oxygen groups. The reported chemical shifts are summarized below:

Structure of oxygen group	Peak Shift (eV)
hydroxyl, phenol, ether	1.5---1.7
carbonyl, quinone	2.0---3.5
carboxyl, ester	4.0---5.0
carbonate	6.0---6.5

Since the peak shifts from the various oxygen groups have been identified, several researchers have used XPS to determine the effectiveness of different oxidation methods. Evans et al. [44] used XPS to determine the extent of the nitric acid oxidation of graphite. They analyzed the C1s peak and found that the samples were well oxidized after eight hours and were almost completely oxidized after 24 hours. Nakayame et al. [45] oxidized carbon fibers by an electrochemical procedure that produced both strongly and weakly oxidized carbon [45]. They used triflouroethanol and dicyclohexyl-carbodimide to label the carboxylic groups and pentaflourobenzaldehyde to label the primary amines. They analyzed the samples using XPS and found that this method primarily increases the carboxylic acid type group.

Treptau [46] used XPS to try to understand how the surface of carbon black and coconut char changes during K_2CO_3 catalyzed hydrogasification. He first verified that heating the samples to the gasification temperature (750°C) outgasses all of the surface oxygen. The surface O/C ratio of the carbon black reduces to ~0.0 for both fresh and HNO_3 oxidized samples. The coconut char O/C ratio reduces to ~0.008 which is well below the bulk value of 0.028 and the initial surface O/C of 0.079.

Catalyzing the carbon black with K_2CO_3 increases the surface O/C ratio by an order of magnitude at 750°C. Also, the surface O/C and K/C ratios increase during hydrogasification and the O/K ratio stays constant at 1.8 for partially gasified samples. This is higher than the expected ratio of 1.5 for the O/K from the catalyst alone. This signifies that the catalyst stabilizes some surface oxygen groups. Treptau was unable to differentiate between acidic and basic oxygen groups using only XPS.

Chapter 3
Equipment and Procedures

3.1 CHAR PREPARATION

3.1.1 PYROLYSIS

The coal and Saran resin were pretreated by several different methods. Both the coal and the Saran resin were initially pyrolyzed to form chars by heating at 10°C/min to 900°C and holding for 30 minutes in a nitrogen flow of 400cc/min. Pyrolysis removed most of the volatile components of the coal, which avoids contaminating the reactor during hydrogasification. The pyrolysis reactor has a three foot long, 2.5 inch ID quartz tube with a quarter inch nipple on one end and a removable flange on the other end. A Lindeberg type 54232 furnace encloses the quartz tube and a downstream cold trap captures the volatiles leaving the samples. The upstream side has a flow meter and a carrier gas cylinder with a regulator to provide controlled gas flow.

3.1.2 DEMINERALIZATION

Some of the coal char was demineralized to further remove mineral matter from the bulk sample. The coal was demineralized by acid washing in HCl and HF to remove the metal oxide contaminants, specifically alumina, silica, CaO, and FeOx. After acid washing, the chars were repyrolyzed to remove the flourine and chlorine left during the demineralization. This pyrolysis also ensured that the samples were well dried. Table 3.1 gives the ultimate analysis of the chars after pyrolysis and demineralization as determined at a commercial laboratory.

Table 3.1 ULTIMATE ANALYSIS OF SAMPLES
(Weight % - Dry Basis)

Element	Coal Char	Demineralized Coal Char	Saran Char
C	75.30	93.01	96.36
H	.53	.27	.53
N	1.34	1.62	1.04
S	3.55	1.82	.43
Ash	17.33	2.28	.08
O (by diff)	1.95	.73	1.56
Cl	-.--	.25	-.--
F	-.--	.02	-.--
	100	100	100

3.2 HYDROGASIFICATION

Zoheidi designed and built the hydrogasification reactor used in this study. A complete description, including the design specifications, is in his dissertation [47]. A new gas chromatograph (GC) is the only change made to the original system. This new GC is a Varian model 3300 equipped with Carbosieve S-II columns.

3.3 SURFACE CHARACTERIZATION

The surface of each of the samples was characterized by four analysis techniques. These techniques measured the surface pH, surface oxygen concentration, active surface area, and the total surface area of the chars. Each method is described in the following sections.

3.3.1 pH MEASUREMENTS

Sample pH determines the general nature of oxygen groups on the char surfaces, ie. whether they are acidic or basic. Since the chars are solids at standard conditions, ASTM method D3838-80 [48] is used to determine the sample pH. The procedure is as follows:

1. Immerse the char samples in a 0.1 molar potassium chloride (KCl) solution (approximately 50mg of char to 20ml of solution in a 25ml Erlenmeyer flask). Potassium chloride (KCl) is used because model carbons will generally wet in KCl when they will not wet in water [47].
2. Boil the char suspensions under reflux for two hours along with a reference solution of KCl.
3. Cool the solutions to room temperature under reflux. A water bath will speed this process.
4. Measure the sample pH and final temperature of each solution. Record the individual pHs and the changes in pH between the coal suspension and the standard KCl solution. The pH of the solution's were measured using a Fisher Scientific Accumet 950 pH/ion Meter. The solution temperature at which the pH was measured was generally 23°C ± 1°C. This temperature is important because sample pH varies with temperature.

The change in pH (ΔpH) is more important than individual pH because pH of each sample, including the standard KCl solution, varies with temperature. The ΔpH determines if the oxygen groups on the carbon surface are acidic or basic: basic oxygen groups increase the ΔpH of the KCl solution and the acidic groups decrease ΔpH of the KCl solution.

3.3.2 X-RAY PHOTOELECTRON SPECTROSCOPY

3.3.2.1 GENERAL INFORMATION

A Perkin-Elmer Model 5400 PHI X-ray photoelectron spectrometer (XPS) located in the Composite Materials and Structures Center at Michigan State University. XPS is used to study the char surfaces in this study. Specifically, the XPS is used to find the surface oxygen to carbon ratio (O/C) of char samples and to determine how this ratio changes with different pretreatments. Two types of analysis scans can be performed with the XPS. The first scanning method usually conducted is a survey scan. Survey scans collect and analyze data over a wide range of energy levels to determine all of the different elements present on the char surface. Once the survey scan is complete and the gross surface concentrations of surface elements is known, a multiplex scan is conducted. A multiplex scan is more accurate than a survey scan because it only scans small ranges of energy levels to specifically look for the elements identified during the survey scan. Information on the bonding states of surface elements can be generated from the multiplex scans.

The XPS system hardware has neutralizer control, a monochromated x-ray source (Al source), and an ion gun (04-300). The neutralizer aids in analyzing samples that build-up a high surface charge and the ion gun enables surface sputtering to analyze the layers initially under the surface. Also, a Zalar Rotation 8 sample mount with auto-tilt stage control permits multiple sample analysis and angle resolve to limit bulk penetration during the analysis.

The XPS has both a magnesium and aluminum x-ray source. Early tests used the magnesium source, while the later analysis used the aluminum

source which provided a better C1s peak for curve fitting. The magnesium source has an anode energy of 1253.6 eV and an anode power of 400 watts, whereas the aluminum source has an anode energy of 1486.6 eV and an anode power of 600 watts. Both sources have an X-ray voltage of 15 KV. The analyzer/detector parameters used in these studies are as follows:

Detector----------Position Sensitive
Input Lens----------Omni Focus II
Omni Focus lens area----------Small
Aperture----------3 or 4
ISS scattering angle (Deg)----------123

3.3.2.2 SURVEY ANALYSIS

The following parameters were used in the survey scans:

Upper limit (eV)	1000.0
Range (eV)	1000.0
Split energy	200.0
Resolution -- Survey	
eV/Step	0.5
1st scan Time/Step (ms)	50.0
2nd scan Time/Step (ms)	200.0
Pass energy (eV)	44.7
Acquisition time (Min)	10.0
X-ray Anode Mg (W)	400.0
Al (W)	600.0

3.3.2.3 MULTIPLEX ANALYSIS SETTINGS

The exact settings used for each multiplex run varied depending on the principal elements found during the survey scan. The following are the most common elements scanned:

Element Name	O1	C1	S1	N1	K1
Acquisition window					
Upper limit (eV)	545.0	300.0	178.0	414.0	307.0
Range (eV)	20.0	20.0	20.0	20.0	20.0
Resolution	UTIL	UTIL	UTIL	UTIL	UTIL
eV/Step	.100	.100	.100	.100	.100
Time/Step (ms)	50	50	50	50	50
Pass/Step (eV)	35.75	35.75	35.75	35.75	35.75
Sweeps	6	6	6	6	6

3.3.2.4 CURVE FITTING ANALYSIS

Curve fitting a multiplexed analysis peak provides some insight into the types of surface functional groups present. Performing a curve fit on the C1s peak gives insight into the bonding state of oxygen that is bound to the surface carbon atoms; ie. if the oxygen complexes are phenolic, quinone, or carboxylic type structures. In doing a curve fit, the following analysis assumptions are implemented: the C1s curve is asymmetric with a 90% gaussian shape, the background is integrated, the full width/half mast

(FWHM) setting is 1.3, all invariance settings are preset to zero, and the lateral movement of the peaks is severely limited. Unfortunately, the curve fitting results were not completed in time to include in this thesis. The C1s peaks of the samples are in the Appendix to show the gross change in the shape of the peak. A broad peak signifies oxygen groups bound to the carbon surface and a narrowing of the peak indicates a decrease in the amount of carbon-oxygen bonds.

3.3.2.5 SAMPLE PREPARATION AND TRANSFER

A. SAMPLE MOUNTING

Prior to XPS analysis, char samples must first be secured to a sample mount suitable for use in both the vacuum pretreatment reactor (VPR) and the XPS instrument. Different methods of securing the samples to the XPS sample mounts were used in the analyses. In earlier work, Treptau [49] formed carbon black samples into pellets using a hydraulic press; however, neither the coal char nor the Saran char would form a pellet. A nitrogen glove box was used to transfer some samples to an XPS sample mount after outgassing; however, XPS analysis showed that oxygen contamination occurred during the transfer. Two methods were useful in securing the samples.

The first method uses standard double-sided tape to mount the chars on the sample mounts. This method limits the outgassing temperature that the chars can be heated in the vacuum pretreatment reactor to 120°C because

the mounting tape will melt at higher temperatures. The procedure is as follows:

1. Preheat Scotch brand mounting tape to 120°C in an oven to preshrink it prior to mounting the sample.
2. After preshrinking the tape, transfer it to the sample mount and press a char sample into the tape, covering a 1.4cm^2 area.
3. Introduce the sample mount into the VPR and heat it to 120°C under vacuum for four hours.

The second method for mounting the sample, used for high temperature runs (200°C to 800°C), involves using a high temperature adhesive (AREMCO 503) to secure the sample onto the mount. To prevent the adhesive from permanently adhering to the sample mounts, it was first mounted on thin strips of tungsten which were then secured to the sample mounts. The high temperature mounting procedure is as follows:

1. Cut a 0.5cm by 1.3cm strip of tungsten and cover the strip with a 1mm thick layer of adhesive. Allow the adhesive to dry in air for one hour at room temperature.
2. Press the sample into one side of the adhesive and cure it for four hours at 120°C in a furnace.
3. When the samples are finished curing, attach them to the XPS mount using a tungsten mask and transfer the mount to the vacuum pretreatment reactor.

XPS analysis of samples mounted with the adhesive showed a larger amount of surface oxygen than the samples mounted on the tape. This analysis also showed a large amount of phosphorous on the surface. Since there is no significant concentration of phosphorous in the chars, the XPS is detecting phosphorous from the adhesive that either migrates to the sample or is exposed in the gaps between char particles. If the XPS scan is analyzing the adhesive through gaps in the char layer, it will record an incorrectly high oxygen concentration, as the adhesive surface is composed of ~60% oxygen. If the increase in phosphorous is due to migration, then oxygen will also likely migrate from the adhesive, causing artificially high surface concentrations.

To account for the increased oxygen content resulting from the adhesive, char samples were analyzed together with uncovered adhesive to determine a ratio of phosphorous to oxygen on the adhesive. This ratio was used to correct the surface oxygen on the char sample by multiplying the ratio of oxygen to phosphorous on the adhesive by the concentration of phosphorous found on the sample. The results are comparable to Treptau's analysis of carbon lampblack pellets and coconut char outgassed at high temperatures [46]. Treptau found that outgassing carbon black and coconut char at 750°C, under high vacuum, decreases the surface concentration of oxygen to the bulk level.

B. VACUUM PRETREATMENT REACTOR

Prior to XPS analysis, a vacuum pretreatment reactor (VPR) is used to outgas the weakly physisorbed surface contaminants. The VPR also can be used to profile the desorption of surface oxygen from the sample by analyzing

samples outgassed at increasingly higher temperatures up to the hydrogasification temperature.

Treptau [49] designed and built the original VPR and he gives a complete description in his dissertation. The VPR can maintain a vacuum less than 1 X 10^{-8} Torr at 25°C or heat samples to 1000°C at pressure up to atmospheric.

Several changes were made to Treptau's design for this study. First, a 6" X 18" stainless steel tube, open at both ends, replaced the original furnace chamber. The thermocouple and heater feedthrough now enters one end of the furnace chamber, while samples are introduced into the other end. The design changes eliminates a snagging problem caused by the sample mount catching on thermocouple and heater element lines when both are introduced into the same end of the furnace. Second, stainless steel interior heat shields replaced the original nickel-chrome alloy shields, but the shield configuration remains unchanged. The new heat shields reduce the heat transfer to the external surface of the reactor. The external surface temperature did not exceed 140°C even after several hours of heating at a furnace temperature of 850°C. Previously, the external temperature would approach 200°C within six hours. The new reactor configuration is shown in Figure 3.1.

C. SAMPLE HEATING AND TRANSFER

Once the chars were mounted on the VPR/XPS sample mount, they were introduced into the VPR and heated under vacuum for four hours. For normal XPS analyses, char samples were heated to 120°C. Higher

FIGURE 3.1. VACUUM PRETREATMENT REACTOR

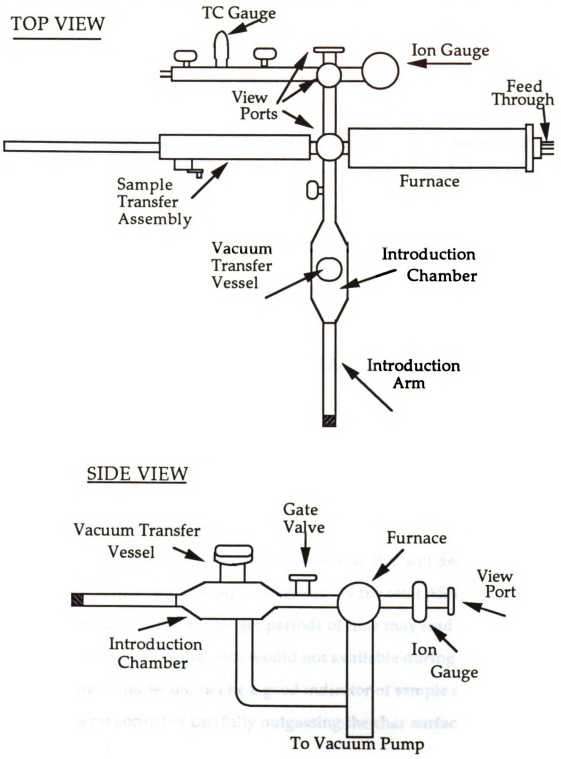

temperatures were used in studies of outgassing. The initial pressure during heating was generally 5 X 10^{-6} Torr, but after heating for just two hours, the pressure was usually less than 9 X 10^{-7} Torr. After cooling and pumping overnight, the system pressure was generally less than 1 x 10^{-8} Torr, the lowest pressure that the system could record.

The transfer to the vacuum transfer vessel occurred at pressures less than 5 x 10^{-6} Torr; however, the vacuum transfer vessel can only maintain pressures at approximately 1 x 10^{-4} Torr. The vacuum transfer vessel was used to transfer and introduce the sample into the XPS. The XPS introduction pressure was generally 2 X 10^{-7} Torr and the analysis pressure was generally less than 4 X 10^{-8} Torr.

3.3.3 ACTIVE SURFACE AREA MEASUREMENT

The measurement of active surface area of carbon samples is accomplished by oxygen chemisorption. The ASA of each sample was determined by first outgassing it at the hydrogasification temperature in helium to prevent any combustion or oxidation of the char surface. The gasification temperature of 725°C was used because this will determine the ASA available during reaction, but not necessarily the total ASA. Outgassing at higher temperatures and for longer periods of time may lead to higher ASA; however, the additional area would not available during hydrogasification and would not be a good indicator of sample reactivity. The ASA experiments consist of carefully outgassing the char surface, then

chemisorbing oxygen onto the active surface area. Details of each step are given in the following sections.

3.3.3.1 SAMPLE OUTGASSING

The sample surface must be "cleaned" prior to determining the active surface area (ASA). This is done by heating the sample under high purity helium to remove the bound surface oxygen which occupies the active sites constituting the ASA. It is extremely important to prevent exposure of the sample to oxygen during outgassing, which could lead to active site reduction and low ASA measurements. This is especially important while the sample is at a high temperature because oxygen chemisorption is an activated process.

Several methods were used to outgas char samples and transfer them to the oxygen chemisorption apparatus. The first method used a separate pretreatment furnace to outgas char samples. The furnace has two 525 Watt Mellen (clam shell) tubular heaters (Model 12-200) which have a maximum temperature of 1200°C. High temperature firebrick encases the heaters; the sample tube enters through an opening in the top brick. An Omega Series CN-2010 programmable temperature controller and a K-type thermocouple control the ramp and soak temperatures. A helium flow rate of 10cc/min prevents the sample from oxidizing as it heats to the soak temperature. The helium was Linde Ultra High Purity (99.999% pure). The method used to outgas and transfer the sample using the pretreatment furnace is as follows:

1. Insert the sample into the sample tube and weigh it with the end stoppers and support cup. The amount of sample varies with

the ASA of the sample. Generally, 50mg of coal char and 100mg of Saran char is sufficient to determine the ASA. A small Styrofoam cup is used to hold the sample tube upright on the scale, which eliminates weighing errors caused by the sample tube extending over the edge of the weighing pan.

2. Attach the sample tube to the furnace and pass helium over the sample to purge the tube of air.
3. Heat the sample to the specified pretreatment temperature at 5°C/min and hold for 30 minutes. Quench the sample to room temperature, remove the downstream tube connection and plug the end with a stopper. This permits helium to flow over the sample while it is being removed. Quenching is extremely important because oxygen chemisorption is an activated process, which occurs extremely slowly at room temperature.
4. Remove the upstream tube connection and quickly plug the end. Weigh the sample tube, stoppers, and cup to find the initial sample weight for the ASA measurement.
5. Attach the sample tube to the chemisorption apparatus and purge the tube with helium to remove any air that may have entered during the transfer.
6. Conduct the ASA measurement using the procedure described in Section 3.3.3.3.

In the second outgassing method, samples were heated under vacuum instead of helium in a special sample tube which permitted the transfer to the chemisorption apparatus while maintaining the vacuum. The sample tube is a large U-tube with two three-way stopcocks which form a bridge between the

two sides of the U-tube. Closing the stopcocks seals the sample so it can be weighed and transferred without exposure to air. Before opening the stopcocks, the bridge is purged of air using the carrier gas from the chemisorption apparatus. When the bridge is purged, the stopcocks are opened and the sample is exposed to helium.

This method had two problems. First, the vacuum tended to pull the sample out of the sample tube. This was prevented by plugging the tube ends with glass wool. The second problem was sample contamination. The vacuum must have pulled air into the sample tube because the ASA measured by this method were much smaller than those measured using the first method.

The third method used was similar to the first, except that the sample was in a special extended U-tube attached to the chemisorption apparatus directly. This special U-tube eliminated the need to transfer the sample and was configured to prevent the high outgassing temperatures from damaging the apparatus. This third method also enable appears to be the method of choice for continuing chemisorption studies.

3.3.3.2 TEMPERATURE PROGRAMMED DESORPTION

Temperature programmed desorption (TPD) is used to determine if the surface is cleansed of oxygen during the heat-up to reaction temperature (725°C) and to identify the temperatures at which desorption occurs. The TPD experiments were conducted by heating samples at 5°C/min to a maximum temperature of 950°C and recording the output signal on a strip chart recorder. In addition to the output signal, the chart recorder integrated

the peak area, which was converted into a volume of CO and CO_2 by multiplying by a calibration factor. The calibration factor was found by passing a pulse of oxygen through an empty sample tube and dividing it by the total integration signal. The ASA found by accounting for the sites vacated by the desorbed CO and CO_2 was over thirty-fold higher than the ASA found by oxygen chemisorption at 295°C. Walker [36] found similar differences between the ASA of carbon black found by TPD and oxygen chemisorption at 300°C. He hypothesized that oxygen chemisorption at 300°C did not cover all of the ASA because the activation energy for some of the active sites was higher than 300°C. The chemisorption temperature of 295°C was used in this study because higher temperatures (450°C) caused significant combustion of the char surface and lower temperatures resulted in a 25% lower ASA. Also, since oxygen chemisorption is an activated process, it takes longer to saturate the surface at lower temperatures.

3.3.3.3 OXYGEN CHEMISORPTION

A Micromeritics Pulse Chemisorb 2700 was used to determine the active surface area using oxygen chemisorption. The Pulse Chemisorb 2700 determines the amount of oxygen that chemisorbs onto the char surface by injecting a known volume of oxygen over the sample and measuring the amount of oxygen that exits the system (the oxygen volume can be varied by changing the injection loop size). The apparatus reads the difference in thermal conductivity between the oxygen pulse and a carrier gas and reports this difference as an electronic signal which is read by an LED meter and a chart recorder. The meter reading is used to determine the volume of oxygen

that by-passes the sample, which is then subtracted from the total amount injected to give the amount of oxygen adsorbed.

The complete apparatus consists of a Micromeritics Pulse Chemisorb 2700 with model 2300 FC flow controller, a Sargent strip chart recorder with an electronic integrator, and Linde ultra high purity (99.999%) gas cylinders of helium, oxygen, and nitrogen.

The chemisorption temperature for most of the runs was 295°C. This temperature was high enough to activate the chemisorption process, yet not cause any significant combustion of the char. A makeshift gas chromatograph (GC) was inserted downstream of the apparatus in several experiments to determine if any combustion occurred during the oxygen chemisorption. The GC consisted of a 1/8 by 18 inch column with Spherocarb 100/120 mesh packing placed in a 90°C water bath. The chemisorption procedure was conducted as follows:

Oxygen Chemisorption to Find the Active Surface Area

1. Outgas the sample using one of the methods described in Section 3.3.3.1.
2. Pass helium over the sample at 10cc/min using the mass flow controller until the detector meter stops fluctuating. This ensures that all gas contaminants are removed from the U-tube prior to heating.
3. Heat the sample to the chemisorption temperature (295°C). Zero the detector meter and peak area signal meter, set the sensitivity to 10X, the relative condition to negative, and wait until the system comes to steady state.

4. Inject a pulse of oxygen into the stream flowing over the char. In most experiments, oxygen pulse size was 0.047cc. Leave the injection lever in the "inject" position.
5. When the detector finishes sensing the peak and the meter reading returns to zero, record the peak area. Continue subsequent injections until there is no change in peak area for several injections. This ensures that the active sites are saturated with oxygen and the procedure is complete. Usually, about 15 injections are sufficient to saturate the char surface with oxygen.
6. Find the volume of oxygen adsorbed on the sample and the active surface area using the following equations:

   a. For each injection:

$$O_2 \text{ Volume injected} - (\text{peak area}) * K = \text{Volume } O_2 \text{ adsorbed}$$

   Where: K = peak correlation factor

$$K = \frac{O_2 \text{ Volume injected}}{\text{Max Peak Area}}$$

   b. Sum the volumes of O_2 adsorbed for each injection and convert the total volume to standard conditions.

c. Determine the active surface area by the following equation:

$$ASA = \frac{(V_{stp}) * (M)}{(\text{weight of sample})}$$

Where:

V_{stp} = Volume O_2 adsorbed at STP.

M = Area covered by one cc of oxygen.
(4.37 m^2/ml O_2)

The area covered by one milliliter of oxygen is determined from the following equation:

$$M = \frac{(16.3\ \text{Å}^2)}{(\text{Molec. } O_2)} \frac{(6.023E23\ \text{Molec.})}{(1\ \text{Mole})} \frac{(1\ \text{Mole})}{(22414\ \text{ml STP})} \frac{(1E{-}20\ \text{m}^2)}{(1\ \text{Å}^2)} = 4.37\ \text{m}^2/\text{ml } O_2$$

3.4 TOTAL SURFACE AREA MEASUREMENT

3.4.1 CARBON DIOXIDE PHYSISORPTION

Surface areas determined by nitrogen and CO_2 adsorption differ in carbons possessing ultra-fine structures (pores with entrances less than 4.2 Å) [50]. Nitrogen is unable to diffuse through the small openings at 77°K in a reasonable time, making analysis difficult. The use of CO_2 at higher temperatures is much more likely to give accurate results than nitrogen at 77°K. A temperature of 273°K or 293°K is better than 195°K for CO_2 physisorption [51] because adequate isotherm coverage at can take weeks at 195°K, but takes less than a day at 273°K or 293°K. Past researchers [51] compared the applicability of the Dubinin equation versus BET theory for surface area measurements of carbon samples, and found that the Dubinin equation gives a better representation of the surface area of carbons than the BET equation.

Carbon dioxide physisorption at 293°K was conducted in a Sartorius Model 4436 Electronic Microbalance to find total char surface area. The apparatus consists of the microbalance, a Heath-Zenith model SR-20R strip chart recorder, a vacuum pump (Cenco-Megaval GM-1917), and assorted pressure gauges. Figure 3.2 shows the complete system.

Prior to analysis, chars were outgassed under vacuum at 150°C in the balance to remove water and other weakly bound contaminants which occupy some of the pore volume. These contaminants cause erroneously low surface areas if they are not removed.

FIGURE 3.2. HIGH PRESSURE MICROBALANCE

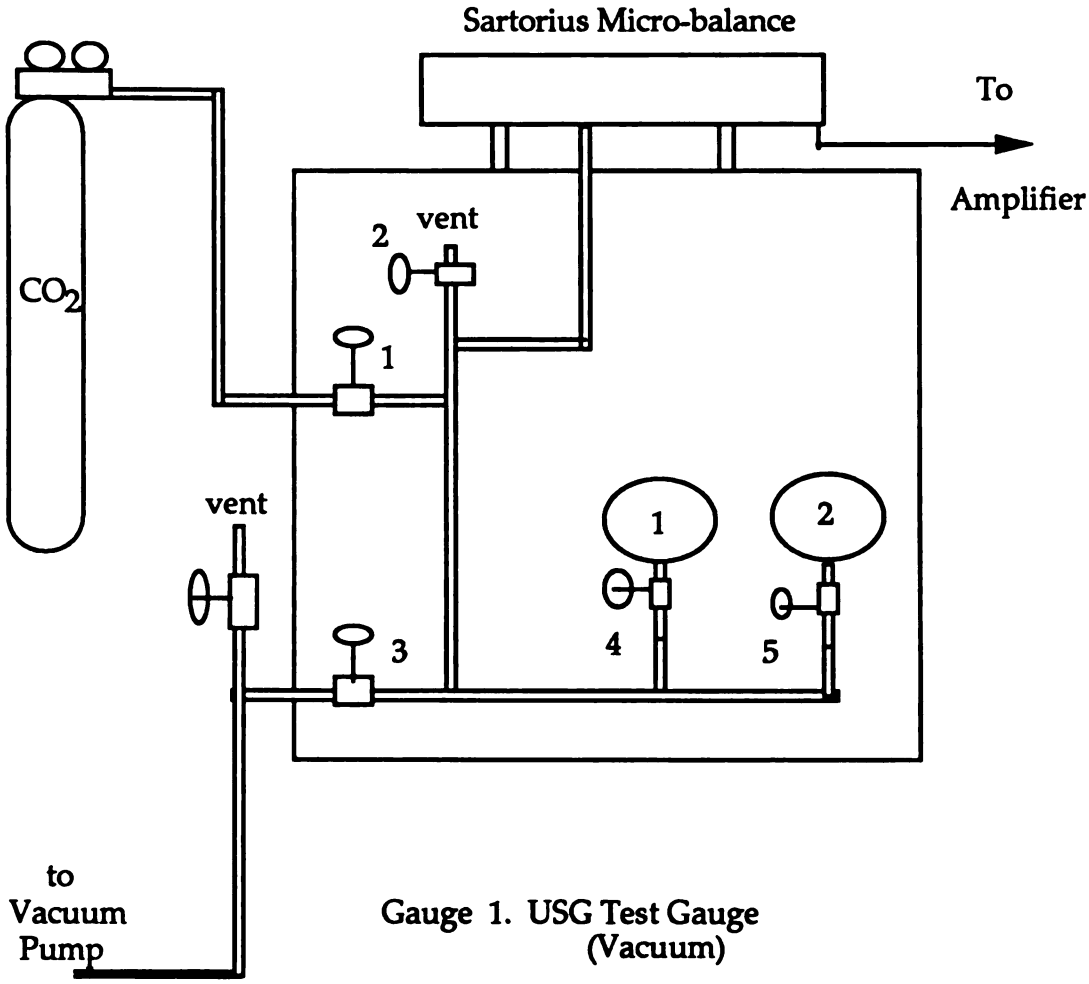

Gauge 1. USG Test Gauge
(Vacuum)

Gauge 2. Matheson No. 63-5652 Test Gauge
(High Pressure)

The basic procedure for determining the total surface area is as follows:

1) Fill the quartz sample boat with approximately 50mg of char.
2) Load sample boat onto the microbalance, seal the system (close valves 1, 2, 3, and 5) and wait until the balance stabilizes (2-4hr).
3) Start the vacuum pump and zero the balance.
4) Open valve #3 slowly to pump down the system. When the pressure is less than 1 torr, heat the sample to 150°C. When the sample stops losing weight (approximately 30 minutes), quench the sample to room temperature in a water bath.
5) When the temperature stabilizes (18-22°C), close valve #3, record the total char weight loss and the bath temperature, and rezero the balance.
6) Open valve #1 slowly to add CO_2 to the system in predetermined pressure increments. Record the total weight gain of the sample at each pressure. Typical pressures at which readings were taken are: 200, 500, 1000, and 1500 torr and 30 and 50 psig.
7) When the system pressure reaches 1500 Torr, close valve #4 and open valve #5 to take the high pressure readings.
8) When all readings are complete, slowly open valve #2 to vent the system. Open the system and replace the sample.

The Dubinin-Radushkevitch method [52] was used to analyze the data and find the total surface area. A brief description of the method follows:

1. Find the monolayer volume W_o of the CO_2 adsorbed on the sample by plotting log W versus $\log^2 (P_o/P)$ and locating the intercept ($\log W_o$).

$$\log W = \log W_o + \log^2(P_o/P)$$

Where:

W = Volume of CO_2 adsorbed on sample.

W_o = Monolayer volume of CO_2 adsorbed (micropore volume).

P = Pressure corresponding to sample weight

P_o = CO_2 saturation pressure.

2. Find the total surface area (m^2/g) of the sample. In this calculation it is assumed that one CO_2 molecule occupies 16.3Å2 on the carbon surface.

$$TSA = \frac{(Wo)}{(wt.\ of\ sample)}(N)(\rho_{co_2})\frac{(1\ g)}{(1000mg)}\frac{(1\ mole)}{(44\ g)}\frac{(16.3\ Å\text{^}2)}{(1\ molec)}\frac{(1E-20\ m\text{^}2)}{(Å\text{^}2)}$$

Where:

N = Avogadro's number (6.023E23 molecules/mole).

ρ_{CO_2} = Liquid density of CO_2 at STP(1.9768mg/ml).

3.4.2 NITROGEN PHYSISORPTION

The Pulse Chemisorb 2700 can also be used to determine the total surface area of a sample via nitrogen physisorption. A suggested procedure follows:

Nitrogen Physisorption to Find Total Surface Area

1. Prepare sample by heating to 120°C under helium for 30 minutes and then quench to room temperature.
2. Set nitrogen/helium mixture 5% nitrogen/95 % helium.
3. Set relative condition to positive and zero peak area meter.
4. Place liquid nitrogen bath around the sample and take peak area reading when counting stops.
5. Set relative condition to negative and zero peak area meter.
6. Remove liquid nitrogen bath and place a room temperature water bath around the sample to desorb the nitrogen.
7. Take peak area reading when the counting stops.
8. Repeat the procedure at higher nitrogen concentrations, usually 10% N_2 and 20% N_2.
9. Calculate the B.E.T. surface area using the same standard BET equations.

Chapter 4
Results

4.1 HYDROGASIFICATION

All of the hydrogasification experiments reported here were conducted at 725°C and 500psig unless otherwise noted. Lussier conducted all of the hydrogasification experiments and provides more details regarding them in his thesis [53].

The hydrogasification rate for all of the samples was highest at the point at which the steady state temperature was reached and rapidly decayed as the sample was converted. The steady state rate of the coal char and Saran char was initially 4.0cc CH_4/min*g carbon and decayed to less than 1cc CH_4 /min*g carbon. The demineralized (PDP) coal char rate was 2.8cc CH_4/min*g carbon at steady state and decayed to 1.2cc CH_4/min*g carbon. Figure 4.1 gives a comparison of hydrogasification rates versus percent carbon conversion for the three samples.

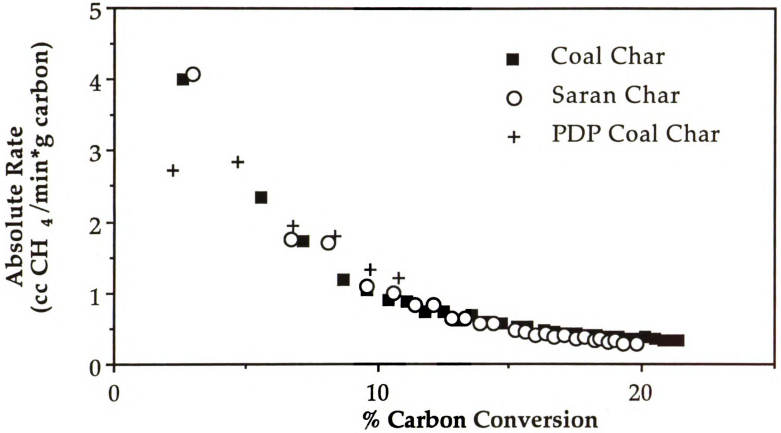

Figure 4.1 Hydrogasification Rate of Prepared Samples at 725 °C and 500psig H_2

4.1.1 REACTION RATES

The first set of hydrogasification experiments were performed at several different temperatures to determine the activation energy of the reaction and to identify the kinetic and mass transfer limited regions. Figure 4.2 shows the Arrhenius plot for coal char reacted at temperatures ranging from 700°C to 775°C. The activation energy of 302kJ/gmol indicates that the reaction is free of mass transfer resistance in this temperature range. A reaction temperature of 725°C was chosen because at this temperature, the hydrogasification reaction is truly limited by kinetics.

4.1.2 EFFECT OF HYDROGASIFICATION ON TOTAL SURFACE AREA

The change in the total surface area (TSA) of the chars was measured using CO_2 adsorption as a function of conversion in hydrogasification. The TSA of the coal chars was not drastically influenced by hydrogasification, and over a range of 34% carbon conversion varied by only 13% (Figure 4.3). The TSA of the initial coal char was 274m^2/g and the TSA of the char gasified to 34% conversion was 295m^2/g. The TSA was highest (313m^2/g) on the char gasified to 9.8% conversion, indicating that a slight opening of the pore structure may be occurring during initial stages of hydrogasification. A summary of the TSA of the starting samples and partially gasified samples is shown in Table 4.1.

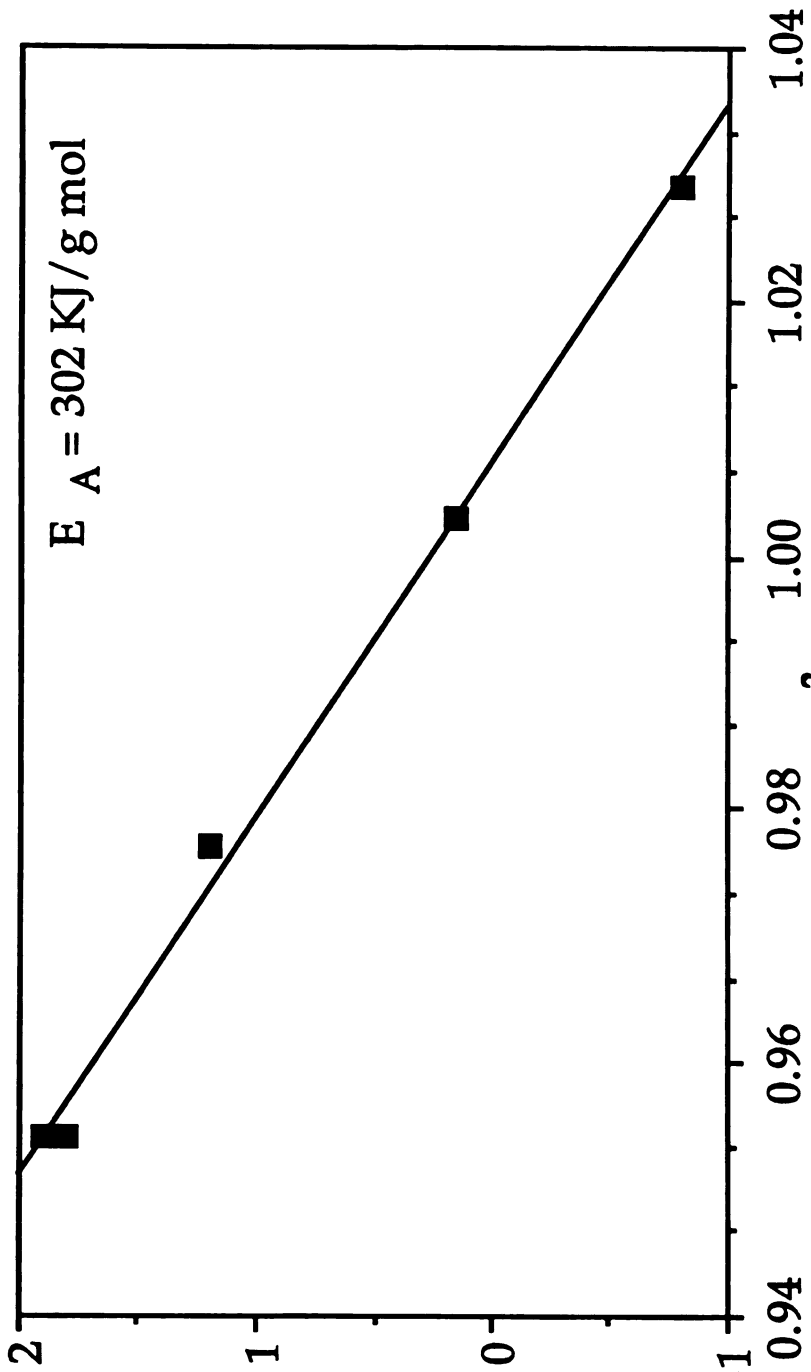

Figure 4.2 Arrhenius Plot for Coal Char

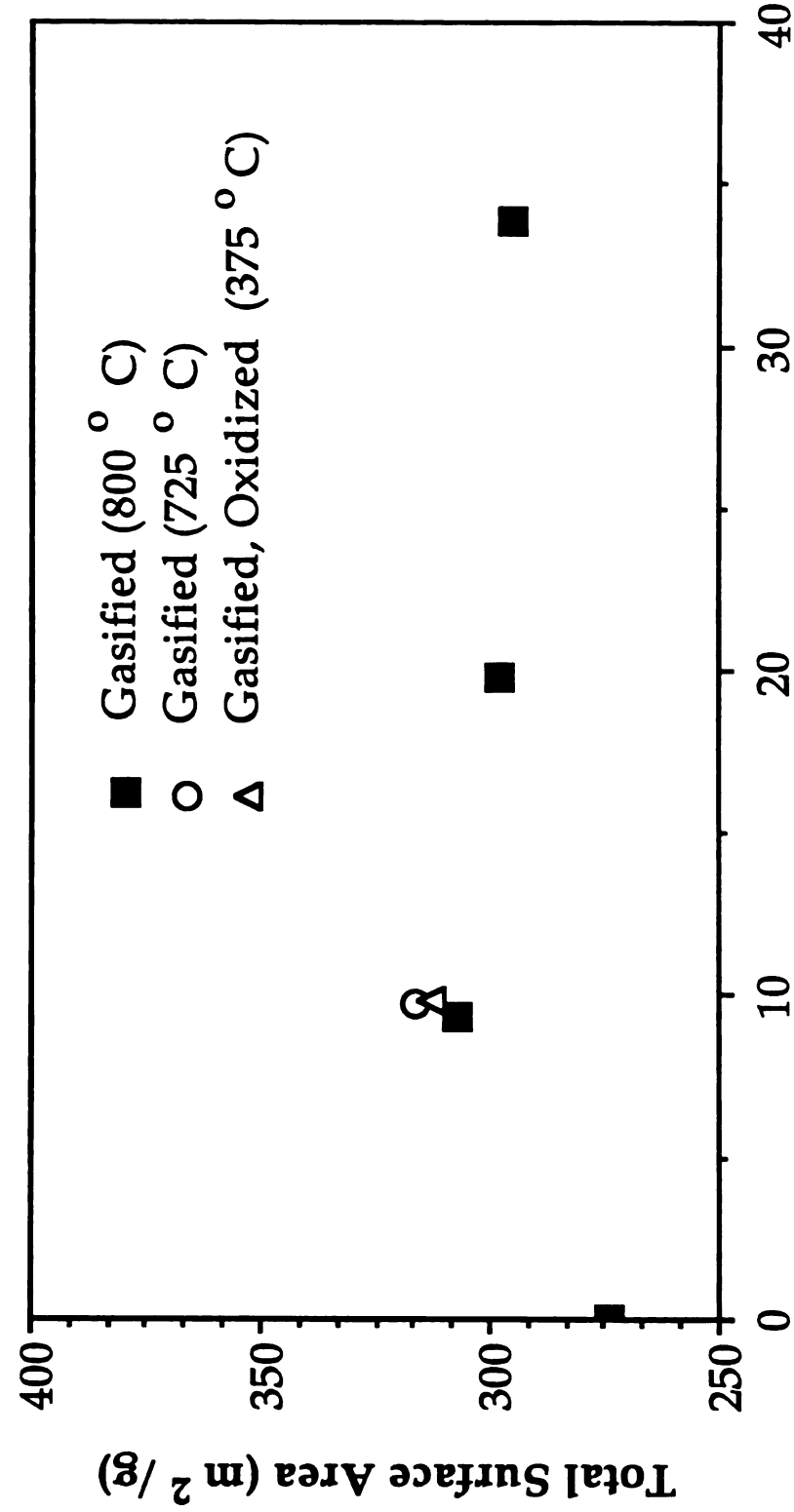

Figure 4.3 Change in Total Surface Area of Coal Char with Carbon Conversion during Hydrogasification

Table 4.1 Comparison of the TSA of Initial and Gasified Samples.

Sample	TSA (m^2/g) Initial	TSA(m^2/g) Gasified
Coal Char	274	313
Saran Char	816	754
PDP Coal Char	322	363

Initial TSA experiments were conducted on samples that were gasified at 800°C. To confirm that TSA was not affected by hydrogasification temperature, TSA was also measured on samples reacted at 725°C. As seen in Figure 4.3, the difference in TSA of a sample gasified at 800°C and 725°C is negligible.

4.2 SURFACE CHARACTERIZATION

4.2.1 SURFACE ΔpH OF CHARS

The surface nature (acidic/basic) of the samples is reported as the change in pH (ΔpH) between a suspension of the sample in 0.1 M KCl and a standard 0.1 M KCl solution. Pyrolyzing, demineralizing and then pyrolyzing the coal char (PDP) not only removes metal contaminants and dries the sample, it also changes the ΔpH of the sample. The initial treatment reduces

the change in sample pH from ΔpH=4.55 for the pyrolyzed coal char to ΔpH=-0.63 for the PDP coal char (Table 4.2).

Table 4.2 Summary of the ΔpH of Initial and Partially Gasified Chars.

Sample	ΔpH Initial	ΔpH Gasified
Coal Char	4.55	3.46
Saran Char	-0.44	2.70
PDP Char	-0.63	3.17

Hydrogasification had a strong effect on surface ΔpH. The sample ΔpH of the initial coal char was ΔpH=4.55 and as this sample was gasified, the ΔpH decreased to 3.46. This indicates the surface is still highly basic. Based only on the coal char, it seems that gasification makes the surface more acidic; however, this is not generally true. Both the Saran char and the PDP coal char become much more basic following gasification. For all three samples, the gasified char surface is extremely basic in nature.

4.2.2 SURFACE OXYGEN CONCENTRATION

Initial surface oxygen contents of the three starting materials were determined via XPS analysis. The concentration of surface oxygen is reported as the ratio of surface oxygen atoms to surface carbon atoms (O/C ratio). The oxygen concentration is adjusted to eliminate oxygen that is strongly bound in SiO_2, Al_2O_3, and SnO_2. The initial O/C ratios were 0.06 for the coal char, the PDP coal char, and the Saran char. As the coal char is heated to gasification temperature (725°C), XPS analyses show that excess oxygen desorbs from the surface, leaving an oxygen content equivalent to that of the bulk sample (Figure 4.4). Although XPS is considered a surface analysis technique, it actually gives a weighted average of about a 30Å layer of the bulk. Therefore, the least amount of surface oxygen detected will be the approximate bulk level.

4.2.3 TEMPERATURE PROGRAMMED DESORPTION

Temperature programmed desorption (TPD) is another technique used to determine if the surface is cleansed of oxygen during the heat-up to reaction temperature (725°C). This method measures the total amount of all gaseous species desorbed from the sample during heat-up, and it identified two temperature zones where gaseous species desorb from the sample. The first zone occurs from ~200°C to 400°C and the second zone occurs from ~575°C to 900°C.

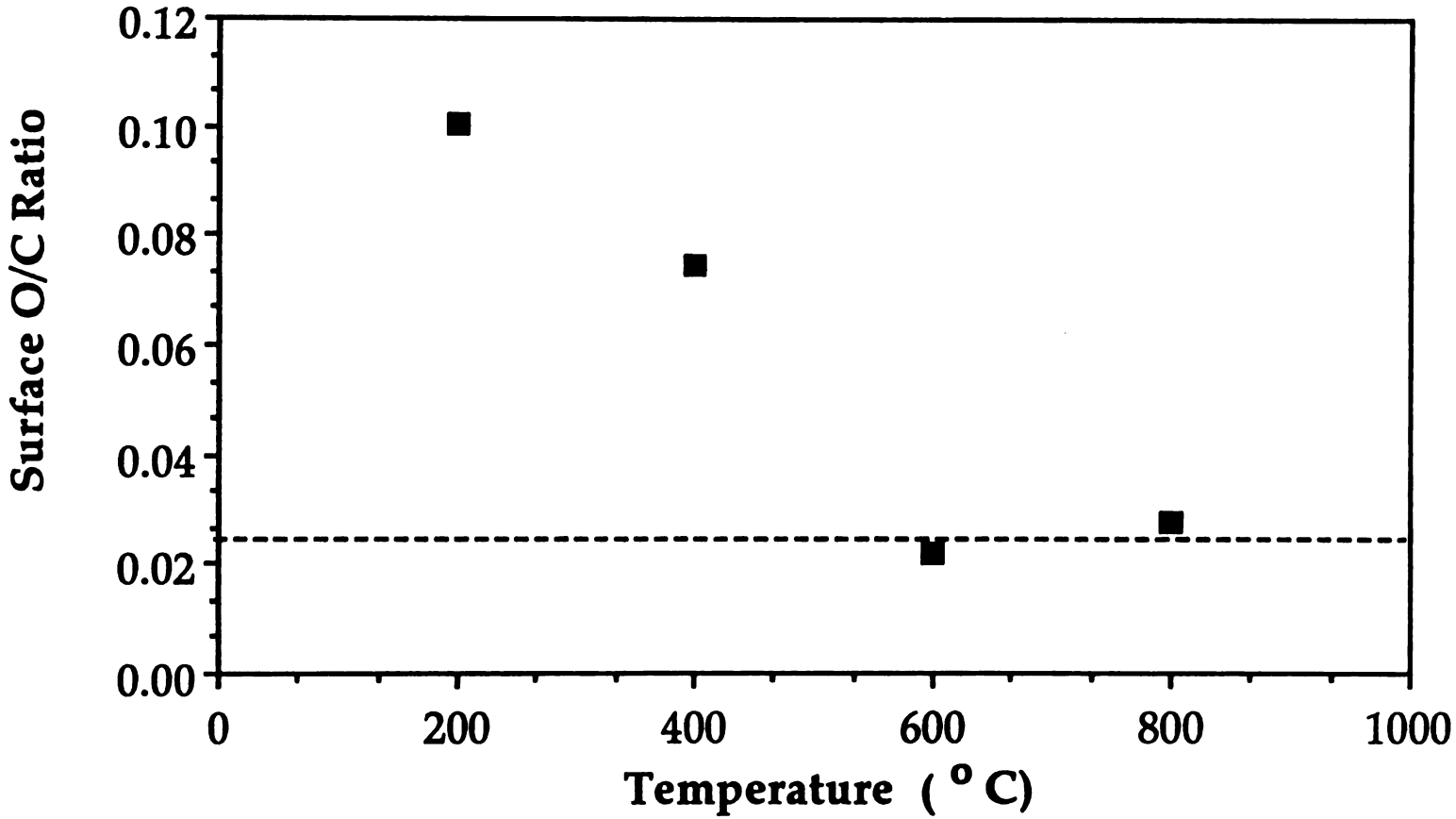

Figure 4.4 XPS Results for As Received Coal Char Heated to Gasification Temperature

Temperature programmed desorption showed that the hydrogasification temperature is in the middle of the second desorption zone. Figures 4.5 and 4.6 show the TPD profiles of the coal char and Saran char respectively.

4.2.4 ASA DETERMINATION

The ASA of each sample was determined by first outgassing it at the hydrogasification temperature in helium, then conducting oxygen chemisorption at 295°C. The gasification temperature was used in outgassing to make available the same ASA that is available during reaction. This is not necessarily the total ASA of the sample because outgassing at higher temperatures and for longer periods of time may lead to higher ASA. The additional area, however, would not be available during hydrogasification so it would not be a good indicator of the sample reactivity. This is evident by the TPD results discussed above (Figures 4.5 and 4.6). The gasification temperature (725°C) is in the middle of the second zone, so any ASA resulting from oxygen desorbing from the upper half of this zone (T>725°C) would not be available during hydrogasification.

To further investigate the dependence of ASA on pretreatment temperature, the ASA for each sample was determined for various temperatures up to 950°C. This was to determine the ASA and how much of the total ASA comes from acidic and/or basic oxygen groups. These results are listed in Table 4.3 and show that approximately half of the total available ASA of the samples come from acidic groups and half from basic groups.

Temperature programmed desorption (TPD) showed that the acidic groups on the coal char have a lower activation energy than those on the

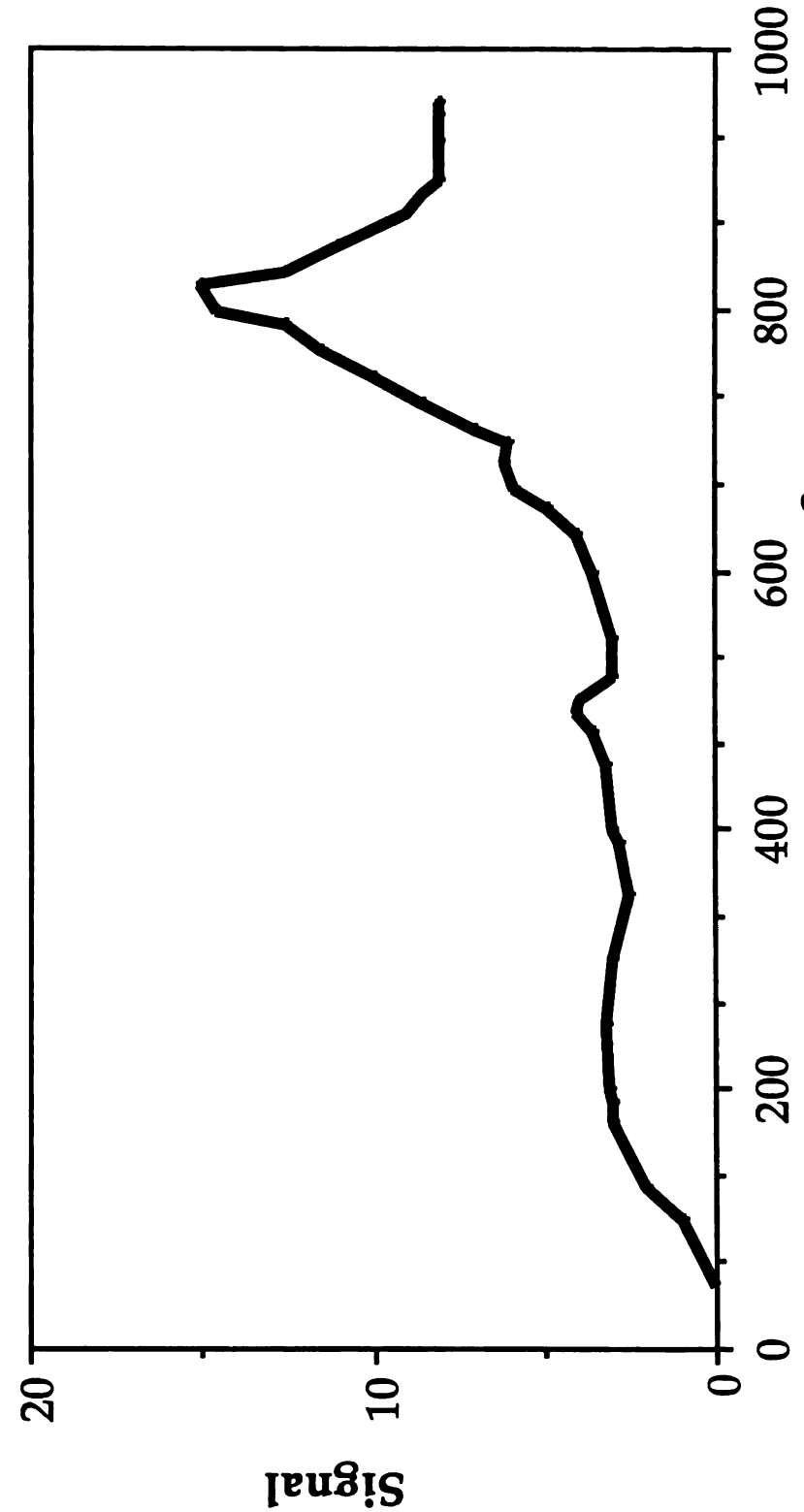

Figure 4.5 Total Gas Desorbed During Temperature Programmed Desorption of Coal Char

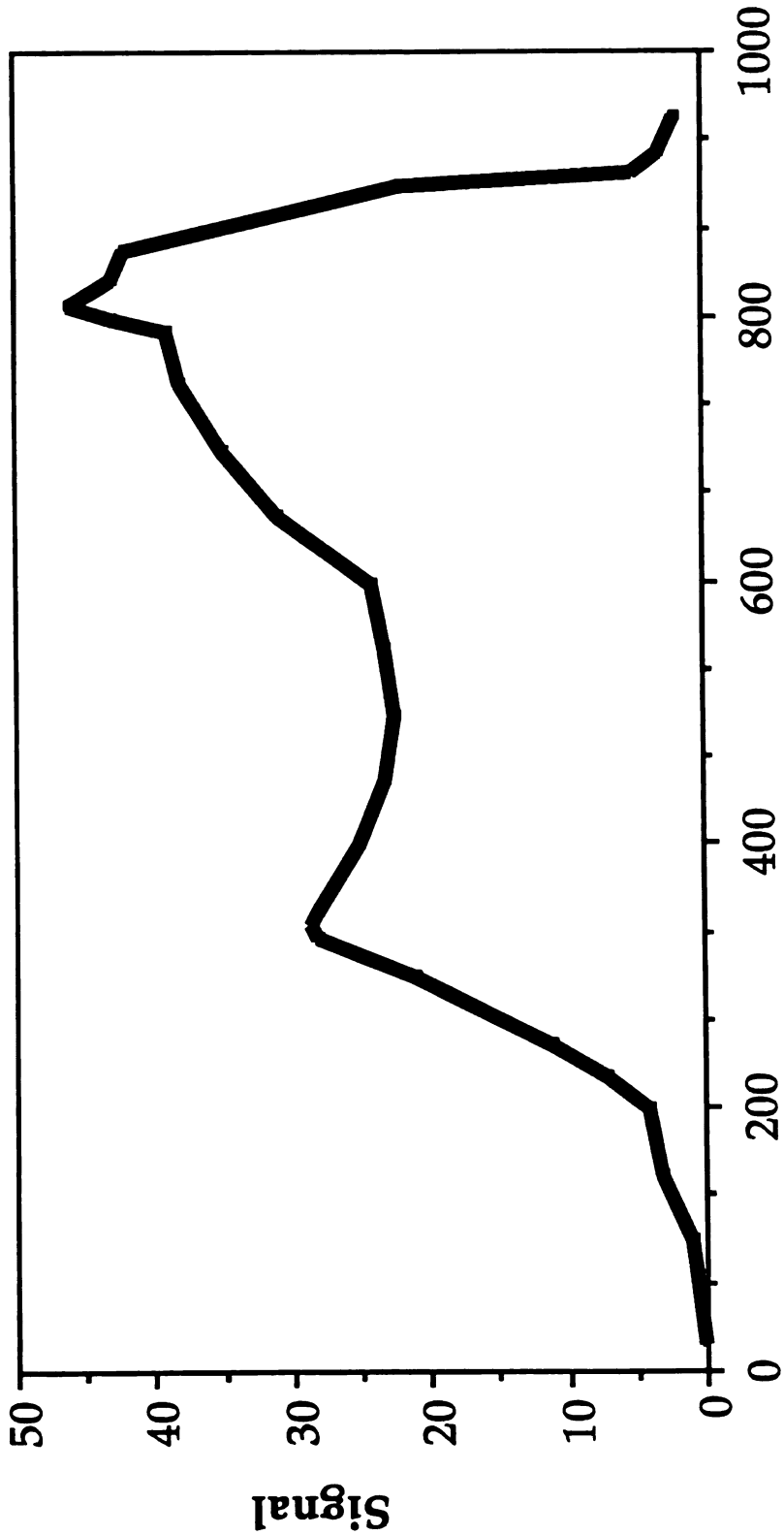

Figure 4.6 Total Gas Desorbed During Temperature Programmed Desorption of Saran Char

Saran char. The acidic groups on the coal char were almost completely desorbed by 250°C, while the acidic groups on the Saran char did not fully desorb until 450°C. This is also evident by the measured ASA. There was no change in the ASA of the coal char between 295°C and 450°C, while the ASA of the Saran char increased by over four-fold in this region.

At temperatures above 900°C, the coal char sinters, leading to a drastic reduction in both the total surface area and the active surface area of the sample. The Saran char does not exhibit signs of this phenomena, and thus can be used more reliably to determine the ASA contributions of the basic oxygen groups at elevated temperatures.

Table 4.3 Active Surface Area at Increasing Temperatures

	Sample	
	Coal Char	Saran Char
Temperature (°C)	ASA* (m^2/g)	ASA* (m^2/g)
295	1.4	0.68
450	1.4	2.92
725	3.0	7.4
950	1.5	7.2

* Note, these ASA were determined using a special, extended sample tube.

One further consideration in determining ASA is a possible dependence of ASA on sample particle size. The Saran char used in the above analysis has a smaller particle size (100-200 mesh) than the Saran char size (60-100 mesh) used in the majority of the experiments. Using the same tube, the ASA of the 60 to 100 mesh Saran char was $3.2 m^2/g$ at an outgassing temperature of 725°C versus $7.4 m^2/g$ for the 100-200 mesh Saran char. This

value is lower than the ASA measured using the first technique described in Section 3.3.3.3, but it is consistent with the coal char ASA using the extended U-tube. Both the coal char and the Saran char have ASA approximately equal to 4.0m^2/g using the normal method and both are approximately 25% lower using the special sample tube.

There were several problems in finding a definitive value for the ASA of the chars. The ASA measurement depends on the size of the sample evaluated, the sample tube used, the resonance time of the oxygen pulse, and the size of the particles in the char. Increasing the resonance time of the oxygen pulse will lead to higher measured ASA values. Oxygen chemisorption on the chars seems to limited by diffusion into the pores. The longer resonance time, either by increasing the downstream pressure or by using a larger diameter U-tube, will lead to higher measured ASA values. The GC raised the downstream pressure to 950 torr and this method gave the largest ASA values; up to two-fold increase over the other methods.

The change in active surface area with carbon conversion may explain why the hydrogasification rate rapidly decreases with conversion. Also, if the ASA can be increased with oxidation, the hydrogasification rate should also increase. Currently, the ASA measurements do not provide definitive values for the ASA of the chars, but they can be used to compare the changes in ASA with different treatments. Figure 4.7 compares the change in ASA with carbon conversion during hydrogasification for two different measurement techniques. The standard tube refers to a short U-tube and the stopcock tube refers to a U-tube with two stopcocks forming a bridge between the legs of the tube. This tube allows the sample to be isolated from air during transfer. The standard tube also was used with the GC attached downstream so the downstream pressure was ~950 torr. This increase in pressure increased the

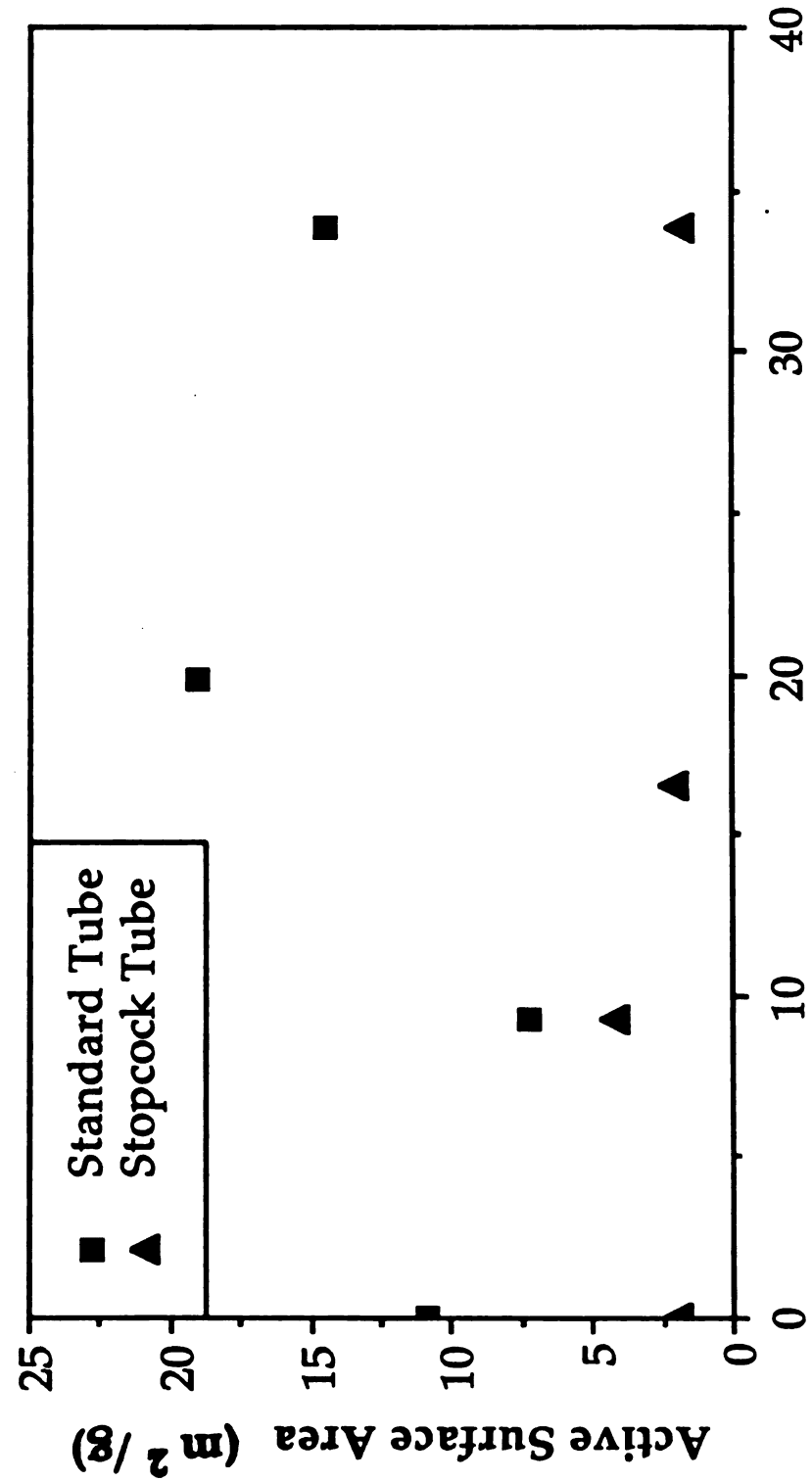

Figure 4.7 Change in ASA of Coal Char with Hydrogasification for Different Sample Tubes

resonance time of the oxygen pulse and aided in overcoming the diffusion limitations. The results from the ASA measurements shown in Figure 4.7 are too erratic to give a definitive answer to how the ASA changes with conversion, but they are useful in showing the differences between the different measurement techniques. Some of the differences in the results may be due to subtle differences in the hydrogasification runs. These data came from early experiments so the experimental technique may not have been perfected.

In addition to learning how the ASA changes with conversion, determining how the ASA changes with intermittent oxidation is also important. Understanding how the ASA is affected by gasification and oxidation may lead to a useful parameter for characterizing a char reactivity. Figure 4.8 shows the change in ASA for the intermittent oxidation of coal char. These values are higher than those reported elsewhere in this thesis because they were conducted before the measurement technique was finalized. The values are useful, however, because they show relative changes in the ASA for the oxidized coal char. The expected trend is apparent through the second gasification; however, the second oxidation and third gasification seem to be transposed. Like the results described in Figure 4.7 these gasification results were from early hydrogasification runs so some of the error may be due to differences in the gasification experiments.

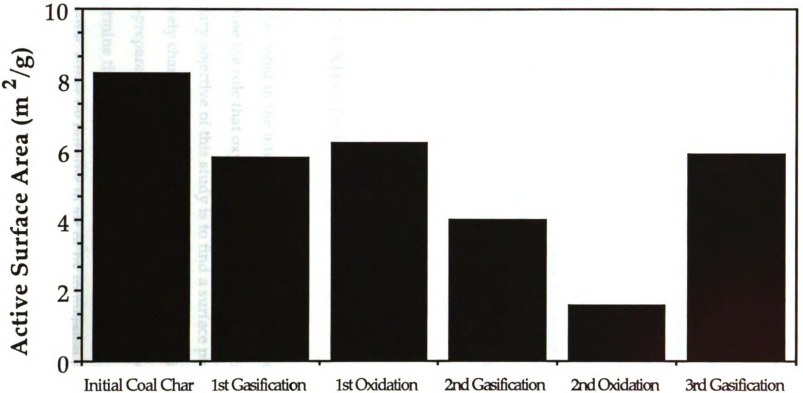

Figure 4.8 Change in ASA of Coal Char with Hydrogasification and Intermittent Oxidation

4.2.5 OUTGASSING PRIOR TO HYDROGASIFICATION

Experiments were performed in which both coal char and Saran char samples were outgassed at 1000°C for 12 hours in vacuum. This procedure cleans most of the oxygen from the char surface and anneals the surface sites. Outgassing the samples reduced the amount of surface oxygen on the coal char by approximately 80% and on the Saran char by approximately 35%.

Outgassing had a more significant effect on the hydrogasification rates. The initial steady state rate of the coal char decreased by 80% and the rate of the Saran char decreased by 82%. Figures 4.9 and 4.10 show the comparative hydrogasification rate curves for the initial samples and the outgassed samples.

4.3 OXIDATION

As stated in the introduction, the main objective of this study is to determine the role that oxygen plays in hydrogasification of carbons. The secondary objective of this study is to find a surface parameter that will effectively characterize the sample reactivity and gasification rate of oxidized and as-prepared samples. Two methods of oxidation were used in this study to determine the effect of oxygen on hydrogasification rate; preoxidation of the sample, either by burning in air or by immersion in HNO_3, and intermittent oxidation of the sample, by burning in air only.

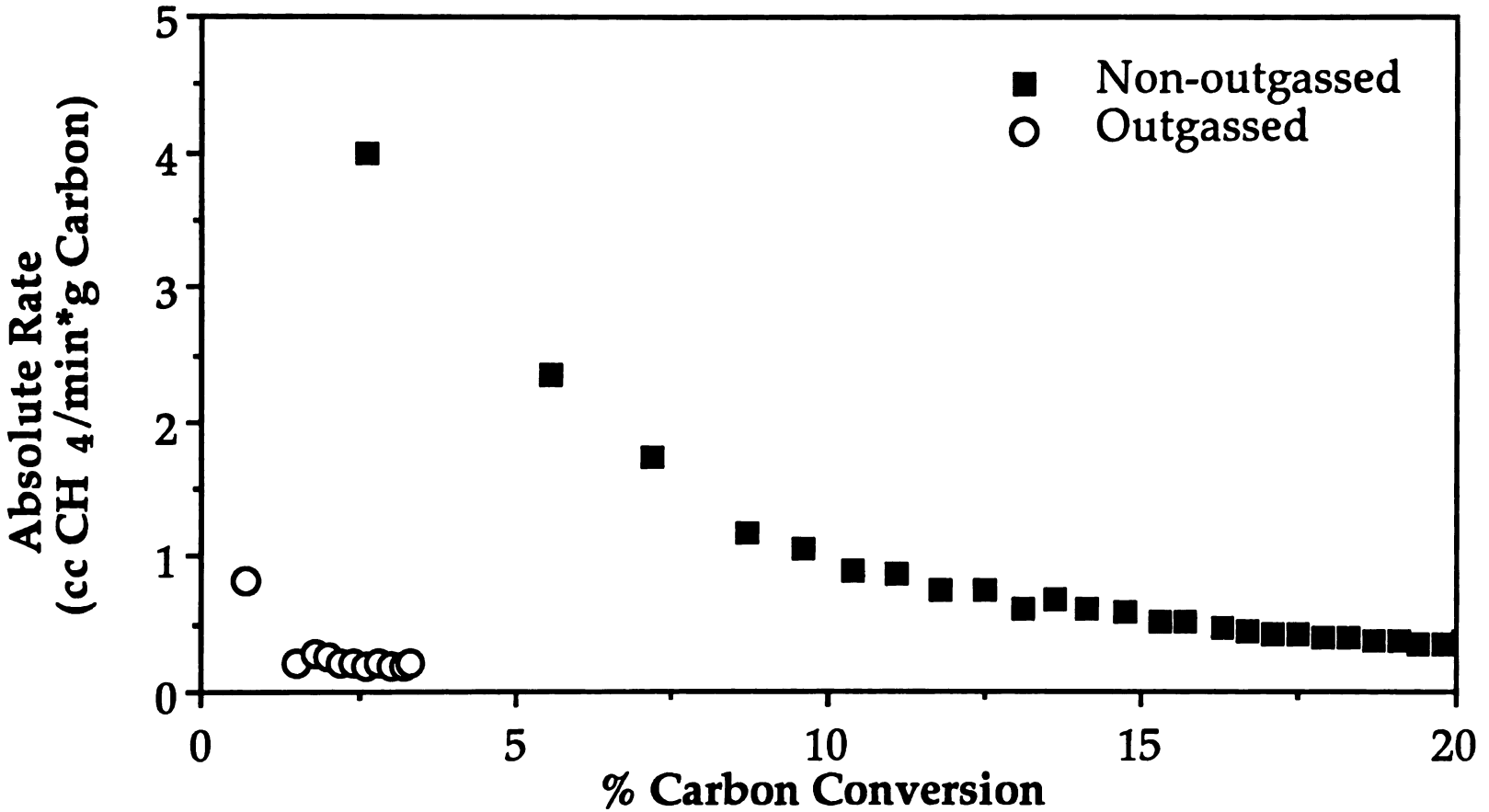

Figure 4.9 Effect of Outgassing at 1000 ^{o} C on the Hydrogasification Rate of Coal Char

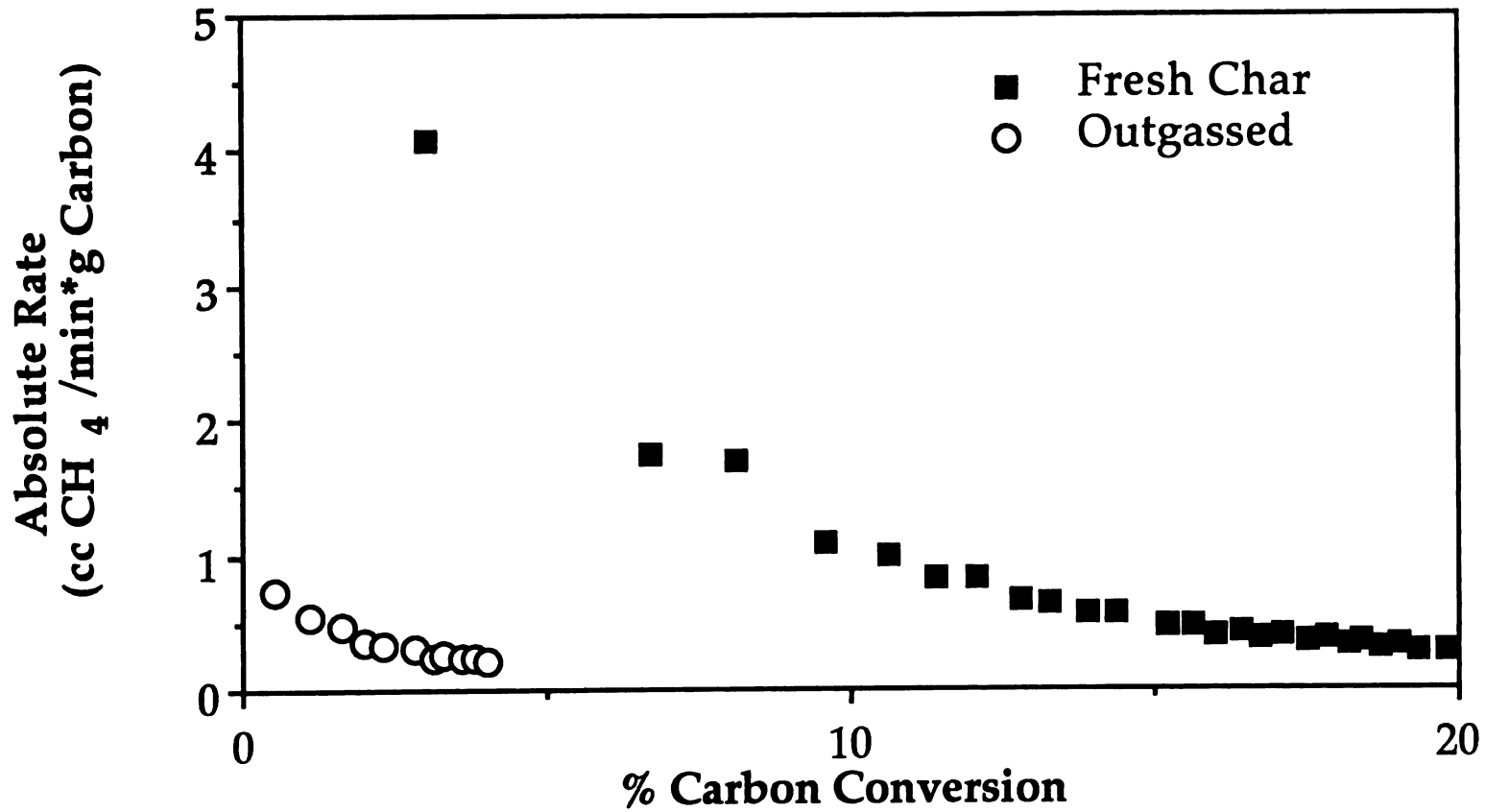

Figure 4.10 Effect of Outgassing at 1000° C on the Hydrogasification Rate of Saran Char

4.3.1 PREOXIDATION

A. BURNING IN AIR

Preoxidation of the samples was used to determine if increasing the initial amount of surface oxygen present on the char surface would have a significant effect on gasification rate. It was also used to provide some insight into what type of oxygen groups (ie. carboxyl, phenolic, carbonyl, etc.) are beneficial to the reaction.

As stated above, two different methods of preoxidation were used to prepare the samples. The first method was to burn the samples in limited amounts of air at 375°C for different time durations. The samples are classified by the percent weight loss during oxidation, which is related to the severity of oxidation. It is well known that oxidation in air at 375°C puts mostly acidic oxygen groups onto the surface; this was confirmed via surface pH measurements and via XPS, which showed a shift in the C1s peak corresponding to the presence of carboxylic acid groups.

All three starting materials were used to determine the effect of preoxidation. As shown in Figure 4.11, preoxidizing coal char by burning in air at 375°C has little effect on the absolute hydrogasification rate. The coal char gasification rate varies by less than 8% at both the steady state gasification rate and the 5% conversion gasification rate. A more severe preoxidation of the coal char (at 725°C) also showed no rate enhancement.

The demineralized coal char (Figure 4.12) appears to show a slight rate enhancement at the steady state point; however, this enhancement is not present at 5% conversion and may be an anomalous result caused by the

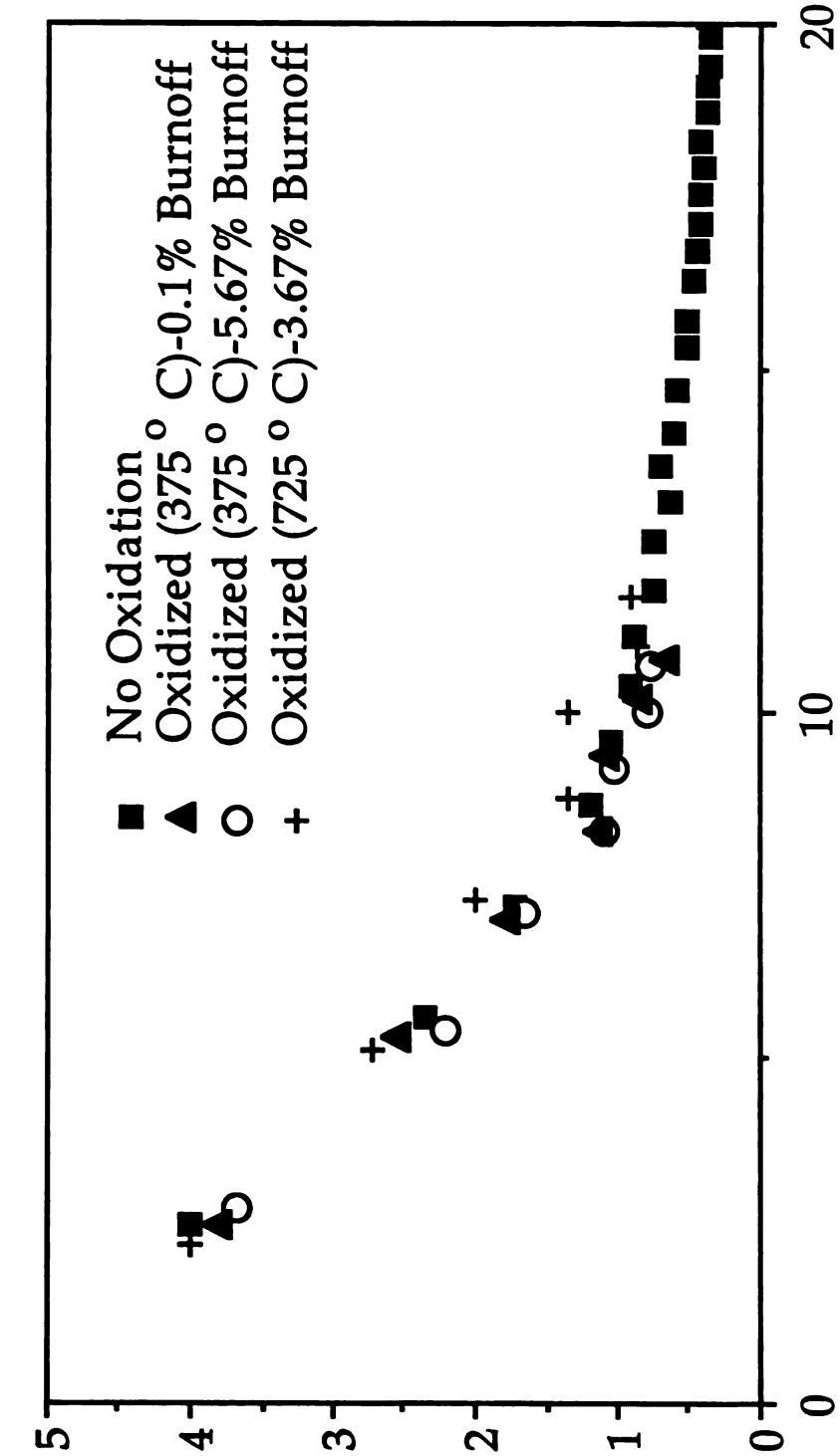

Figure 4.11 Effect of Preoxidation on the Hydrogasification Rate of Coal Char

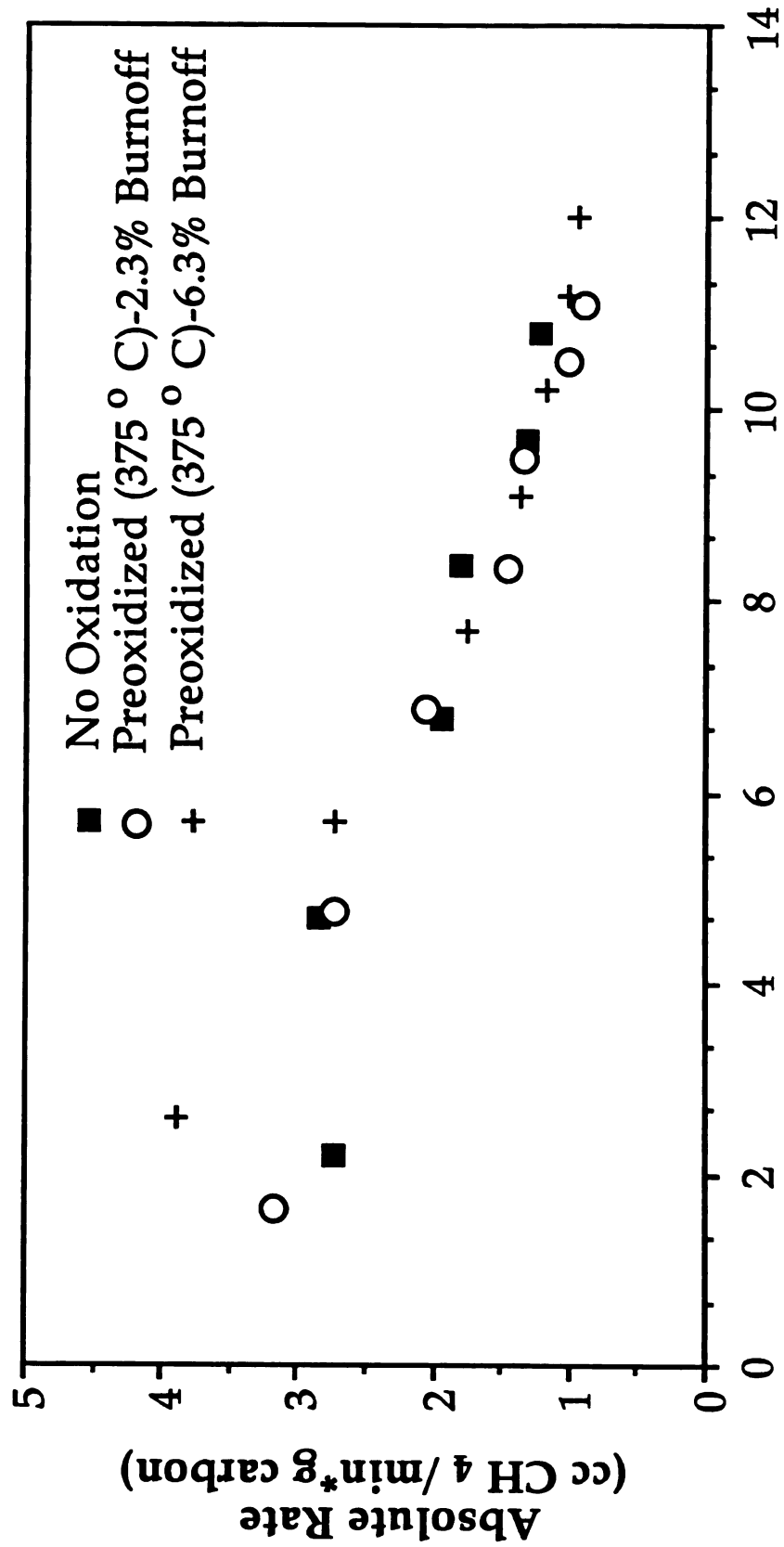

Figure 4.12 Effect of Preoxidation on Hydrogasification Rate of Demineralized Coal Char

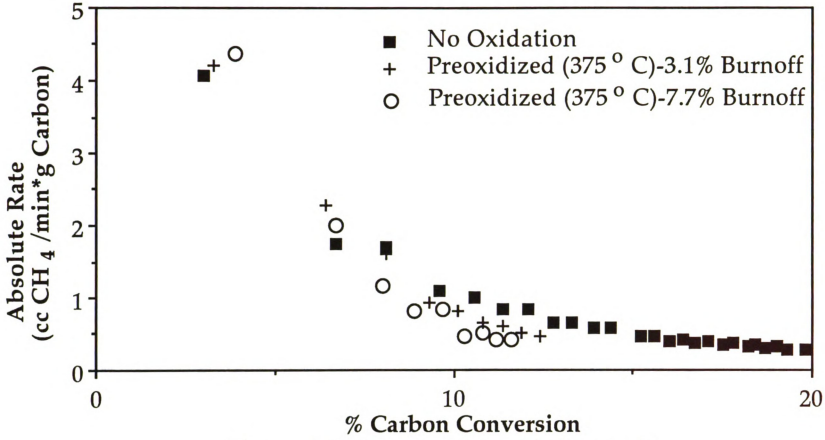

Figure 4.13 Effect of Preoxidation on the Hydrogasification Rate of Saran Char

difficulty in obtaining the initial steady state point. This is explained in more detail by Lussier [53]. Preoxidation of the Saran char (Figure 4.13) also has no effect on the rate.

Based solely on the hydrogasification rates, it may seem that preoxidation does not affect the sample. However, as shown in Table 4.4, preoxidation of the coal char increases the amount of surface oxygen by 30% and decreases the pH of the surface from very basic (ΔpH=4.55) to acidic (ΔpH=-1.66). The more severely oxidized coal char (725^{o}C) had a 10% increase in surface oxygen, but these groups were generally basic in nature (ΔpH=2.88).

Preoxidizing by burning in air increases the ASA of the PDP coal char and the Saran char, but it does not enhance the reaction rate. This increase in ASA shows that oxidation does increase the ASA, yet the increase in the ASA does not affect the hydrogasification rate of a fresh sample.

B. OXIDATION WITH NITRIC ACID

The second method of preoxidation was by contacting with an aqueous solution of 70% nitric acid for approximately twelve hours. This method was only performed on the coal char . Nitric acid oxidation increases the amount of surface oxygen by more than 50% but there is no significant change in the absolute hydrogasification rate (Figure 4.14).

The most dramatic effect of this method of preoxidation is the large decrease in the active surface area of the coal char from 4.0m^2/g initially to 1.5m^2/g. This dramatic decrease may be caused by a demineralization of the

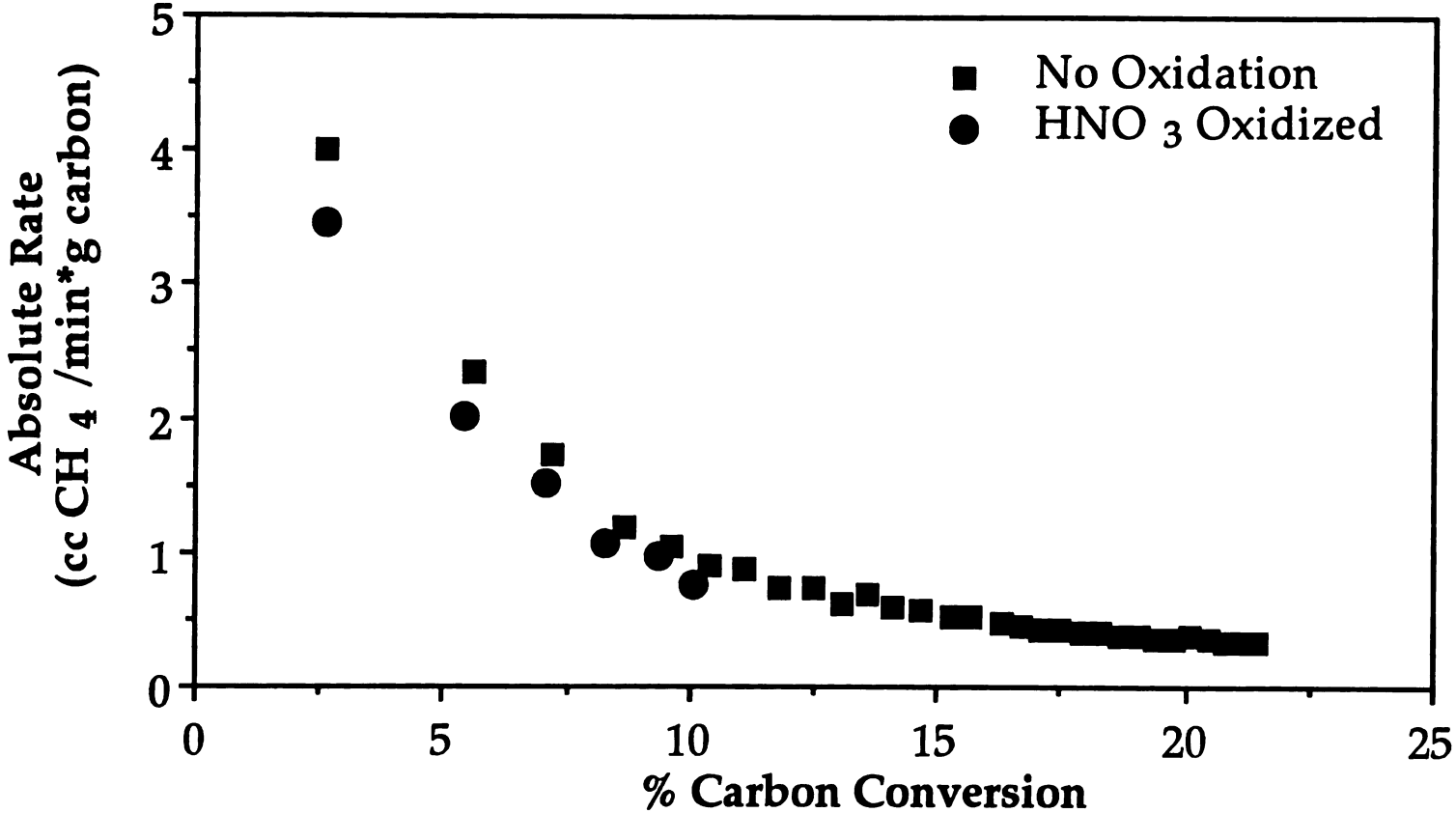

Figure 4.14 Effect of Preoxidation Via Contacting with HNO_3 on the Hydrogasification Rate of Coal Char

coal char. The PDP coal char had approximately the same decrease in ASA. The large increase in acidity of the HNO_3 oxidized coal char (ΔpH=-2.27) either confirmed that the increase in surface oxygen came from the addition of acidic oxygen groups or was caused by some nitric acid left in the pores after the char was rinsed.

Table 4.4 Effect of Preoxidation on the Surface Nature of Coal Char and Saran Char.

SAMPLE	O/C RATIO	ΔpH	ASA (m^2/g)
Coal Char	0..062	4.55	4.0
-Preoxidized Coal Char			
0.1% Mass Burnoff (375°C)	0.052	0.82	NA
5.67% Mass Burnoff (375°C)	0.128	-1.66	NA
3.67% Mass Burnoff (725°C)	0..093	2.88	NA
-HNO_3 Preoxidized Coal Char	0..007	-2.27	1.5
Demineralized Coal Char	0.066	-0.63	1.3
-Preoxidized, Demin. Coal Char			
2.3% Mass Burnoff (375°C)	0.094	-1.29	6.9
6.3% Mass Burnoff (375°C)	0.092	-2.75	6.7
Saran Char	0.066	-0.44	4.0
-Preoxidized Saran Char			
3.1% Mass Burnoff (375°C)	0.108	-2.54	6.1
7.7% Mass Burnoff (375°C)	0.152	-3.38	9.9

4.3.2 INTERMITTENT OXIDATION

Intermittent oxidation of the samples proved to be a more effective method of enhancing hydrogasification rates of all three types of samples. Oxidation was performed on samples that had already undergone hydrogasification to approximately 10% conversion by removing the sample from the reactor and burning it in air. The majority of the samples were burned in air at 375°C for various lengths of time, and one sample was oxidized at 725°C.

Hydrogasification of the Saran char results in more than a three-fold decrease in surface oxygen content and a 3.14 increase in the ΔpH. Intermittent oxidation of a gasified coal char replenishes the surface oxygen (Table 4.5) and changes the nature of the char surface. The original coal char was extremely basic; however, with oxidation, the char becomes almost neutral. This is a major decrease in the ΔpH and proves that the oxygen groups fixed by burning in air at 375°C are strongly acidic.

As shown in Figure 4.15 and 4.16, intermittent oxidation results in over a a two-fold increase in hydrogasification rate for both Saran char and coal char. This enhancement, however, decays rapidly back to the baseline gasification rate upon further conversion. Increasing the duration of the oxidation does not enhance the effect. This is evident in Figure 4.16, which shows the effect of a two hour oxidation compared to a half hour oxidation. The increase in oxidation time does not increase the rate enhancement. The oxidation temperature also does not seem to be a factor. Increasing the oxidation temperature to 725°C (Figure 4.17) did not affect the rate enhancement.

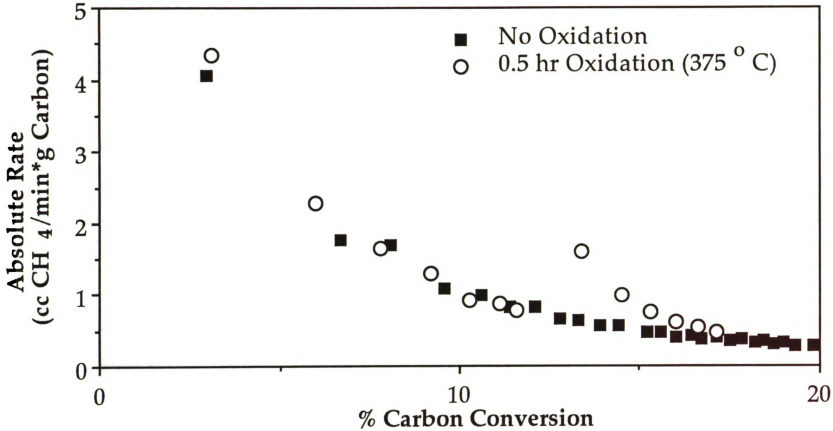

Figure 4.15 Effect of Intermittent Oxidation on the Hydrogasification Rate of Saran Char

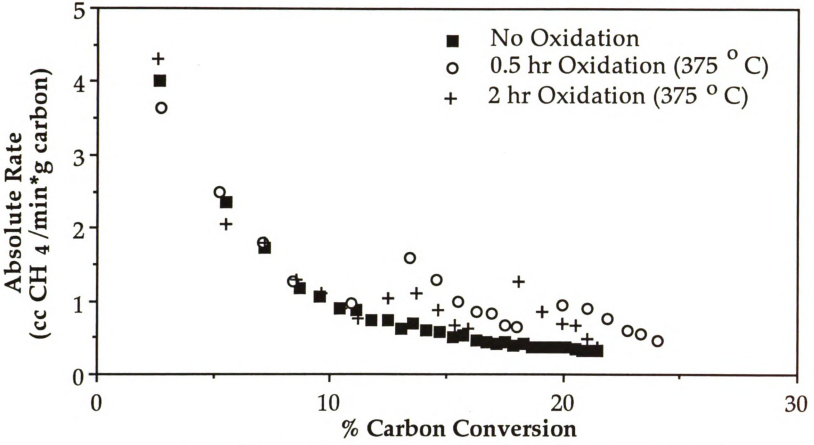

Figure 4.16 Effect of Two Intermittent Oxidations on the Hydrogasification Rate of Coal Char

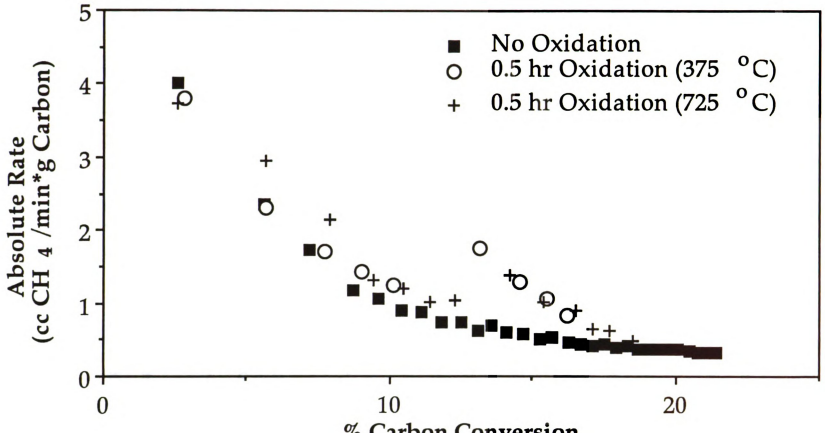

Figure 4.17 Effect of Intermittent Oxidation on the Hydrogasification Rate of Coal Char

The rate enhancement from intermittent oxidation seems to be limited either by extent of conversion before oxidation or by the number of times that the sample was previously oxidized. Figure 4.16 illustrates the rate enhancement for two successive oxidations and shows a lesser enhancement is achieved for the second oxidation.

Table 4.5 Effect of Intermittent Oxidation on the Surface Nature of Coal Char and Saran Char.

SAMPLE	O/C RATIO	ΔpH
Coal Char	0.062	4.55
-gasified (725°C)	0.052	3.46
-gasified, oxidized (375°C)	.NA	0.91

4.3.3 PREOXIDATION OF OUTGASSED SAMPLES

The effect of preoxidation by burning in air at 375°C on outgassed samples was also investigated. Unlike the as-prepared coal char and Saran char samples, preoxidation enhanced the hydrogasification rate of the outgassed samples.

The amount of surface oxygen on the outgassed samples following oxidation increased by approximately eight-fold for the coal char and almost two-fold for the Saran char. Preoxidation had a minor effect on the surface pH of the coal char, which changed from ΔpH=3.71 to ΔpH=2.92, and a major effect on the Saran char, for which ΔpH changed from .55 to -2.42 (Table 4.6).

Preoxidation of the outgassed samples had a major effect on the surface area of the samples (Table 4.7). The ASA of both the coal and Saran char increased by 50% while the TSA of the coal increased by 12-fold and the TSA of the Saran char decreased by 12%. The dramatic increase in the TSA of the coal char is due to opening of the coal pore structure. Coal char sintering during outgassing caused the majority of the pores to become blocked; these pores were reopened during oxidation when some of the carbon surface was burned away.

Table 4.6 Effect of Outgassing and Preoxidation on the Surface Nature of Coal Char and Saran Char.

SAMPLE	O/C RATIO	ΔpH
Coal Char	0.062	4.55
-outgassed (1000°C)	0.012	3.71
-outgassed, Preoxidized (375°C) .52% Mass Burnoff	0.100	2.92
Saran Char	0.066	-0.44
-outgassed (1000°C)	0.043	0.55
-outgassed, Preoxidized (375°C) .42% Mass Burnoff	0.080	-2.42

Table 4.7 Effect of Outgassing and Preoxidation on the Total Surface Area (TSA) and Active Surface Area (ASA) of Coal Char and Saran Char Samples.

SAMPLE	TSA (m^2/g Carbon)	ASA (m^2/g Carbon)
Coal Char	274	4.0
-outgassed (1000°C)	7*	0.6
-outgassed, Preoxidized (375°C) .52% Mass Burnoff	87	0.9
Saran Char	816	4.0
-outgassed (1000°C)	870	1.5
-outgassed, Preoxidized (375°C) .42% Mass Burnoff	762	2.3

* Determined by nitrogen BET.

Hydrogasification rates of both the outgassed coal char and outgassed Saran char were enhanced by preoxidation (Figures 4.18 and 4.19). The coal char rate was initially enhanced by ~160% but the rate quickly decayed to the nonoxidized rate. The Saran char rate was improved by ~250% and the effect also decayed, but not as quickly as the coal char. The hydrogasification rate enhancement of the Saran char was still evident up to 6% carbon conversion, whereas the rate enhancement of the coal char ceased by 3% carbon conversion.

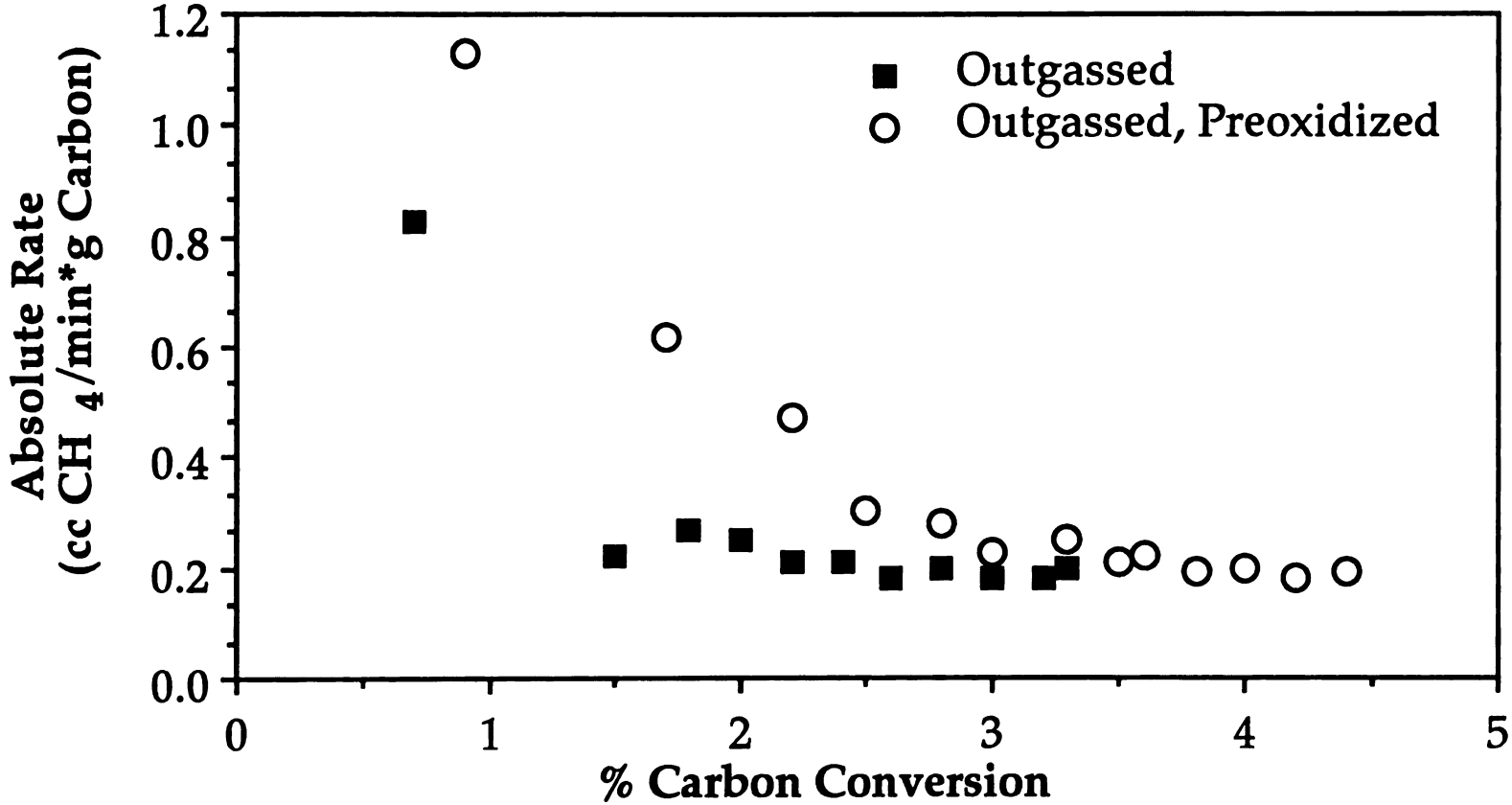

Figure 4.18 Effect of Preoxidation at 375 °C on the Hydrogasification Rate of Outgassed Coal Char

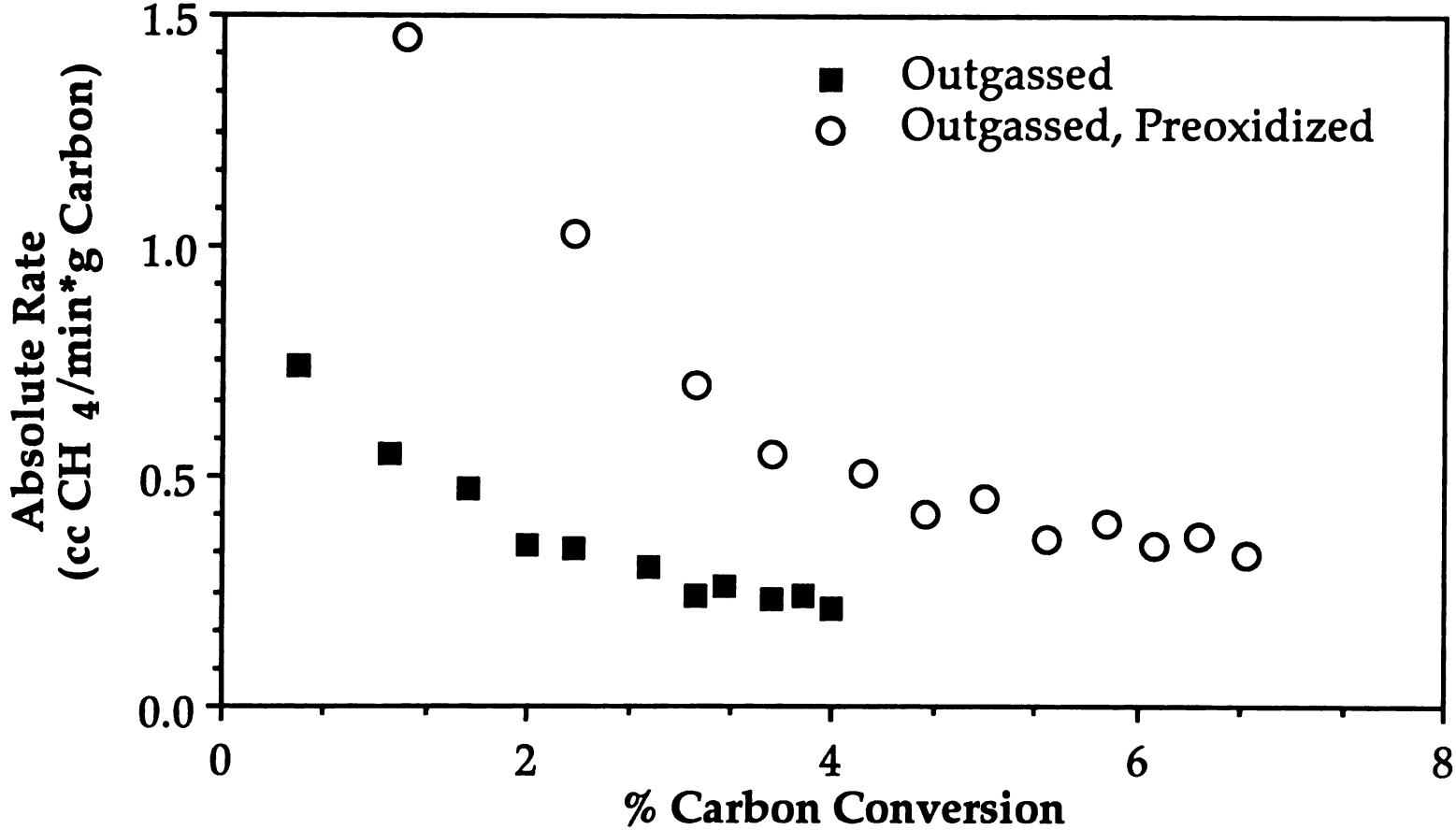

Figure 4.19 Effect of Preoxidation at 375 °C on the Hydrogasification Rate of Outgassed Saran Char

Chapter 5
Discussion

5.1 OBJECTIVE

The objective of this study was to determine what role oxidation plays in coal hydrogasification. Surface oxidation is studied because oxygen is an important contributor in active site formation and increasing the number of active sites should enhance the reactivity of a char. Oxygen creates new active sites because it desorbs from carbon surfaces as either CO or CO_2; these cleave carbon atoms from the surface leaving behind new site vacancies. These additional site vacancies (ASA) should enhance the hydrogasification rate because they provide new locations for hydrogen to attack the carbon structure of the char.

In addition to determining the role of oxidation, a secondary objective was to find a parameter that could be used to normalize the hydrogasification rate and predict char reactivity. The active surface area (ASA) and surface oxygen concentration are the most important parameters because they directly characterize the number of active sites or the probability of forming more active sites during hydrogasification.

5.2 INITIAL CHAR PROPERTIES

The three types of samples used, an Illinois #6 bituminous coal, a demineralized form of the coal (PDP), and a Dow Saran Resin, provided a good cross-section of char properties. This cross-section of char properties was beneficial in isolating the role of oxygen and assessing the importance of properties such as the amount of ash, sulfur, and surface oxygen.

Of the three starting chars, the Saran char was the most pure and the coal char the least pure. The Saran char had the lowest ash content (0.08%) and lowest sulfur content (0.43%), while the coal char had the highest ash (17.33%) and sulfur content (3.55%). The amount of sulfur present in the char is most important in potassium catalyzed hydrogasification because small amounts will deactivate the catalyst.

After correcting for oxygen bound in mineral oxides, all of the initial chars had approximately the same amount of surface oxygen (O/C ratio = 0.06). This method of accounting for the bound surface oxygen is not exact because it assumes that all of these minerals are in their normal oxide configuration and this may not be the case.

5.3 HYDROGASIFICATION

It is evident from all of the hydrogasification plots of absolute rate versus percent carbon conversion that initial activity in hydrogasification decays with conversion. Also all of the starting samples have the same gasification rate after 5% carbon conversion and only slightly different values initially (Figure 4.1). The initial hydrogasification rates for the chars were

~4.0cc CH_4/min*g carbon for the coal char and Saran char and 2.8cc CH_4/min*g carbon for the PDP coal char. The hydrogasification rate for the PDP char is probably incorrect. The PDP coal char was analyzed before the new GC was attached; with the old GC, accurately judging the peak rate was more difficult. By comparing the hydrogasification rate versus conversion curve, it is evident that there is no real difference in the gasification rate between the PDP char and the other initial chars.

The primary process affecting the hydrogasification rate is the consumption and destruction of active sites. Initially, we postulate that there is a large amount of active surface area so the hydrogasification rate is high. As the reaction proceeds, active sites are destroyed so the rate rapidly decreases because fewer and fewer sites are available for hydrogen to react with the surface. Also, as the carbon surface is converted, new active area is exposed, which is then consumed during hydrogasification. A secondary process affecting hydrogasification is the desorption of carbon monoxide from the carbon surface. According to the final step in the mechanism for steam gasification (Eqn 3.), hydrogen and carbon monoxide combine to form methane and water. Increasing the amount of surface oxygen that desorbs as CO should also enhance the gasification rate; however, this effect is probably negligible because only 1-2% of the carbon surface is converted to CO during hydrogasification.

All three of the initial samples have approximately the same rate and the same amount of surface oxygen; this suggests that the O/C ratio must be a good indicator of hydrogasification rate. The dependence of reaction rate on the initial amount of surface oxygen was confirmed by outgassing the samples. After outgassing, the hydrogasification rates of the chars were

drastically reduced (Figures 4.9 and 4.10) as a result of the decrease in amount of surface oxygen and active surface area.

As shown in Figure 4.4, most of the surface oxygen is outgassed by 600°C, but the surface O/C ratio never reaches zero. It does, however, reach a level approximately equal to the bulk oxygen content of the coal char. This result is comparable to Treptau's [46] findings; when he outgassed coconut char at 750°C, he found that the surface O/C ratio decreased to the bulk level. The surface oxygen concentration does not completely reach zero because the XPS is not surface specific. XPS analysis actually represents the average concentration of the top 30Å layer of the bulk char.

To further confirm the importance of oxygen in enhancing hydrogasification, samples were preoxidized. This procedure, however, did not enhance the hydrogasification rates of any of the initial samples (Figures 4.9, 4.10, and 4.11) even though the ASA was of each sample was increased. The PDP char seems to show a slight enhancement in the reaction rate, but this is within experimental error. The failure of preoxidation to enhance the reaction rate is contrary to the original hypothesis; however, preoxidizing the fresh chars may not enhance the rate because these chars may already be in their most reactive state. To confirm this theory, outgassed samples were also preoxidized and did show significant rate enhancement (Figures 4.18 and 4.19). Therefore, increasing the amount of surface oxygen on some samples does lead to rate enhancement. This effect was also significant for the gasified chars. Intermittent oxidation of partially gasified chars significantly increased the reaction rates; however, within a few percent conversion, the hydrogasification rate decays back to its original level (Figures 4.15, 4.16, and 4.17) as gasification proceeds.

5.4 NORMALIZED HYDROGASIFICATION RATES

The secondary objective of this study was to identify a parameter that can be used to normalize the hydrogasification rate. Table 5.1 shows a comparison of the hydrogasification rate normalized by each parameter studied. It is evident that ASA and surface O/C ratio show the most promise for predicting the reactivity of a sample.

5.4.1 ACTIVE SURFACE AREA

The ASA of a sample seems to be a good indicator of reactivity. This is evident by comparing the ASA to the reaction rate for the coal char and the Saran char. The ASA of each of these chars was ~4.0m^2/g carbon and their normalized rates were almost identical. Considering how different these two chars are in TSA, pH, porosity, etc. , this is extremely encouraging. The ASA normalized rates for the outgassed and outgassed-oxidized coal chars were also similar to the normalized rate for the initial chars (~1.1±.2cc $CH_4/min*m^2$ ASA). For Saran char, the variation is somewhat greater, but rates based on ASA are all within ±50% as compared to absolute rates which change five-fold. None of the preoxidized samples followed this trend because the preoxidation increased ASA but did not affect hydrogasification rate.

Table 5.1 Comparison of Hydrogasification Rate Normalized by Different Surface Parameters.

	HYDROGASIFICATION RATE			
SAMPLE	Absolute[1]	per TSA[2] (X100)	per ASA[3]	per O/C Ratio[4] (unbound)
Coal Char	4.0	1.46	1.00	64.5
-HNO_3 oxidized	3.5	1.64	2.33	500.0
-Preoxidized (375°C)				
0.1% Mass Burnoff	3.8	1.74		58.5
5.67% Mass Burnoff	3.7	1.90		26.1
-Preoxidized (725°C)				
3.67% Mass Burnoff	4.0			43.0
-Outgassed (1000°C)	0.8	11.43	1.33	66.7
-Outgassed-oxidized (375°C)				
.52% Mass Burnoff	1.1	1.26	1.23	11.0
-Gasified (725°C)	0.5	0.18		--.-
-Gasified-oxidized	2.2	0.70	0.34	
Demineralized (PDP Char)	4.0*	1.24*	3.08*	60.6*
-Demin-oxidized (375°C)				
2.3% Mass Burnoff	3.2	0.90	0.46	34.0
6.3% Mass Burnoff	3.9	1.04	0.58	42.4
Saran Char	4.4	0.54	1.10	66.7
-Preoxidized (375°C)				
3.1% Mass Burnoff	4.3	0.53	0.70	39.8
7.7% Mass Burnoff	4.4	0.50	0.44	29.0
-Outgassed (1000°C)	0.8	0.09	0.50	18.6
-Outgassed-oxidized (375°C)				
.42% Mass Burnoff	1.4	0.78	0.61	17.5
-Gasified (725°C)	0.5	0.06		27.8

* Adjusted to a rate of 4.0 cc CH_4/min*g carbon, see section 5.3 for discussion.
1 = units in cc CH_4/min*g carbon.
2 = units in cc CH_4/min*m^2 TSA.
3 = units in cc CH_4/min*m^2 ASA.
4= units in cc CH_4/min*g carbon*unit O/C ratio.

5.4.2 SURFACE ΔpH AND O/C RATIO

Normalizing the hydrogasification rate with unit O/C ratio provided the most encouraging results. The normalized rates for the initial chars and the outgassed coal char were all ~65cc CH_4/min*g carbon*unit O/C ratio. The outgassed Saran char and the outgassed-oxidized Saran and coal chars formed another grouping of normalized rates at ~17cc CH_4/min*g carbon*unit O/C ratio. The amount of surface oxygen a good predictor of reactivity because it is directly related to the amount of available ASA and the amount of desorbing carbon monoxide. Thus, both possible processes that influence the hydrogasification rate are characterized by this parameter.

In addition to the amount of oxygen on the sample surface, the type of group that the oxygen is bound in is also important. Acidic groups are more reactive than basic groups, and most acidic groups desorb well below the gasification temperature. This makes the amount of oxygen in acidic groups an important consideration when using oxygen content to normalize hydrogasification rate. The ΔpH and oxygen concentration are important in determining how the amount and type of oxygen groups relate to the active surface area. The importance of these parameters cannot be determined individually because all oxygen groups do not contribute equally to enhancing hydrogasification rate.

The initial coal char was extremely basic in nature. Its pH was over 10.0 with a ΔpH of 4.55. Both the PDP char and the Saran char were slightly acidic in nature when compared to the coal char. They had changes in pH of -0.44 and -0.63 respectively. The pH of the boiled KCl solution was normally around 7.0 so these samples are actually fairly neutral. Based on the large decrease in pH caused by the demineralization of the coal char, most of the

oxygen that is initially on the coal char must be contained in basic groups that are bound in mineral oxides. Since these oxygen groups are not bound to carbon, they do not desorb as CO or CO_2, so their desorption does not increase the active surface area of the char. This explains why the coal char and the Saran char have the same initial hydrogasification rate when the coal char has twice as much total surface oxygen. This assumption is confirmed by the unbound organic O/C ratios for these samples. All three of the initial chars had approximately the same unbound organic O/C ratio (~0.06) and the same hydrogasification rate.

The ΔpH of the chars after gasification also indicates that the basic oxygen groups are not as important as the acidic groups. The ΔpH of the Saran char increases from -0.44 to 2.70 and the ΔpH of the PDP char increases from -0.63 to 3.17. The ΔpH increases because the acidic oxygen groups are desorbed during the reaction leaving only unreactive basic groups. Primitive curve fitting analysis of the carbon C1s peak showed a definite decrease in the concentration of carboxylic acid groups upon gasification. This reduction in carboxylic groups was evident for both the coal char and the Saran char. Since the Saran char did not have the excess basic groups, the effect of outgassing was not masked like it was in the coal char. The ΔpH of the Saran char increased ΔpH=-0.44 to 0.55 with the outgassing. This is strong evidence that the outgassing reduces the reactivity of the samples by removing the acidic groups.

5.4.3 TOTAL SURFACE AREA

The total surface area of each of the chars was examined to ensure that physical changes in the surface structure are not responsible for changes in reaction rate. As shown in Figure 4.3, the total surface area is not significantly affected by hydrogasification. The coal char does show some slight change in TSA during hydrogasification; however, this effect is too small to account for such large decreases in reaction rate. Since the TSA is not affected by hydrogasification, it is not a good predictor of reactivity.

The study on the total surface area was conducted on samples reacted at 800°C. Since the later hydrogasification experiments were conducted at 725°C, a link between the reaction temperatures was established. Comparison of the TSA for two samples reacted at 800°C and 725°C (Figure 4.3) shows conclusively that the different reaction temperature does not alter the TSA of the coal char.

The TSA was also examined to ensure that outgassing and oxidation do not physically change the surface structure of the chars. The Saran char was not physically affected by either treatment; however, the coal char sintered during the outgassing; its TSA decreased 39-fold to $7 m^2/g$. The fact that the coal char sinters during outgassing is significant in understanding the rate enhancement from oxidizing the outgassed coal char. The rate is enhanced by two-fold while the TSA of the coal char appears to increase by twelve-fold. The rate enhancement may appear to be caused by the increase in TSA; however, the increase in TSA should also happen during the initial stages of hydrogasification. The large increase in TSA caused by oxidation is due to the opening some of the pores blocked by the sintering during outgassing. These blocked pores would also be opened as the carbon surface is reacted away

during hydrogasification, so there is no real change in the TSA between the outgassed and the outgassed-oxidized coal char.

5.5 HYDROGASIFICATION RATE ENHANCEMENT

Intermittent oxidation proved to be the best method for enhancing the hydrogasification rates of the chars. This method involved partially gasifying the sample then oxidizing it by burning in air at 375°C. Intermittent oxidation enhances the reaction rate two-fold for both the coal char and the Saran char; however, the rate enhancement lessens with each successive oxidation of the same sample or with the extent of conversion. Figures 4.13 and 4.14 show a comparison between the reaction rates for an initial char and an intermittently oxidized char.

This increase in the hydrogasification rate is most likely due to an increase in the ASA of the chars or an increase in surface oxygen. Figure 4.8 shows how the ASA of a sample changes with intermittent oxidation. The figure clearly shows that hydrogasification consumes ASA while oxidation increases ASA. The subsequent increases in hydrogasification rate after oxidation verify the link between ASA and rate. The results for the last oxidation and gasification seem reversed. This may be due to the small amount of sample available to conduct the experiments. Each gasification and subsequent oxidation reduces the total mass of sample available.

Comparing the different oxidized samples, it is evident that increasing the surface oxygen concentration also increases the active surface area; however, the preoxidized samples show that increasing the ASA does not always increase the reaction rate. The theory that ASA is consumed by

hydrogasification is challenged by the results shown in Figure 4.7. This figure compares the change in ASA with conversion and unfortunately shows no definitive trend; however, this series of experiments was conducted before the oxygen chemisorption technique was finalized. Thus, a definitive trend may be hidden by experimental error.

Changing the oxidation temperature seems to have no effect on the reactivity of a sample. Figure 4.9 compares the rate of a coal char preoxidized at 725°C to the rates of two different coal chars preoxidized at 375°C. It is clearly evident that there is no rate enhancement from the higher preoxidation temperature. Also, it is apparent that the increase in basic oxygen groups from oxidation at 725°C does not inhibit the hydrogasification reaction.

The most important conclusion that can be made from these data is the confirmation that increasing the amount of surface oxygen also increases the active surface area of a sample. A lesser finding is that a sample that is initially well oxidized will not become more reactive via preoxidation even though the ASA increases. This suggests that there may be more than one process that is important to hydrogasification and that these processes compete with each other at different points in the reaction.

Currently, the effect of preoxidizing a char with nitric acid is inconclusive. This method was only performed on the coal char and seemly had no effect on the hydrogasification rate. The most significant differences between preoxidizing via combustion and via contacting with nitric acid are that with nitric acid, none of the carbon structure is reacted away and that the active surface area decreases drastically. The ASA of the coal char decreased by 60% with HNO_3 oxidation but this effect is misleading. Initially, one may think that the decrease in ASA is linked to the increase in acidic oxygen

groups; however, it is possible that the actual decrease is caused by the demineralization of the coal char. When the HNO_3 oxidized coal char is compared to the PDP char, there is no difference in ASA. The ASA of the nitric acid oxidized coal char was $1.5m^2/g$ and the ASA of the PDP char was $1.3m^2/g$.

Table 4.3 shows a comparison of the ASA measured at increasing temperature for both the coal char and the Saran char. Two important conclusions can be drawn from this analysis. First, the ASA is not increased by outgassing the samples at temperatures above the reaction temperature. This is contrary to results indicated by the temperature programmed desorption. The second conclusion is that both acidic and basic groups contribute to the total ASA.

Chapter 6
Conclusions

The objective of this study was to find the role that surface oxidation plays in hydrogasification of coal char and Saran char. The secondary objective was to isolate a sample characteristic that would be a good indicator of reaction rate.

This study gives some insight into the general role that oxygen plays in the reaction. Surface oxidation enhances the reactivity of coal and Saran chars which were previously reacted or outgassed; however, it has no effect on the reactivity of fresh chars. The reactivity of gasified and outgassed chars increases because the oxidation creates new active sites; however, the reactivity does not return to its original level. The fresh chars are not affected by oxidation, even though oxidation increases the ASA, because they are already well oxidized during formation.

Varying oxidation conditions does not affect the degree of enhancement of the reactivity of the char; apparently the additional oxygen fixed in more severe oxidation either competes with another mechanism or it is bound in the wrong type of oxygen group.

A definitive parameter that could predict the reactivity of a sample prior to hydrogasification was not isolated during this study; however, two parameters investigated do show some promise. Active surface area and the

unbound organic surface oxygen O/C ratio may be used to predict sample reactivity, whereas the total surface area is definitely not a good indicator of reactivity. The ΔpH shows some promise, but the results are currently inconclusive.

The total surface area (TSA) is not a good predictor of reactivity because it does not change during hydrogasification. The rapid decrease in reaction rate with conversion is not due to a reduction in TSA; the rate enhancements are also not a result of increases in TSA.

The surface ΔpH of the samples is also not a good predictor of sample reactivity. The importance of ΔpH in hydrogasification of the coal char is masked by the large amount of mineral oxides bound to the surface, and the other samples do not show a quantitative trend in hydrogasification rate with either an increase or decrease in ΔpH. The ΔpH does, however, conclusively show that hydrogasification removes acidic oxygen groups from the sample surface; although increasing the acidic or basic nature of the sample surface does not solely influence the sample reactivity. The preoxidation by burning in air at 375°C increased the acidic nature of the char surface and preoxidation by burning in air at 725°C increased the basic nature of the char surface yet neither affected the rate.

The active surface area of a sample is a better indicator of reactivity. There were two general results obtained when normalizing rate by ASA (Table A.3). The normalized rate for the preoxidized Saran char, the preoxidized PDP coal char, and the initial coal char was 0.55±0.1 cc CH_4/ min*m^2 ASA and the initial Saran char and the outgassed and outgassed-oxidized coal char were 1.2±0.1 cc CH_4/min*m^2 ASA. These variations may be due to errors in the rate or ASA determination, or they might signify two different reactivities. The fact that some predictability is evident when

normalizing with ASA is encouraging and verifies that this method warrants further investigation.

The concentration of unbound surface oxygen is currently the best indicator of sample reactivity used in this study. Fresh chars have O/C normalized initial rates of ~65cc CH_4/min*g carbon*unit O/C. The PDP char rate was much lower; however, the maximum reaction rate was probably low. If the rate is adjusted to 4.0cc CH_4/min*g carbon, as implied by the rate versus conversion curve, then the normalized rate would be ~60.6cc CH_4/min*g carbon. This is in good agreement with the fresh coal char and Saran char. The outgassed chars have consistent O/C normalized rates, but they are lower than the normalized rates of the fresh samples. The normalized outgassed rates are 18±0.5 cc CH_4/min*m^2 ASA both before after oxidation. The outgassed coal char is an exception to this trend. Its normalized rate was 66.7±0.1 cc CH_4/min*m^2 ASA, which is in line with the fresh chars.

Further work still needs to be done to verify the validity of using ASA and surface oxygen concentration to predict the reactivity of a char in hydrogasification. Future ASA experiments should concentrate on overcoming the diffusion limitations of oxygen chemisorption on coal and Saran chars. Increasing the residence time of the oxygen pulse should be investigated first. This can be done by decreasing the carrier gas flow rate or increasing the downstream pressure (with the GC). If these methods do not enhance the reproducibility of the ASA measurements, then the reaction conditions should be standardized. The sample weight, particle size, and the number of oxygen pulses should be the first parameters standardized. This method may not provide exact ASA values, but the measured ASA would be useful in a comparative study of reactivity versus ASA for the chars.

The second area that warrants further investigation is the surface oxygen concentration. The amount of surface oxygen that is not strongly bound as mineral oxides is more important than determining the gross amount of oxygen. Further work to isolate the effects of minor mineral concentrations may lead to better results. This study only isolated the major mineral oxides like SiO_2, Al_2O_3, and SnO_2, which were on the char surface in concentrations greater than 0.5% of the total surface atoms. Also, using the XPS curve fitting routine to identify the relative concentrations of different oxygen groups, which are bound to the carbon lattice, may provide more insight into the mechanism by which surface oxidation enhances hydrogasification. The fact that not all surface oxygen is useful to the reaction is evident by both the ΔpH changes caused by different oxidations and the total surface oxygen concentration. Thus, finding exactly which oxygen group causes the best rate enhancement and finding a way to increase the relative concentration of that group would be extremely beneficial in coal hydrogasification. Also, since many of the different coal gasification processes have mechanisms similar to hydrogasification, the rate enhancement technique should be beneficial to the entire field of coal gasification.

LIST OF REFERENCES

LIST OF REFERENCES

1. R.L. Hirsch, J.E. Gallagher Jr., R.R. Lessard, R.D. Wesselhoft, Science, 215, 121 (1982).

2. H.H. Schobert, Coal, The Energy Source of the Past and Future, The American Chemistry Society, Washington D.C. 1987.

3. J. Huebler, SNG SYMPOSIUM I, 371, (1973).

4. W.F. HEDERMAN Jr., Prospects for the Commercialization of High-BTU Coal Gasification, Rand, Santa Monica, (1978).

5. M. Steinberg, 1987 International Conference on Coal Science, 11, 953 (1987).

6. L.R. Radovic, P.L. Walker Jr., and R.G. Jenkins, Fuel, 62, 849 (1983).

7. K. Miura, M. Makino, and P.L. Silveston, Fuel, 69, 580 (1990).

8. J.D. Blackwood, Aust. J. Chem.,12, 14 (1959).

9. Anthony, Howard, AICHE Journal, 22, No. 4, 625 (1976).

10. S. Matsumoto and P.L. Walker Jr., Carbon, 27, 395 (1989).

11. J.R. Cao and M. H. Back, Carbon, 23, 141 (1985).

12. P.L. Walker Jr., F. Rusinko Jr., and L.G. Austin, Advan. Catalysis, 11, 133 (1959).

13. A Linares-Solano, E.J. Hippo, and P.L. Walker Jr., Fuel, 65, 776 (1986).

14. H. Zoheidi and D.J. Miller, Carbon, 25, 265 (1987).

15. M.H. Treptau, and D.J. Miller, ACS Division of Fuel Chemistry Prepr., 34(1), 176 (1989).

16. C.W. Zielke, E. Gorin, Ind and Engin. Chem., 47, 820 (1955).

17. J-R. Cao, M.H. Back, Carbon, 20, No. 6, 505 (1982).

18. Z.J. Pan and R.T. Yang, Journal of Catalysis, 123, 206 (1990).

19. J.T. Shaw, Proc Intern Conf on Coal Science, 209 (1981).

20. R.J. Lang and R.C. Neavel, Fuel, 61, 620 (1982).

21. H. Zoheidi, and D.J. Miller, Carbon,25, 265 (1987).

22. J.M. Saber, J.L. Falconer, and L.F. Brown, Journal of Catalysis,90, 65 23. S.R. Keleman, H, Freund, and C.A. Mims, Journal of Catalysis, 97, 228 (1986).

23. S.R. Keleman, H. Freund, and C.A. Mims, Journal of Catalysis, 97, 228 (1986).

24. J.M. Saber, J.L. Falconer, and L.F. Brown, Journal of Catalysis,90, 65 (1984).

25. Y. Otake and R. G. Jenkins, ACS Division Fuel Chemistry Prepr., 32, 310 (1987).

26. C. Sellitti, J.L. Koenig, and H. Ishida, Carbon,28, 221 (1990).

27. P.L. Walker Jr., Carbon, 28, 261 (1990).

28. J.S. Noh and J.A. Schwarz, Carbon, 28, 675 (1990).

29. Y. Ohtsuka, K. Itagaki, K. Higashiyama, A. Tomita, and Y. Tamai, Neaoyo Kyokaishi, 60, 437 (1981).

30. C. A. Mims and J. J. Krajewski, Journal of Catalysis,102,140 (1986).

31. H. Zoheidi, and D.J. Miller, Carbon,25, 809 (1987).

32. K.E. Adams, D.R. Glasson, and S.A.A. Jayaweera, Carbon, 27, 95 (1989).

33. R. Cypres, D Planchon and C. Braekman-Danhuex, Fuel,64, 1375 (1985).

34. A DeKoranyi, Carbon, 27, 55 (1989).

35. N.R. Laine, F.J. Vastola, and P.L. Walker Jr., Journal of Physical Chemistry, 67, 2030 (1963).

36. P.L. Walker Jr., Carbon,28, 261 (1990).

37. A.W. Adamson, Physical Chemistry of Surfaces, 4th Ed., Wiley and Sons, New York (1982).

38. D.T. Clark, and R. Wilson, FUEL, 62, 1034 (1983).

39. C. Kozlowski, and P.M.A. Sherwood, Carbon, 21, 53 (1983).

40. A. Ishitani, Carbon, 19, 269 (1981).

41. C. Kozlowski, P.M.A. Sherwood, Journ. Chem. Soc. Faraday Trans, 1,80, 2099 (1984).

42. D.L. Perry, A. Gint, Fuel, 62, 1024 (1983).

43. A. Proctor, P.M.A. Sherwood, Journ. of Electron Spectroscopy and Related Phenomena, 27, 39 (1982).

44. E.L. Evans, Carbon, 13, 461 (1975).

45. Y. Nakayama, F. Soeda, and A. Ishitani, Carbon,28, 21 (1990).

46. M. Treptau, Carbon, 29, 531 (1990).

47. Zoheidi, H, Ph.D. Dissertation, Michigan State University, East Lansing, Michigan (1987).

48. ASTM Designation: D 3838-80 (Reapproved 1986).

49. Treptau, M, Ph.D. Dissertation, Michigan State University, East Lansing, Michigan (1989).

50. H. Marsh and W.F.K. Wynne-Jones, Carbon, 1, 269 (1964).

51. T.G. Lamond and H. Marsh, Carbon,1, 281, (1964).

52. S.J. Gregg, K.S.W. Sing, Adsorption, Surface Area and Porosity, 2nd Ed, Academic Press Inc, New York, (1982).

53. M. Lussier, Masters Thesis, Michigan State University, East Lansing Michigan (unpublished).

APPENDICES

APPENDIX A

APPENDIX A. SUMMARY DATA TABLES

Table A.1 Pretreatment Effects on the Total Surface Area (TSA) and Active Surface Area (ASA) of Coal Char and Saran Char Samples.

SAMPLE	TSA (m^2/g Carbon)	ASA (m^2/g Carbon)
Coal Char	274	4.0
-HNO_3 oxidized	214	1.5
-Preoxidized		
0.1% Mass Burnoff	218	
5.67% Mass Burnoff	195	
-outgassed (1000°C)	7*	0.6
-outgassed-oxidized (375°C)		
.52% Mass Burnoff	87	0.9
-gasified (725°C)	313	
-gasified-oxidized	316	6.3
Demineralized	322	1.3
-demin-oxidized (375°C)		
2.3% Mass Burnoff	354	6.9
6.3% Mass Burnoff	376	6.7
Saran Char	816	4.0
-oxidized(375°C)		
3.1% Mass Burnoff	815	6.1
7.7% Mass Burnoff	876	9.9
-outgassed (1000°C)	870	1.5
-outgassed-oxidized (375°C)		
.42% Mass Burnoff	762	2.3

* TSA found via nitrogen BET; all other TSAs via CO_2 Dubinin method.

Table A.2 Pretreatment Effects on the Surface Properties of Coal Char and Saran Char.

SAMPLE	BOUND O/C RATIO	UNBOUND O/C RATIO	ΔpH
Coal Char	0.136	0.062	4.55
-HNO_3 oxidized	0.186	0.007	-2.27
-Preoxidized (375°C)			
0.1% Mass Burnoff	0.1304	0.052	0.82
5.67% Mass Burnoff	0.2102	0.128	-1.66
-Preoxidized (725°C)			
3.67% Mass Burnoff		0.093	2.88
-Outgassed (1000°C)	0.063	0.012	3.71
-Outgassed-oxidized (375°C)			
.52% Mass Burnoff	0.138	0.100	2.92
-Outgassed (725°C)	0.102	.NA	4.16
-Outgassed-O_2 chemisorbed	0.117	.NA	3.88
-Gasified (725°C)	0.103	—.—	3.46
-Gasified-oxidized			0.91
Demineralized (PDP Char)	0.066	0.066	-0.63
-Demin-oxidized (375°C)			
2.3% Mass Burnoff	0.094	0.094	-1.29
6.3% Mass Burnoff	0.092	0.092	-2.75
Saran Char	0.066	0.066	-0.44
-Preoxidized (375°C)			
3.1% Mass Burnoff	0.108	0.108	-2.54
7.7% Mass Burnoff	0.152	0.152	-3.38
-Outgassed (1000°C)	0.043	0.043	0.55
-Outgassed-oxidized (375°C)			
.42% Mass Burnoff	0.080	0.080	-2.42
-Gasified (725°C)	0.018	0.018	2.70

Table A.3 Pretreatment Effects on the Surface Oxygen Concentration Coal Char and Saran Char as Determined by XPS.

SAMPLE	TOTAL O/C Ratio	TOTAL % Oxygen	UNBOUND* O/C Ratio	UNBOUND* %Oxygen
Coal Char	0.136	9.3	0.062	4.27
-HNO_3 oxidized	0.186	15.5	0.007	0.56
-Preoxidized (375°C)				
0.1% Mass Burnoff	0.1304	11.02	0.052	4.38
5.67% Mass Burnoff	0.2102	16.58	0.128	10.08
-Preoxidized (725°C)				
3.67% Mass Burnoff	0.1508	12.45	0.093	7.65
-Outgassed (1000°C)	0.063	5.9	0.012	1.17
-Outgassed-oxidized (375°C)				
0.52% Mass Burnoff	0.138	12.0	0.100	8.71
-Outgassed (725°C)	0.102	9.16	N.A	.NA
-Outgassed-O_2 chemisorbed	0.117	10.42	2.053	4.69
-Gasified (725°C)	0.104	8.88	<0.00	<0.000
Demineralized (PDP Char)	0.066	6.1	0.066	6.10
-Demin-oxidized (375°C)				
2.3% Mass Burnoff	0.094	8.5	0.094	8.50
6.3% Mass Burnoff	0.092	8.4	0.092	8.40
Saran Char	0.066	6.2	0.066	6.10
-Preoxidized(375°C)				
3.1% Mass Burnoff	0.108	9.5	0.108	9.50
7.7% Mass Burnoff	0.152	12.9	0.152	12.90
-Outgassed (1000°C)	0.043	4.1	0.043	4.10
-Outgassed-oxidized (375°C)				
.42% Mass Burnoff	0.080	7.3	0.080	7.33
-Gasified (725°C)	0.018	1.8	0.018	1.81

* Unbound oxygen refers to the surface oxygen atoms that are not bound in the surface metal oxides like SnO_2, Al_2O_3, and SiO_2.

APPENDIX B

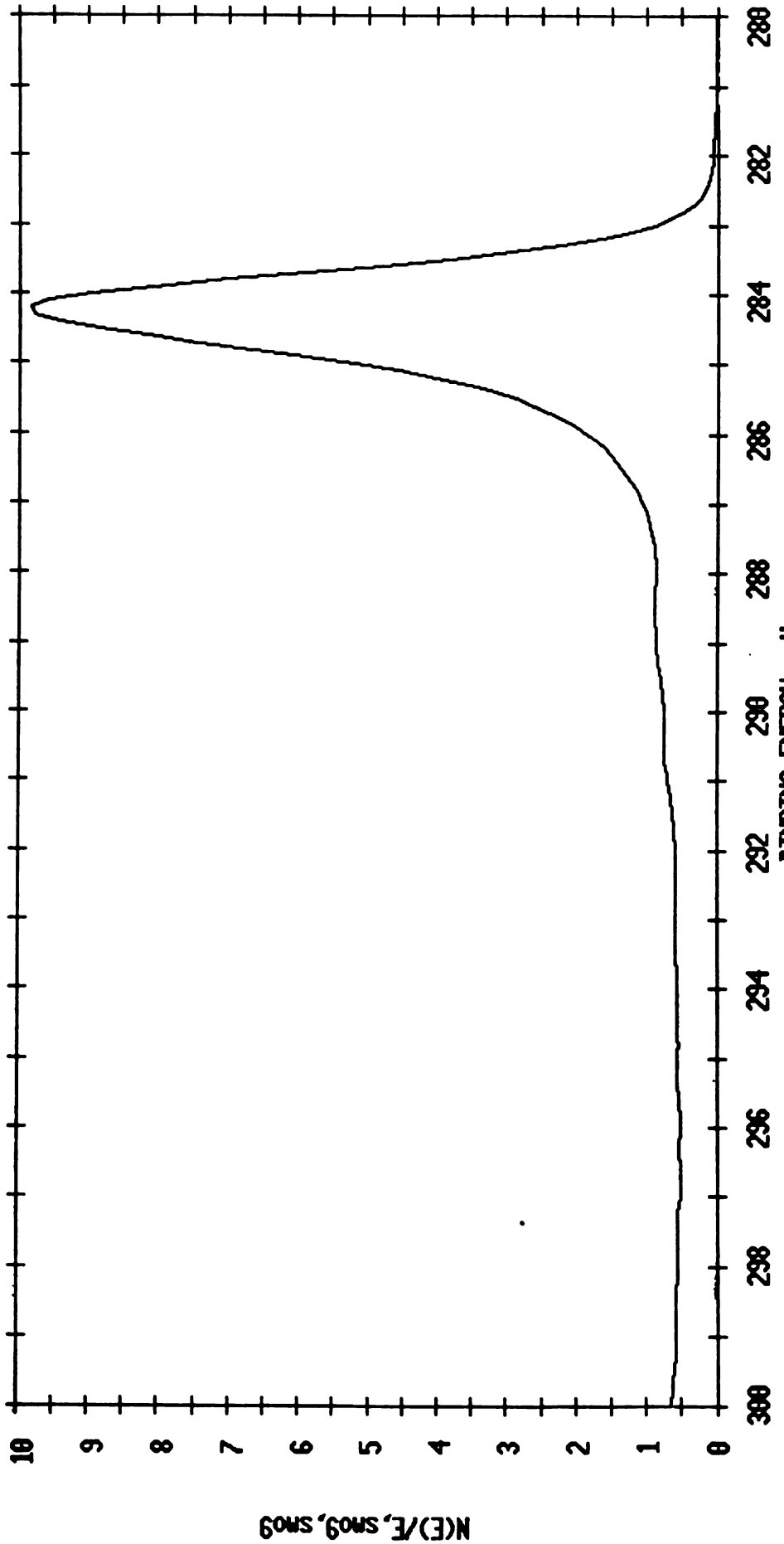

Figure B1. The XPS C1s Peak of Fresh Coal Char--Outgassed at 120°C Under High Vacuum.

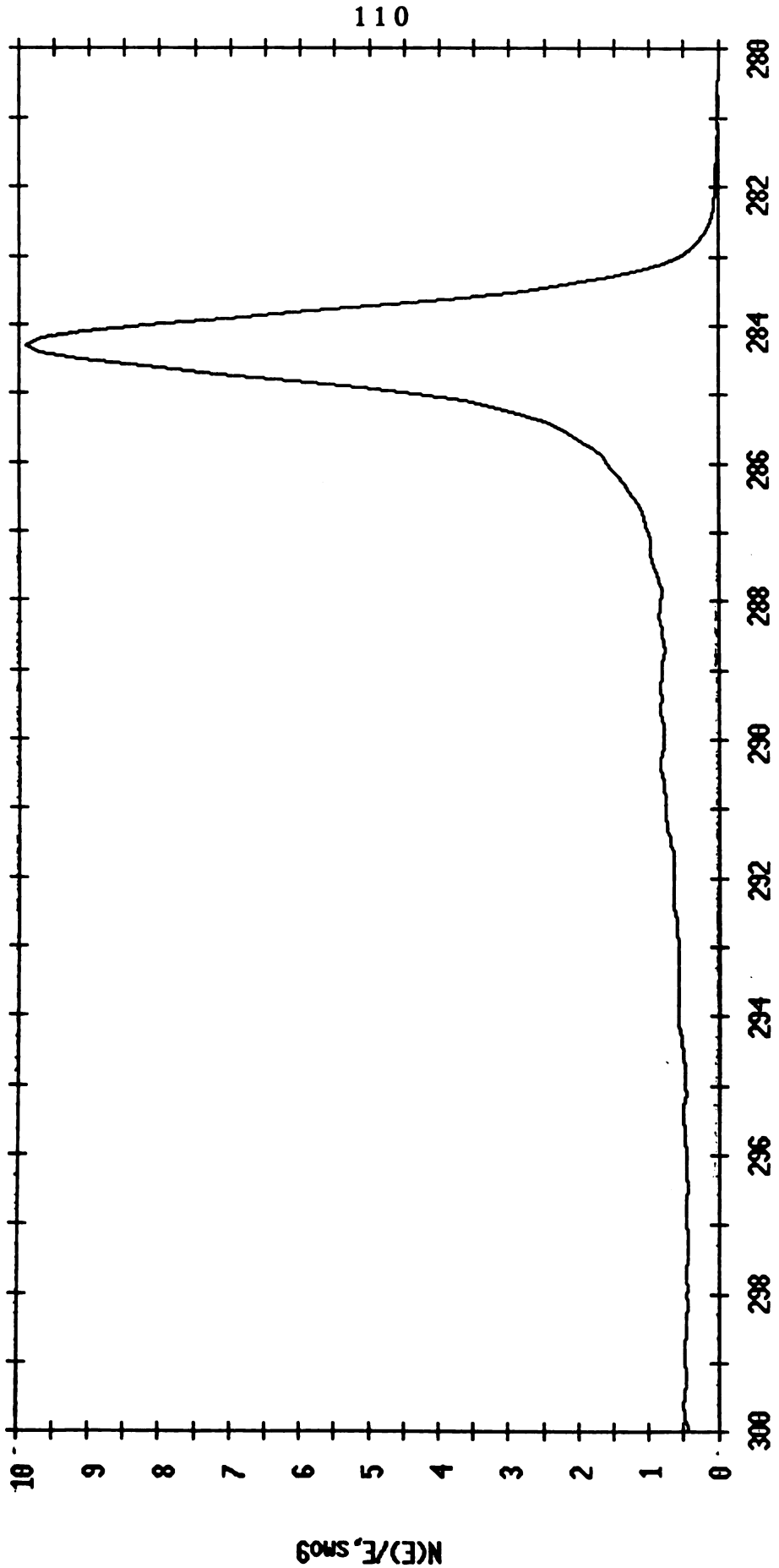

Figure B2. The XPS C1s Peak of Gasified Coal Char--Outgassed at 120°C Under High Vacuum.

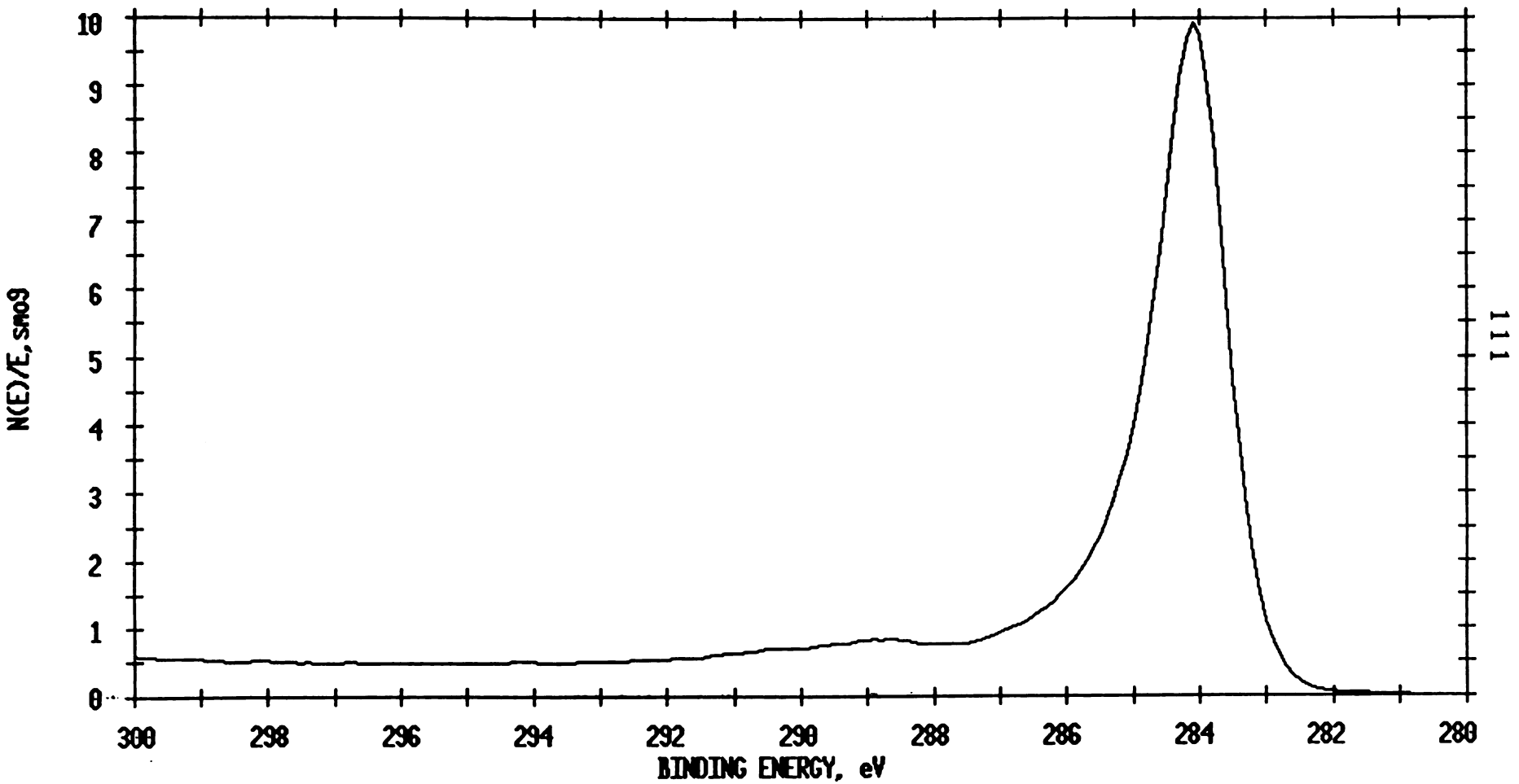

Figure B3. The XPS C1s Peak of Outgassed (1000°C) Coal Char--Outgassed at 120°C Under High Vacuum.

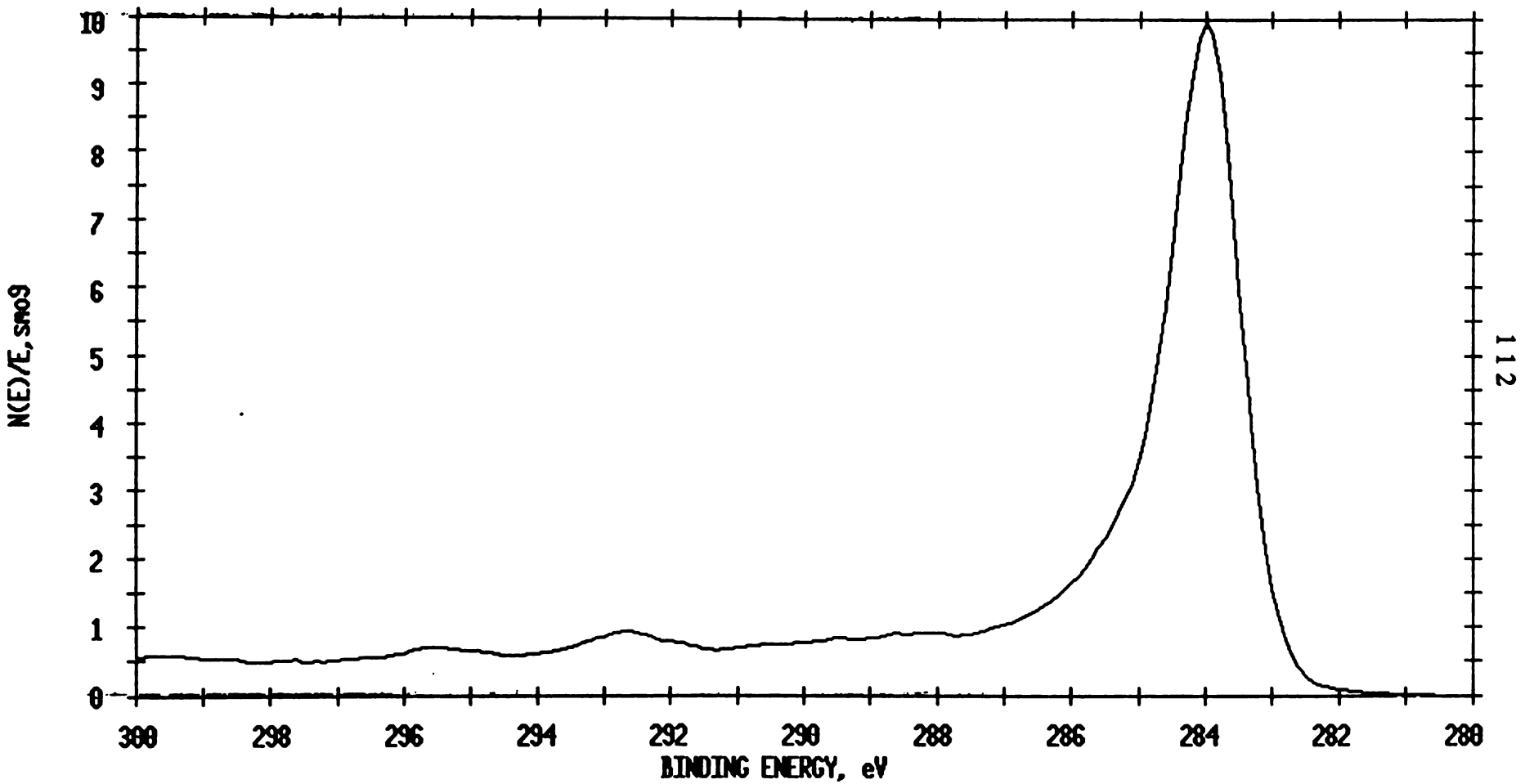

Figure B4. The XPS C1s Peak of Outgassed (1000°C)-Oxidized Coal Char--Outgassed at 120°C Under High Vacuum.

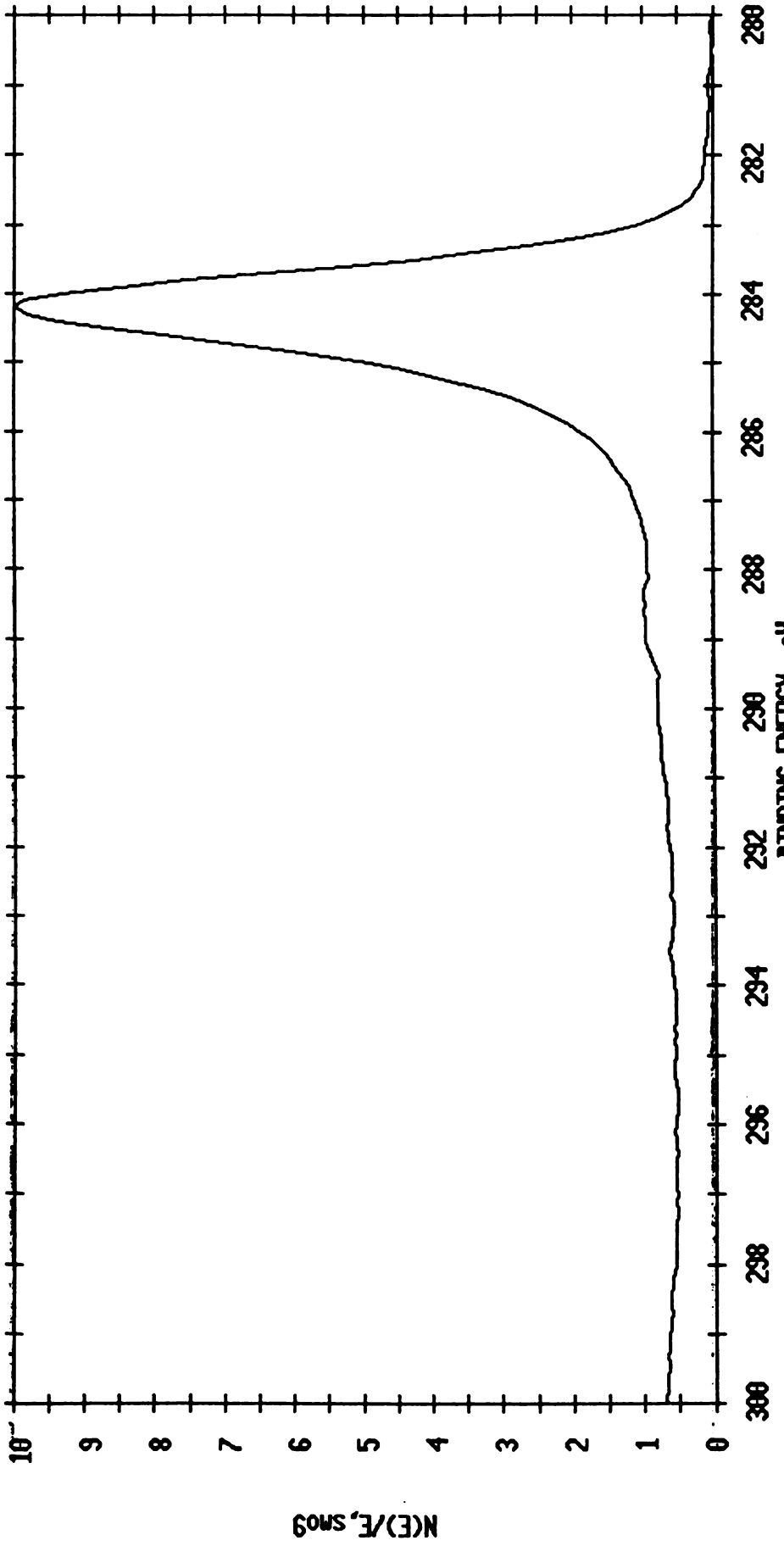

Figure B5. The XPS C1s Peak of Coal Char Preoxidized at 375oC (0.1% Mass Burnoff)-
-Outgassed at 120oC Under High Vacuum.

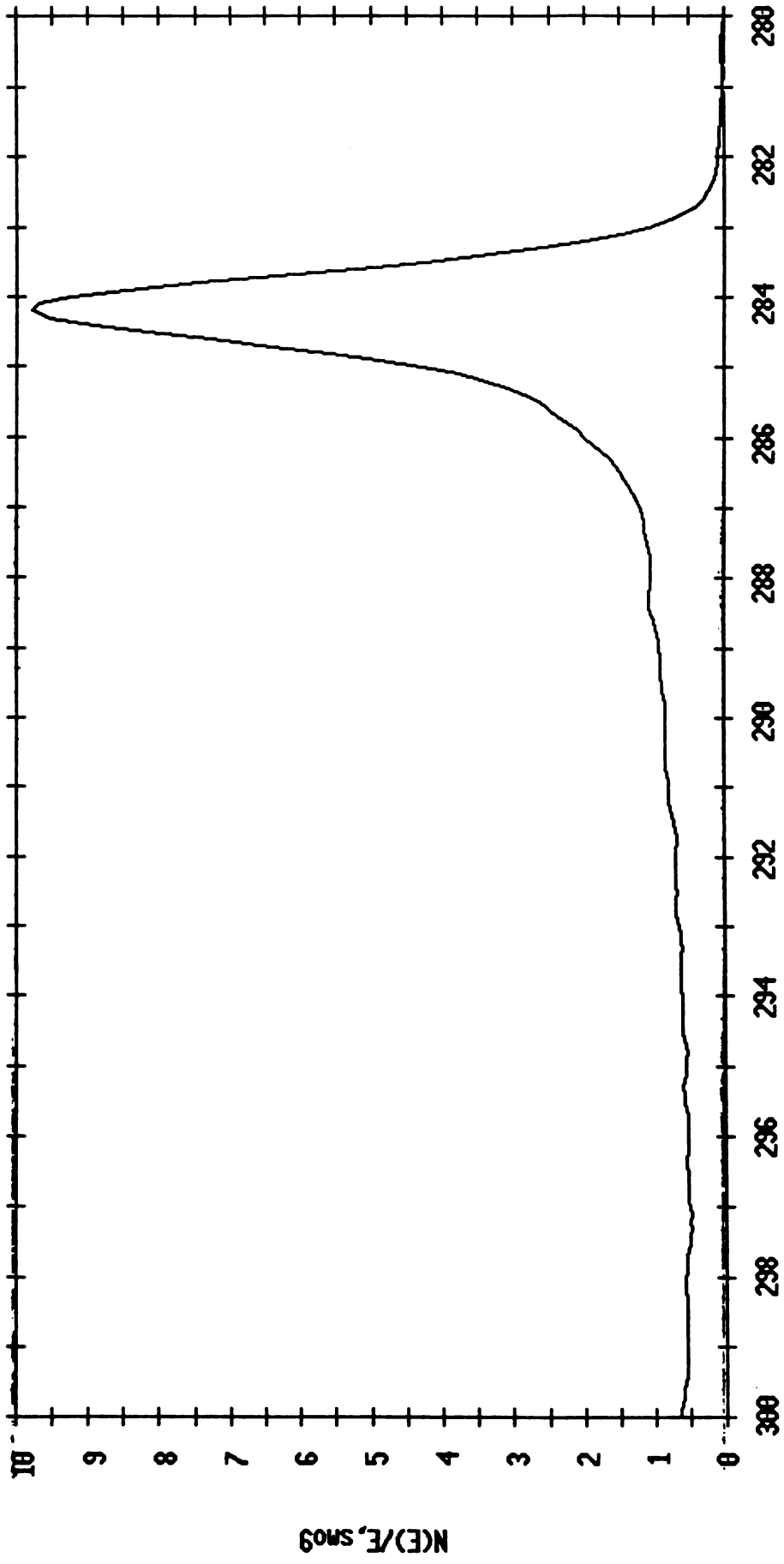

Figure B6. The XPS C1s Peak of Coal Char Preoxidized at 375oC (5.67% Mass Burnoff)-
-Outgassed at 120oC Under High Vacuum.

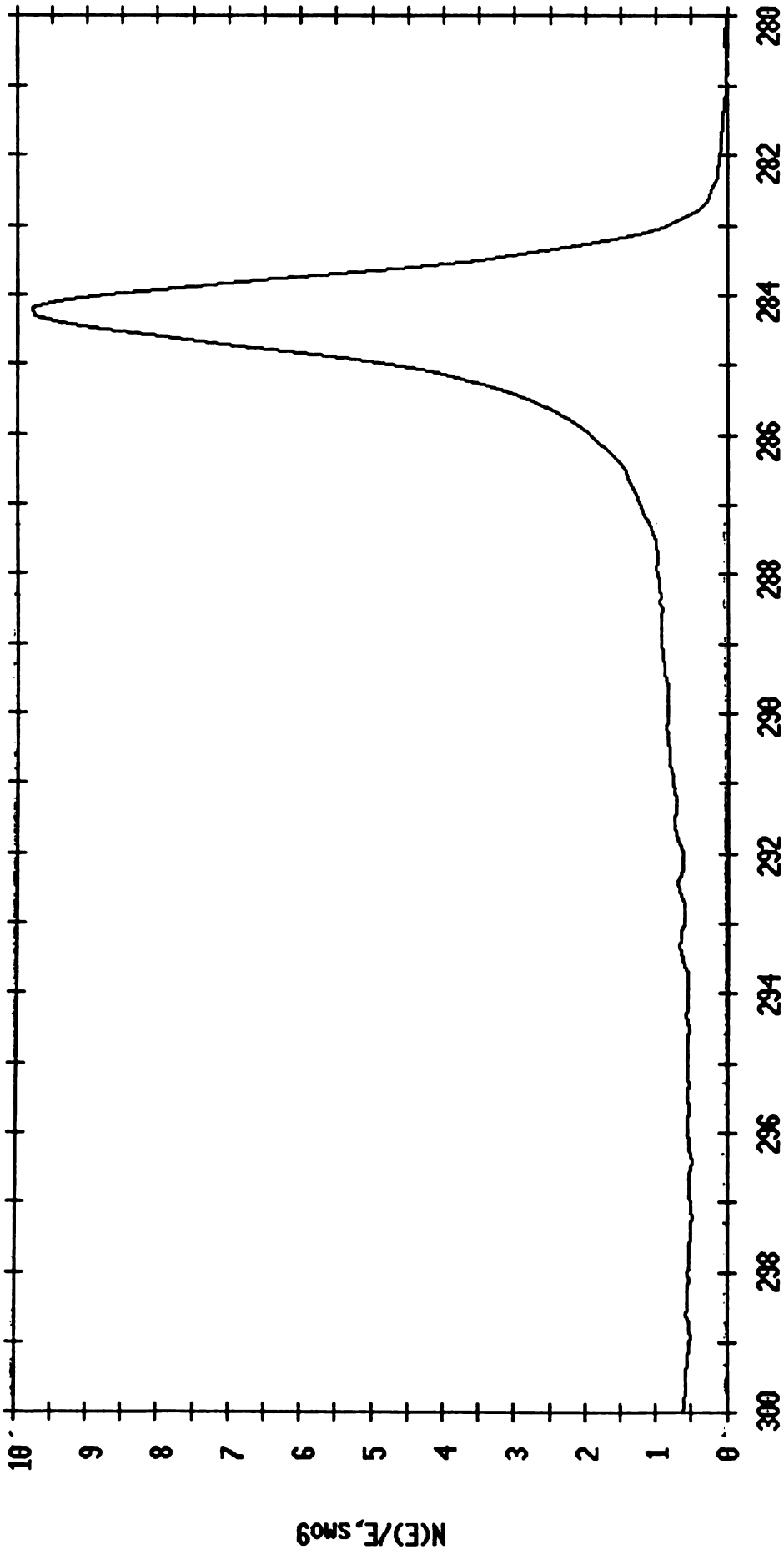

Figure B7. The XPS C1s Peak of Coal Char Preoxidized at 725°C (3.67% Mass Burnoff)-
-Outgassed at 120°C Under High Vacuum.

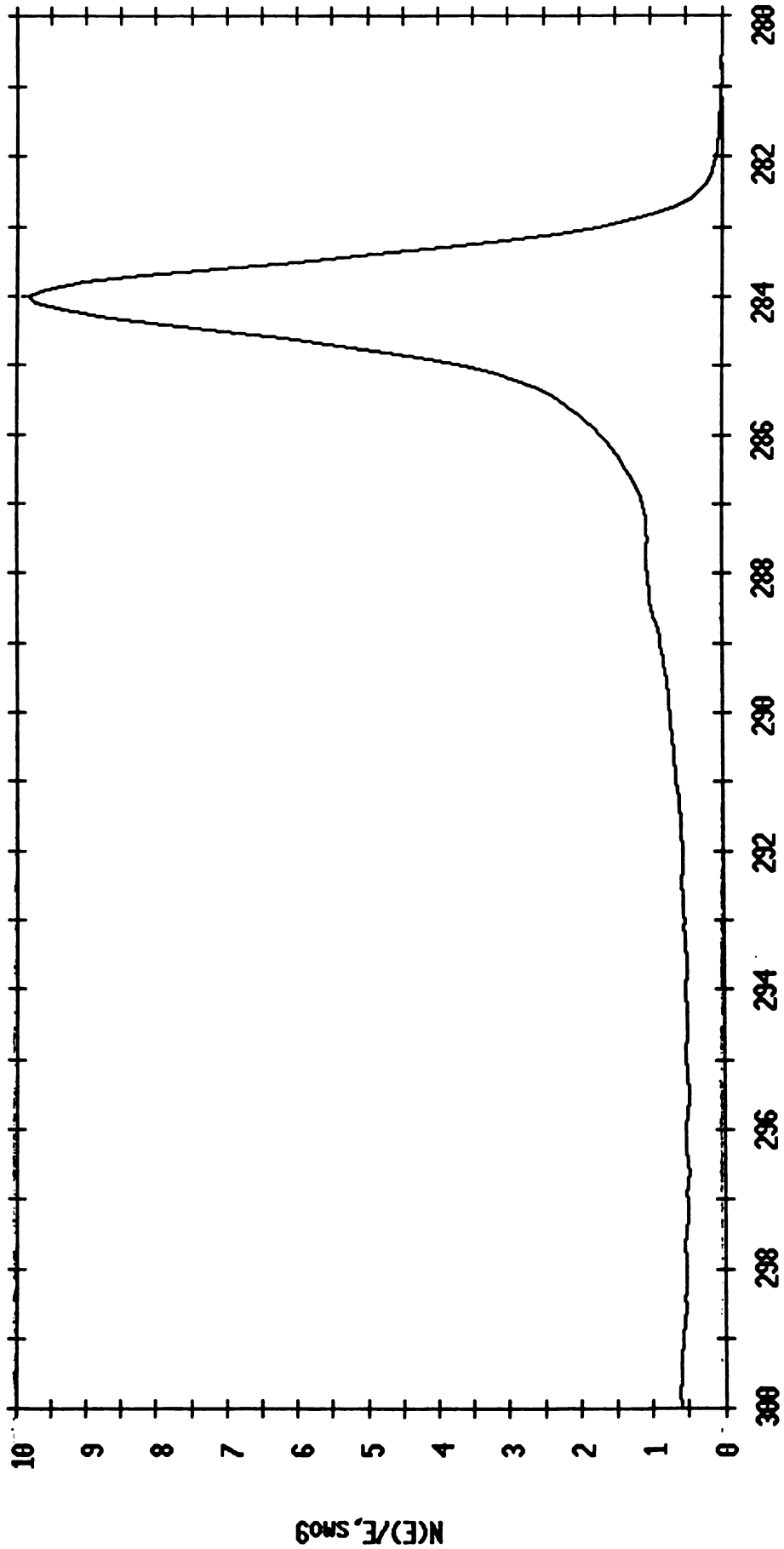

Figure B8. The XPS C1s Peak of Coal Char Preoxidized with Nitric Acid--Outgassed at 120°C Under High Vacuum.

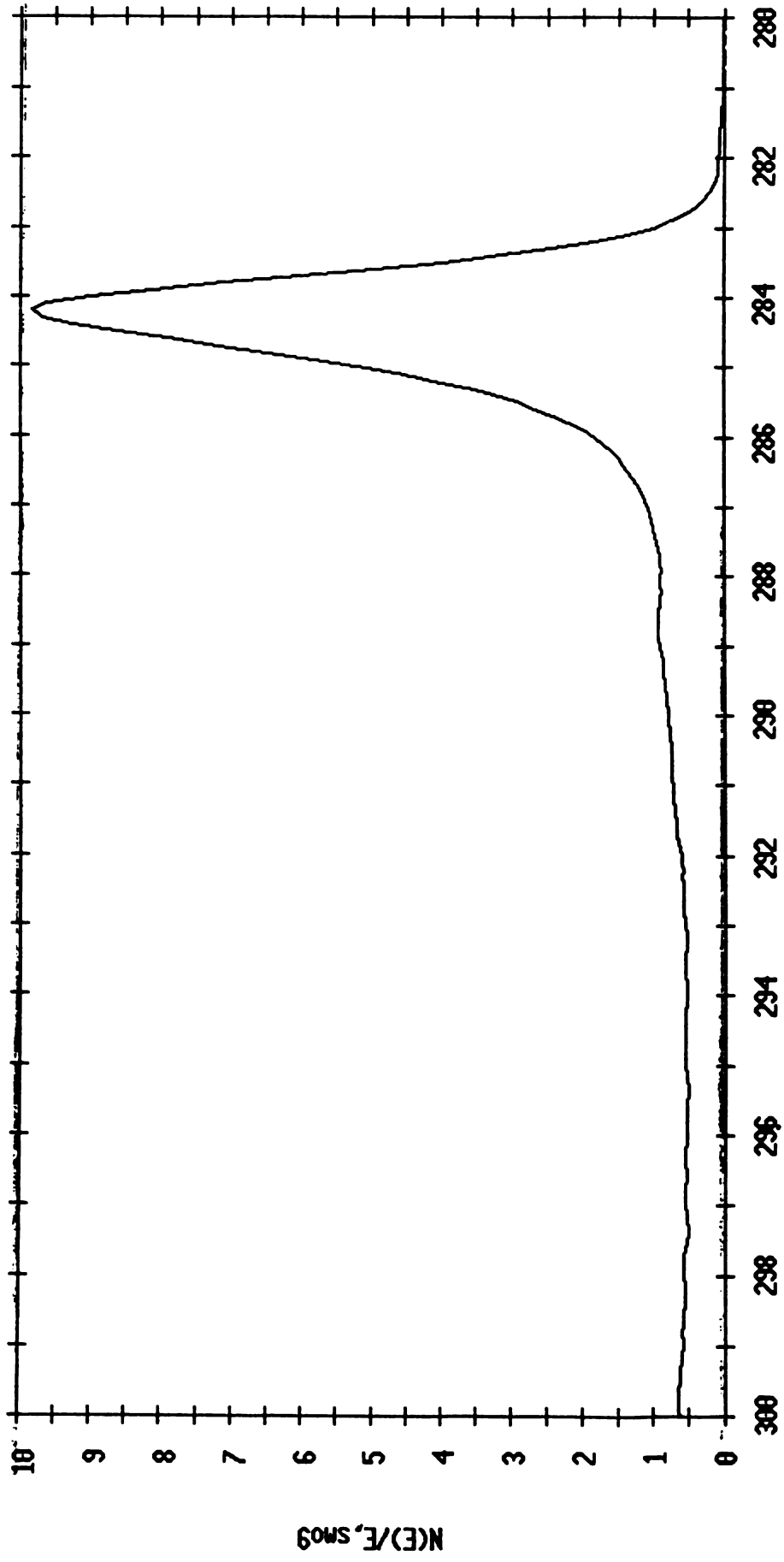

Figure B9. The XPS C1s Peak of Demineralized (PDP) Coal Char –Outgassed at 120°C Under High Vacuum.

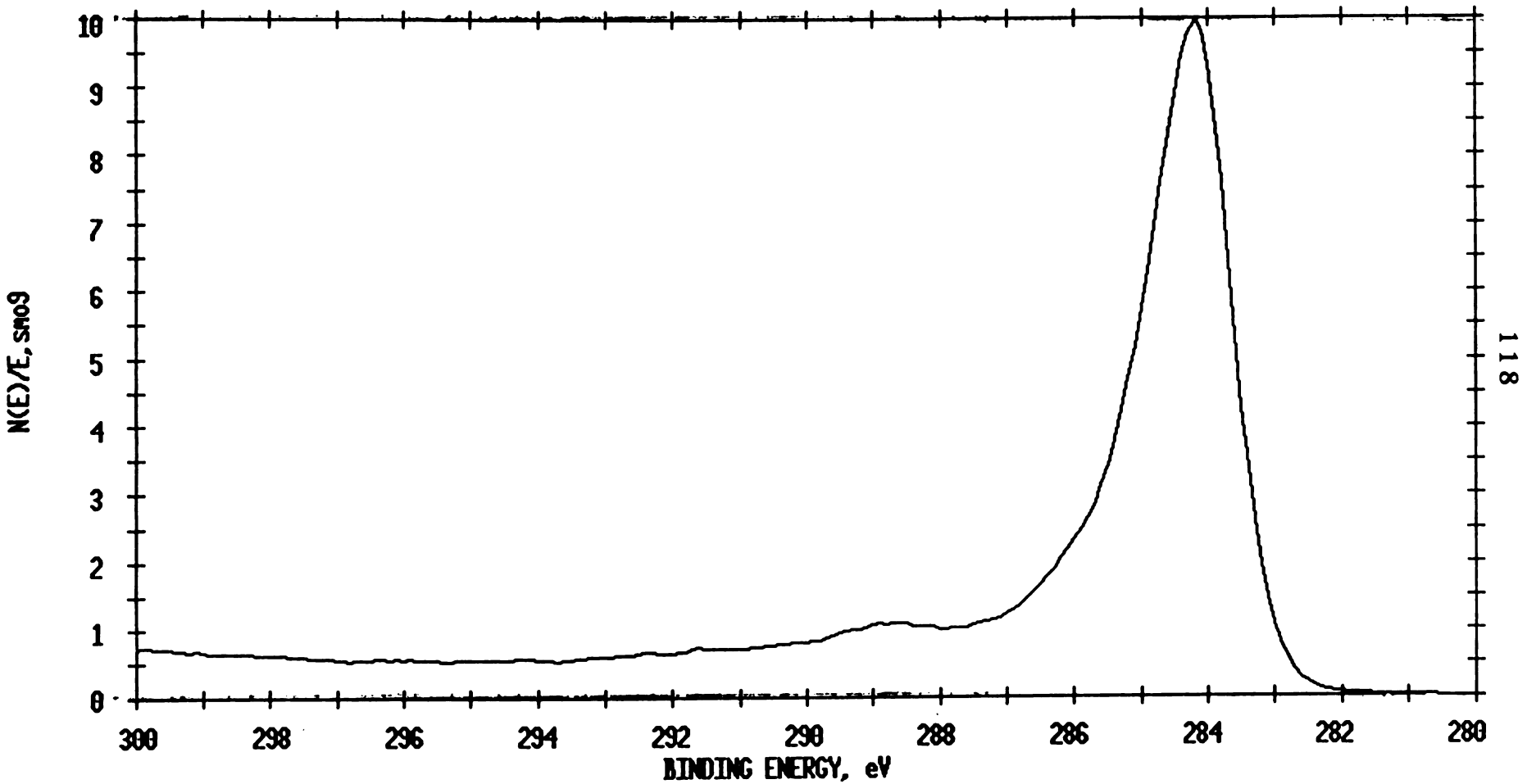

Figure B10. The XPS C1s Peak of PDP Coal Char Preoxidized at 375°C (2.13% Mass Burnoff) –Outgassed at 120°C Under High Vacuum.

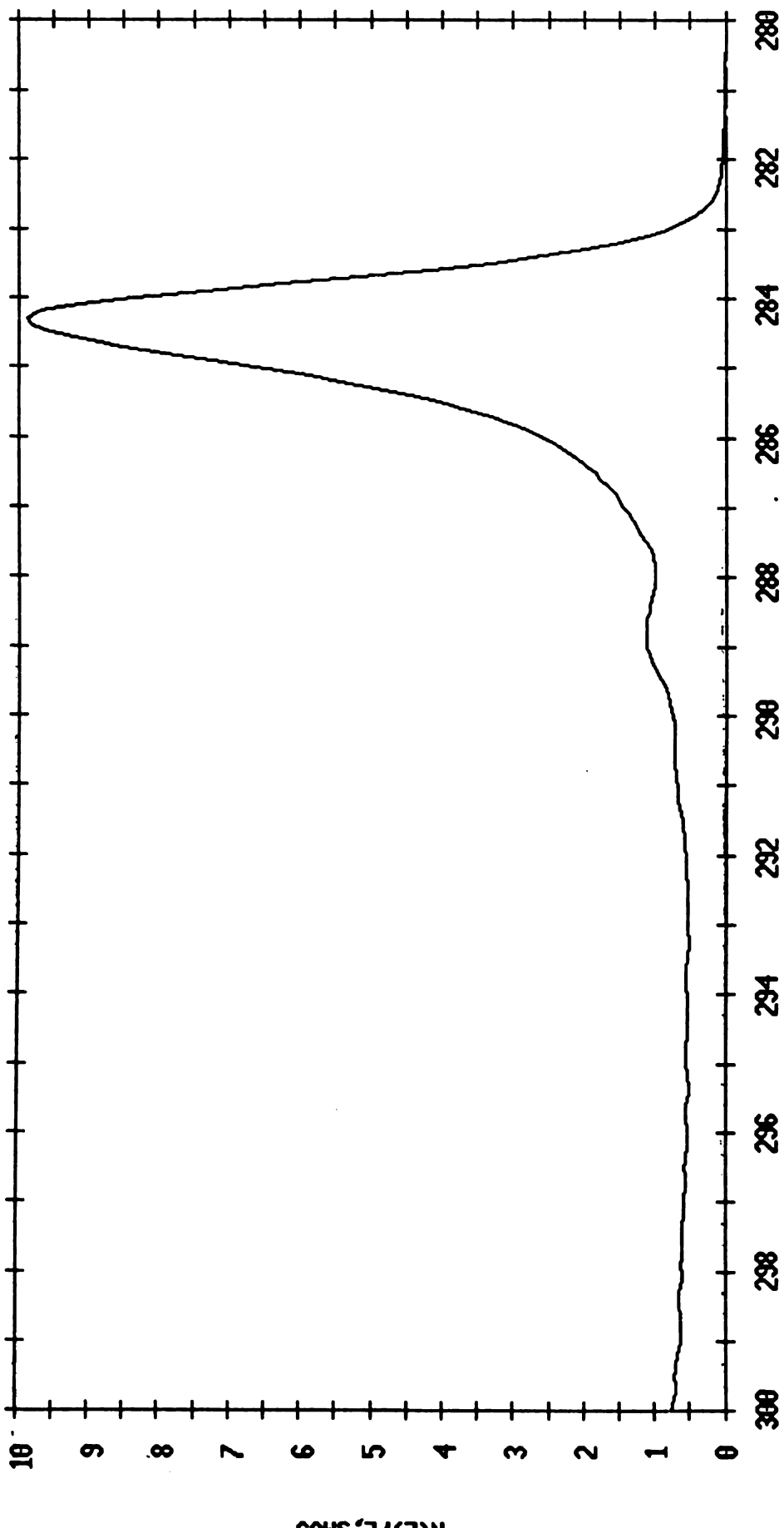

Figure B11. The XPS C1s Peak of PDP Coal Char Preoxidized at 375oC (6.33% Mass Burnoff) –Outgassed at 120oC Under High Vacuum.

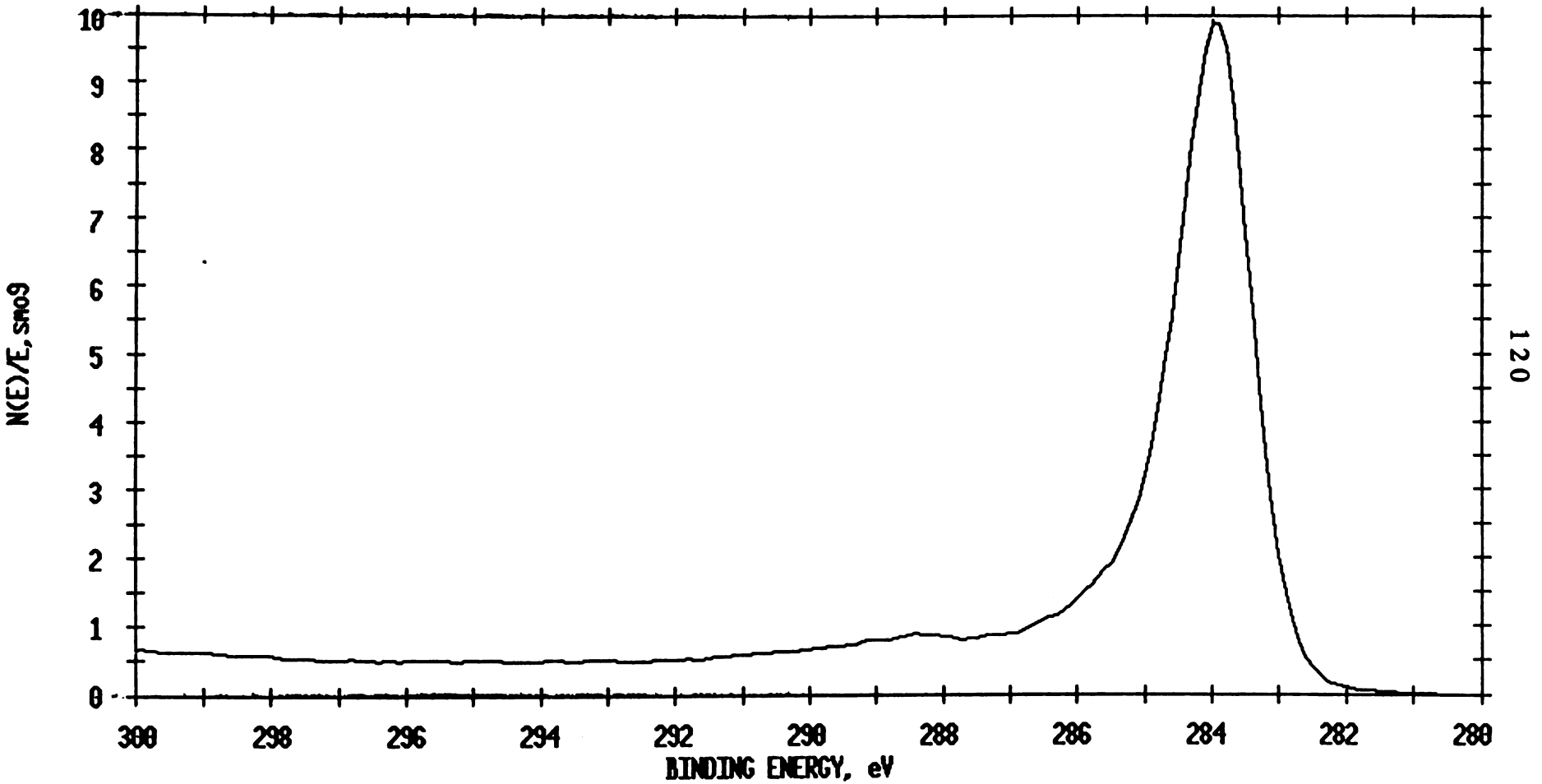

Figure B12 The XPS C1s Peak of Fresh Saran Char --Outgassed at 120°C Under High Vacuum.

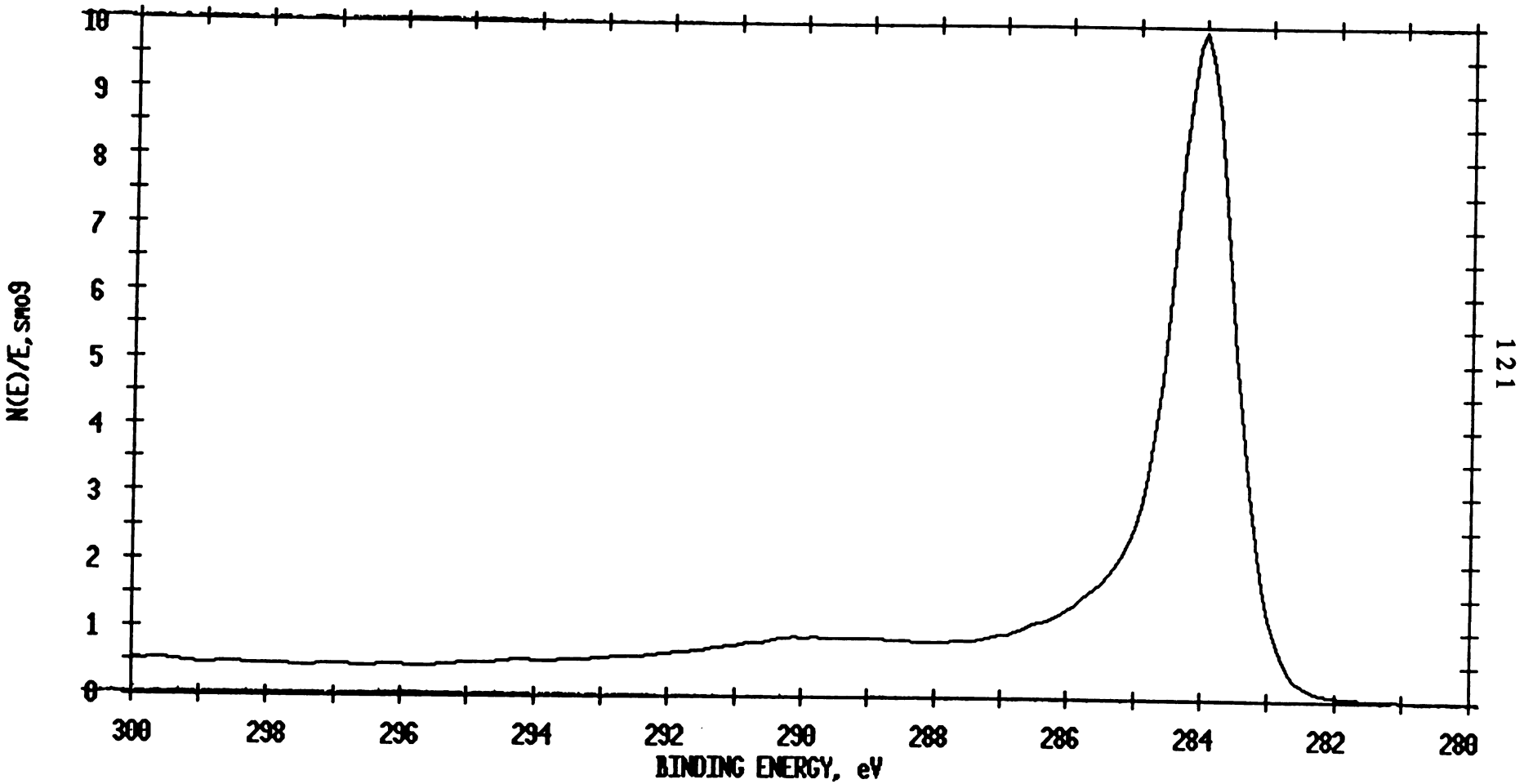

Figure B13. The XPS C1s Peak of Gasified Saran Char --Outgassed at 120°C Under High Vacuum.

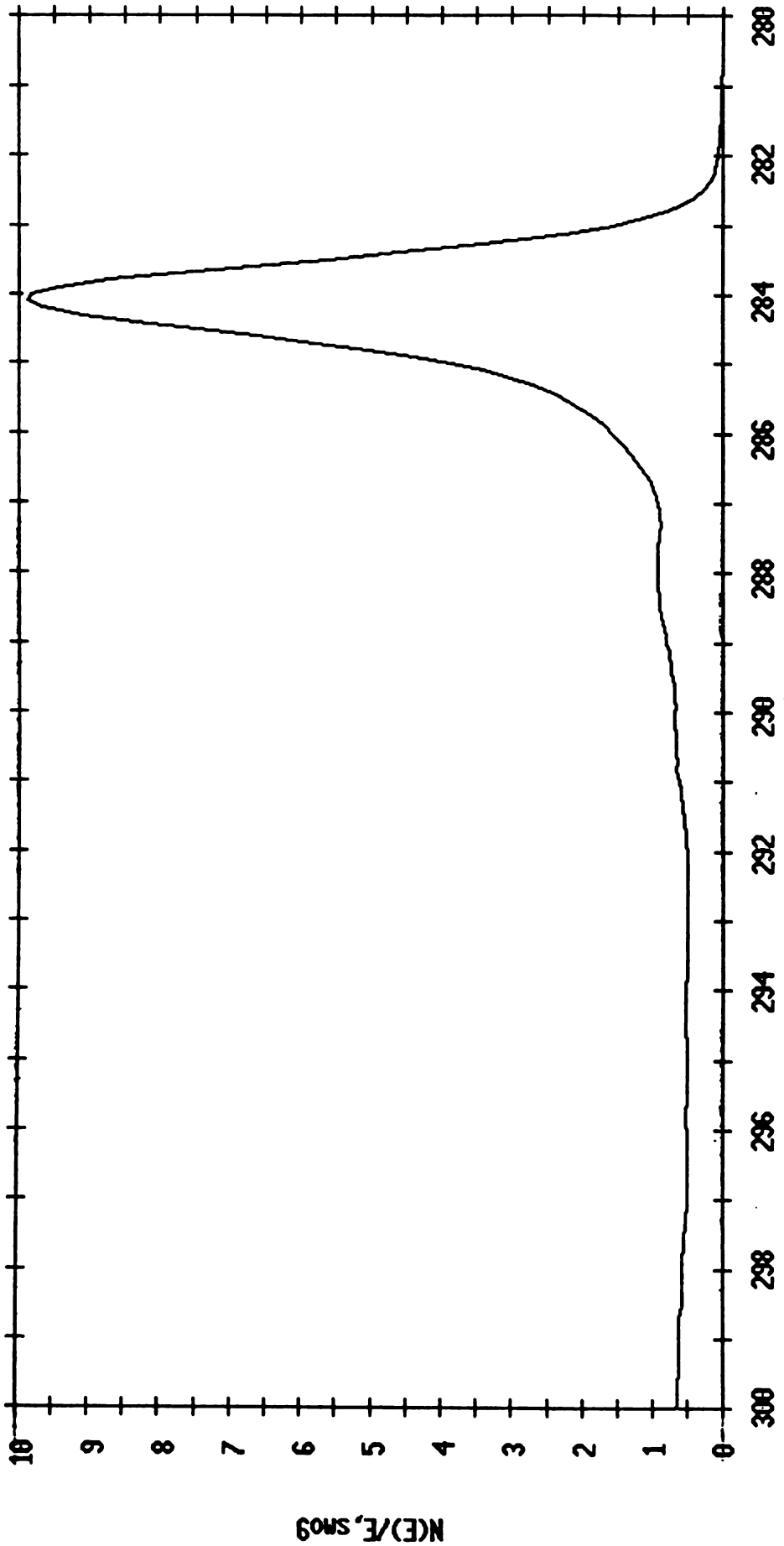

Figure B14. The XPS C1s Peak of Saran Char Preoxidized at 375°C (3.14% Mass Burnoff) - -Outgassed at 120°C Under High Vacuum.

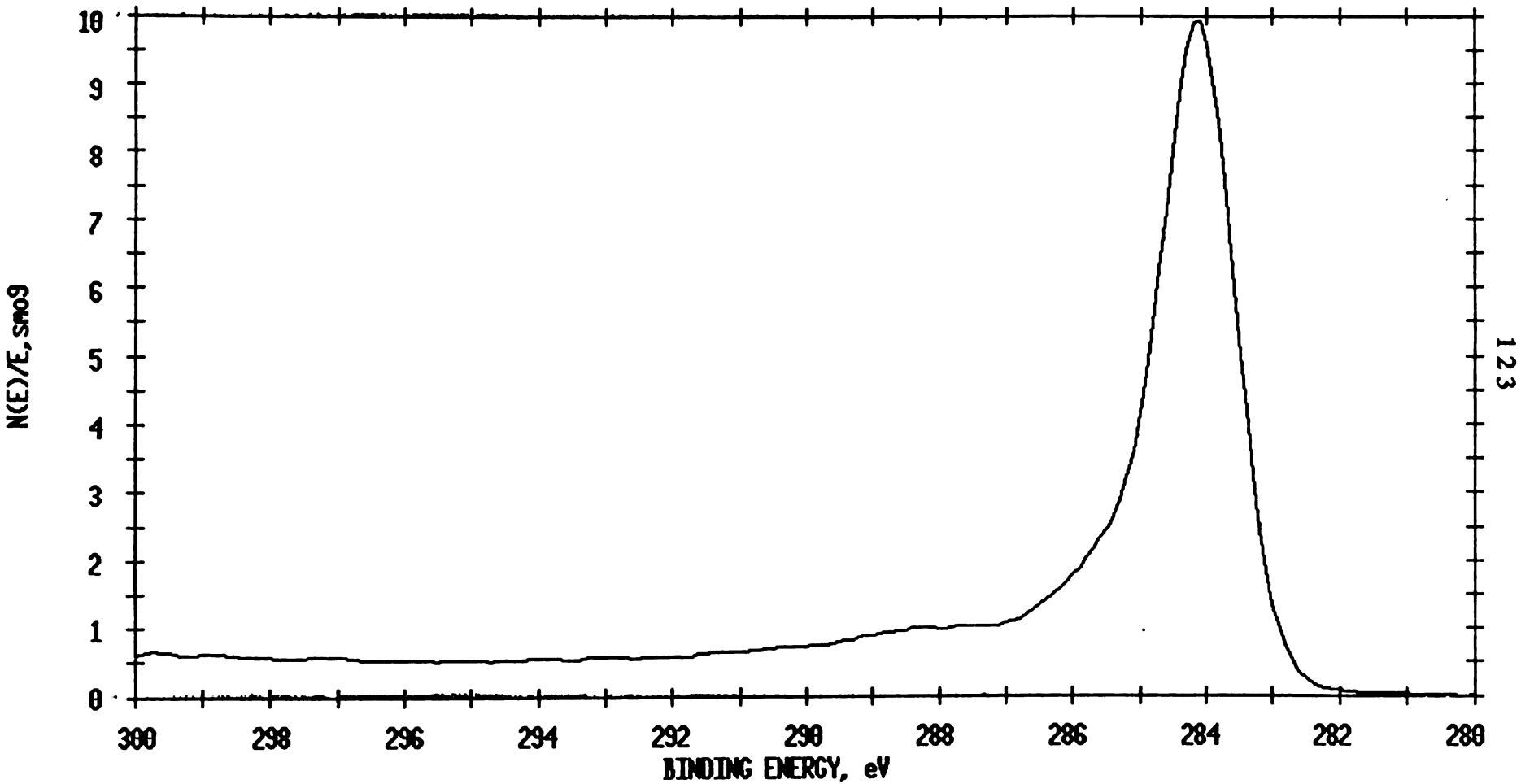

Figure B15. The XPS C1s Peak of Saran Char Preoxidized at 375°C (7.77% Mass Burnoff) - -Outgassed at 120°C Under High Vacuum.

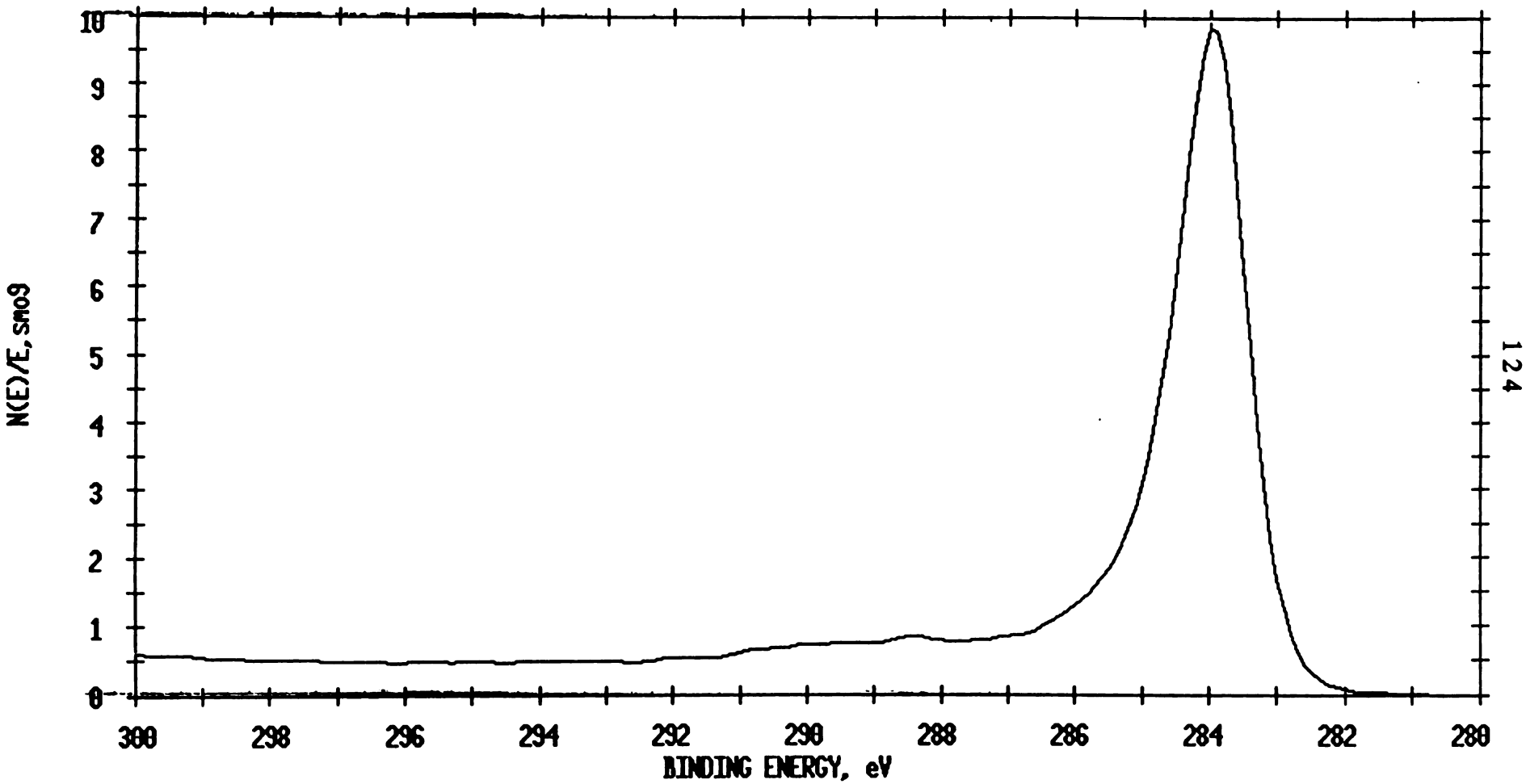

Figure B16. The XPS C1s Peak of Outgassed (1000°C) Saran Char--Outgassed at 120°C Under High Vacuum.

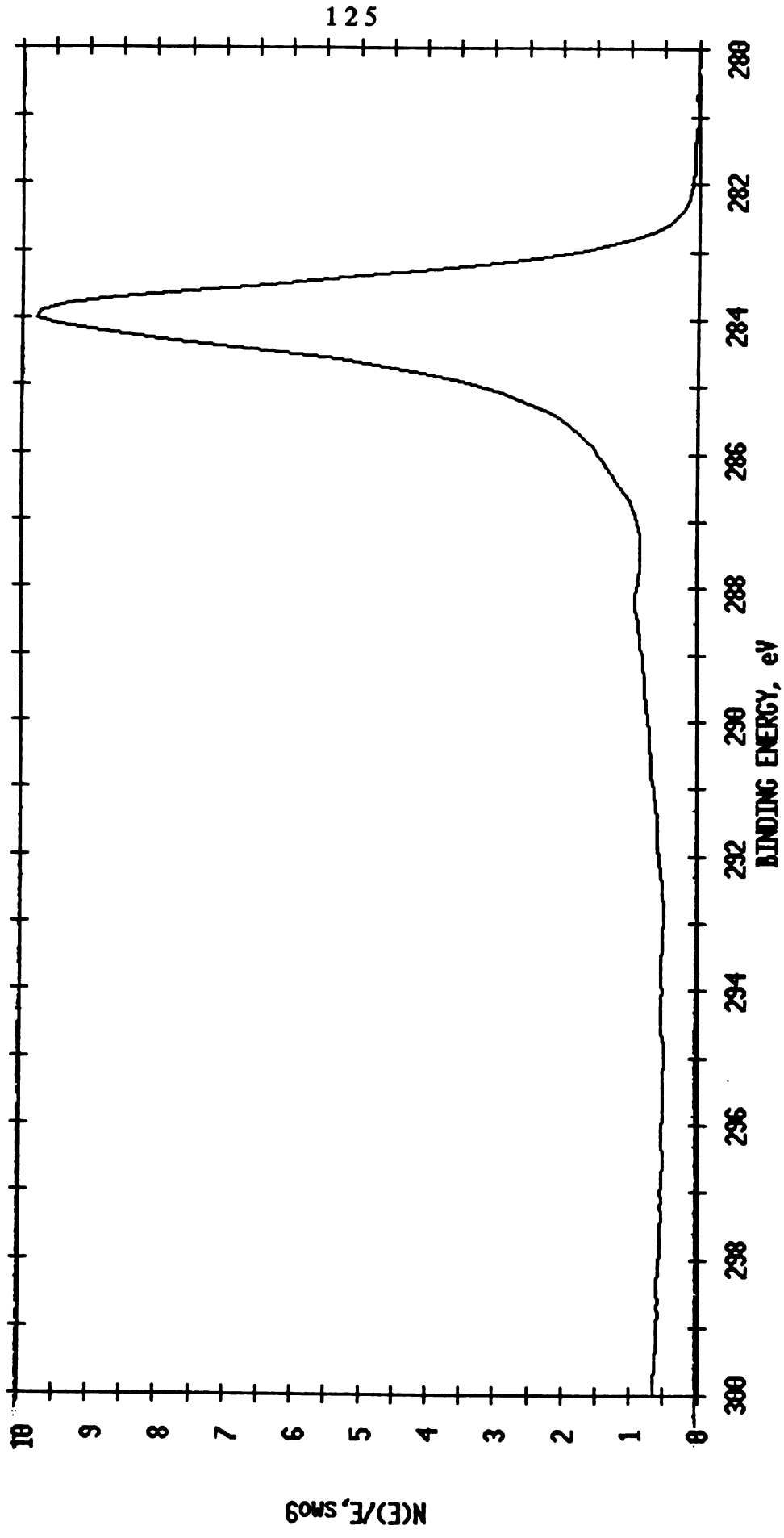

Figure B17. The XPS C1s Peak of Outgassed (1000°C) Saran Char Preoxidized at 375°C (0.42% Mass Burnoff)-Outgassed at 120°C Under High Vacuum.

APPENDIX C

APPENDIX C.

CARBON SURFACE GASIFIED DURING OXYGEN CHEMISORPTION

A_{CO_2}=Area of CO_2 peak from chart recorder.

A_{O_2}=Area of O_2 peak from chart recorder.

M=D.E.T. meter reading.

M_{O_2}=Fraction of meter reading due to O_2.

Ø=Volume fraction.

$Ø_{CO_2} = A_{CO_2} / (A_{CO_2} + A_{O_2})$

$Ø_{O_2} = A_{O_2} / (A_{CO_2} + A_{O_2})$

X=Correlation factor for CO_2 response factor.

k=Scaling factor for peak area reading.

Π=Volume of gas adsorbed on char surface.

$Π_{O_2}$= Volume of oxygen injected - $k(M_{O_2})$.

π=Volume of gas not adsorbed on char.

$π_{O_2} = k(M_{O_2})$.

$π_{CO_2} = X(_{O_2})/(1-X)$ [typical value is 0.00864cc CO_2].

Mass Carbon Lost = $(_{CO_2})$*(M_w of Carbon)/(vol of 1 mol STP).

Mass Carbon Lost (mg) = (0.00864cc CO_2)(1gmol / 22414cc)(12000mg C / 1gmol CO_2) = 0.00463mg C

% Carbon Lost as CO_2 = (100%)*(0.00463mg C / 0.079mg C) = 5.8%